The response of prograding wave-dominated delta systems to rising relative sea level

Trajectory analysis as an approach to recognise controls on palaeogeographic evolution and stratigraphic architecture

Kristian Helle

Dissertation for the Degree of Philosophiae Doctor (PhD)

Department of Earth Science
University of Bergen, Norway
2008

The response of prograding wave-dominated delta systems to rising relative sea level

Trajectory analysis as an approach to recognise controls on palaeogeographic evolution and stratigraphic architecture

Preface

This dissertation entitled “The response of prograding wave-dominated delta systems to rising relative sea level; trajectory analysis as an approach to recognise controls on palaeogeographic evolution and stratigraphic architecture” is presented for the degree of Philosophiae Doctor (PhD) at University of Bergen (UiB), Norway. The project has been funded by VISTA (www.vista.no) which is Statoil’s (now StatoilHydro) basic research programme conducted in collaboration with the Norwegian Academy of Science and Letters.

The research presented here was carried out between spring 2005 and autumn 2007 with Professor William Helland-Hansen (UiB) as project leader and supervisor, and Sverre Henriksen as technical contact in Statoil. The research took place at UiB, Statoil Research Centre in Trondheim and Colorado School of Mines (Golden, USA) and these institutions are acknowledged for providing facilities during work with the dissertation.

Numerous persons at UiB, Statoil and other institutions are thanked for contributions and discussions. In particular, Professor William Helland-Hansen is thanked for excellent supervision and is along with Tor Sømme (UiB) acknowledged for numerous stimulating discussions. Sverre Henriksen, Alf Ryseth, Scott Bullimore, Knut Inge Brendeland and Inge Kaas at Statoil are acknowledged for proposing data sets and approving access to these, as well as for discussions. John Howell (Centre for Integrated Petroleum Research at UiB) is acknowledged for introducing the Book Cliffs stratigraphy in Utah, USA. Adrian Read is acknowledged for reviewing the English. Thanks are also extended to my co-authors and field assistants.

My family and friends, and in particular my wife Ana Silvina Peréz Teséyra, are warmly thanked for all the good times.

The response of prograding wave-dominated delta systems to rising relative sea level

Trajectory analysis as an approach to recognise controls on palaeogeographic evolution and stratigraphic architecture

THE RESPONSE OF PROGRADING WAVE-DOMINATED DELTA SYSTEMS TO RISING RELATIVE SEA LEVEL

Trajectory analysis as an approach to recognise controls on palaeogeographic evolution and stratigraphic architecture

Chapter 1

Background, purpose of study, data base and methodology

Kristian Helle

Sequence stratigraphic background

In the 1960s and 1970s, sedimentological research was mainly concerned with recognising links between sedimentary processes, sedimentary structures and depositional environments (e.g. Reineck, H. E. & Singh, I. B., 1973; Friedman, G. M. & Sanders, J. E., 1978; Reading, H., 1978; Walker, R. G., 1979). With a few exceptions, little attention was attributed to larger scale geometries within stratigraphic packages until the introduction of the Exxon seismic sequence stratigraphic model (Fig. 1) (Payton, C. E., 1977; Wilgus, C. K. *et al.*, 1988). Along with the development of plate tectonics in the 1960s which increased the understanding of the evolution of sedimentary basins, the Exxon model enabled depositional systems to be studied at a more regional scale than before. As a result, allogenic mechanisms (e.g. Milankovitch, M., 1941) became increasingly recognised as important controls on sedimentation, and the Exxon global sea level chart was presented. Later, the Exxon group developed high resolution sequence stratigraphy based on well logs, cores and outcrop analysis (Fig. 2) (Van Wagoner, J. C., 1985; Van Wagoner, J. C. *et al.*, 1990). This sequence stratigraphic framework provided tools which significantly refined stratigraphic resolution and increased the understanding of the controlling mechanisms on depositional systems, compared to the traditional lithostratigraphic methodology.

The Exxon model and the global sea level chart were subsequently criticised for lacking documentation and omitting local to regional controls on sedimentation, such as sediment supply and tectonics (e.g. Miall, A. D., 1986; Hubbard, R. J., 1988). The terminology in the Exxon model was unnecessarily complex and the emphasis on allogenic controls on in depositional systems was too simplistic. In scientific communities outside Exxon, the importance of linking the systems tract to change in *relative* sea level (combining global sea level and tectonics), and not merely *global* sea level emerged. In particular, focus on the importance of deposition during falling relative sea level, which was largely neglected in the Exxon model, resulted in the development of a forced regressive systems tract (or equivalent terminology, Hunt, D. & Tucker, M. E., 1992; Nummedal, D., 1992; Helland-Hansen, W. & Gjelberg, J. G., 1994).

Alternative sequence stratigraphic models to the Exxon one were proposed, based on other data sets than seismic. These included the Genetic Stratigraphic model (Galloway, W. E., 1989) based on well data, and the Transgressive-Regressive model (Embry, A. F., 1993) which is based on outcrops. For a more comprehensive historic overview of sequence stratigraphy, see Nystuen (1998).

Trajectory Analysis

Following the introduction of the conceptual basis of modern sequence stratigraphy (Payton, C. E., 1977; Wilgus, C. K. *et al.*, 1988), some authors started to focus on the development of the sediment surfaces and the migration of facies belts with time, employing a semi-quantitative approach. Larue and Martinez (1989) used principles of bedform climb models and discussed variable climb angles for shoreline successions in explaining different scenarios of erosion and deposition; Cant (1991) presented geometrical modelling of facies belt migration during fluctuating relative sea level; Muto and Steel (1992; 1997; 2002a) emphasised the effect of increasing clinoform surface (or increasing clinoform size) associated with progradation during rise in relative sea level. They argued that the ratio between the rate of sediment supply and the rate of relative sea level rise can never be in equilibrium, and that with constant sediment supply and rising relative sea level, shoreline or shelf edge progradation will eventually turn into transgression (auto retreat). Ross et al. (1994) introduced the principle of slope readjustment which builds on by Hedberg's (1972) concepts of graded and erosional margins. The graded margin type progrades in equilibrium with depositional and erosional processes, whereas the erosional margin type is recognised by oversteepening of the basin margin resulting in sediments being transported to the basin floor.

Helland-Hansen and Gjelberg (1994) further developed the ideas of facies migration presented by Cant (1991) and Larue and Martinez (1989), and introduced the *shoreline trajectory* concept (Fig. 3) which they defined as the cross-sectional migration path of the shoreline through time (Helland-Hansen, W. & Gjelberg, J. G., 1994). This concept emphasises the angle of shoreline migration, and thereby directly incorporates the effects of sediment supply and basin physiography (in addition to relative sea level) into the sequence stratigraphic methodology. The trajectory approach was later further developed by Helland-Hansen and co-workers (Helland-Hansen, W., 1995; Helland-Hansen, W. & Martinsen, O. J., 1996). Helland-Hansen (2007) defined *trajectory analysis* as the study of the lateral and vertical migration of sedimentary successions with emphasis on migration patterns and their directions. Although trajectory analysis can be performed at any scale, ranging from ripple-migration through to continental margin accretion, the methodology has so far mostly been applied to 2D, depositional dip directed, studies of shoreline migration (shoreline trajectory) and shelf-edge migration (shelf edge trajectory).

The obvious reason for using shorelines to study migration patterns is that the shoreline is located at the continental-marine facies transition which is also associated with a break in the depositional profile. This facies transition is a very distinct boundary that can relatively easily be traced compared to other facies boundaries. This makes outcrop data the most useful source for investigating shoreline trajectories, even if ground penetrating radar data and high resolution seismic data may provide good sources for mapping the displacement of the break in slope through time (cf. Helland-Hansen, W., 2007).

The angle of the shoreline trajectory is controlled by sediment supply, relative sea level change and basin physiography, and the concept allows the sum of these variables to be viewed as a continuous spectrum. There are two main categories of shoreline trajectories: transgressive and regressive. The transgressive trajectories can further be divided into accretionary and non-accretionary, whereas the regressive trajectories can be divided into normal regressive, accretionary forced regressive, and non-accretionary forced regressive (Fig. 3) (Helland-Hansen, W. & Martinsen, O. J., 1996). Since the introduction of the concept it has been applied to depositional systems by several authors (e.g. Mellere, D. & Steel, R. J., 1995; 1995b; Hampson, G.

J., 2000; Bhattacharya, J. P. & Willis, B. J., 2001; Løseth, T. M. & Helland-Hansen, W., 2001; Bullimore, S. A. & Helland-Hansen, W., 2002; Crabaugh, J. P., 2003; Hampson, G. J. & Storms, J. E. A., 2003; Løseth, T. M. *et al.*, 2006).

The *shelf edge trajectory* concept (Fig. 4) (Steel, R. J. *et al.*, 2000) is based on the same principles as outlined by Helland-Hansen and Gjelberg (1994), but is defined as the cross-sectional migration path of the shelf edge through time. A notable difference between the shoreline and shelf edge trajectory concepts is that the former is applied to shoreface clinoforms (metres to 10s of metres high) whereas the latter is applied to shelf-slope-basin floor scale clinoforms (100s to a couple of 1000s of metres high). Although exceptions occur (e.g. Steel, R. J. & Olsen, T., 2002), this scale difference makes seismic data the best source for studying shelf edge trajectories. The shelf edge trajectory can be used as a reliable indicator for long term relative sea level fluctuations; falling, flat and rising shelf edge trajectories represents falling, stable and rising relative sea level, respectively (Fig. 4).

Subsequent to the introduction of the shelf edge trajectory concept, Steel and Olsen (2002) used it to suggest that the formation of significant basin floor fans is associated with flat or falling shelf edge trajectories, while Porebski and Steel (2003) related varying shelf edge delta architectures to different shelf edge trajectory trends (their Fig. 11). The concept has also been applied in other studies (e.g. Mellere, D. *et al.*, 2002; Plink-Björklund, P. & Steel, R., 2002).

In general, trajectories can be divided into descriptive (observable) and inferred (not observable) types. *Descriptive trajectories* are typically well-displayed trajectory patterns from seismic data and these patterns can be used as a descriptive basis for how the sum of sediment supply and relative sea level changes through time. The trajectory pattern can then be coupled with other information obtained from the studied data, such as interpretation of depositional environments and facies geometries. This may form the basis for suggesting the relative importance of changes in sediment supply versus changes in relative sea level as controls on the stratigraphic architecture of a depositional system. Further, the integration of trajectory patterns and facies interpretations can be used to investigate if the occurrences of certain depositional environments or stratigaphic architecture are genetically linked to specific trajectory patterns. If such connections are successfully recognised, these relationships can be used to predict stratigraphic architecture in areas where data quality or coverage is poor.

Examples of *inferred trajectories* could be seismic or outcrop data were the trajectory pattern needs to be inferred e.g. due to insufficient lateral outcrop control to decide trajectory orientation. In these cases, the trajectory pattern can be inferred from facies geometries such as aggrading coastal plains or shallow marine sandstones implying relative sea level rise and rising trajectories, or a basinward shift in facies implying a progradational component in the trajectory. Once the trajectory pattern has been documented, the inferred trajectories can be used in much the same way as descriptive trajectories.

There are several advantages in applying the trajectory analysis approach to sequence stratigraphy compared to the traditional sequence stratigraphic methodology. Traditional sequence stratigraphic analysis subdivides stratigraphic successions into systems tracts which are largely defined by their position on a sea level curve. Clearly, the approach presupposes that relative sea level is, in fact, oscillating and the systems tract terminology therefore automatically favours relative sea level as the main control on the development of the depositional system and the resulting stratigraphic architectures. However, in many study areas (e.g. chapters 2-4 in this dissertation), it is not obvious that the effect of fluctuating relative sea level is the dominant control on the development of a depositional system. In such cases, it may be inappropriate to genetically incorporate the relative sea level term in the naming of the units of which the stratigraphic succession is subdivided (the system tracts).

In contrast to the systems tract approach, the trajectory approach directly incorporates the effects of sediment supply and basin physiography on evolution of the depositional system, *in addition* to change in relative sea level. Trajectory analysis therefore honours gradual changes of deposition and has the potential to embrace models for whole ranges of depositional conditions, including those in which oscillating relative sea level is *not* the dominant control on sedimentation. Thus the trajectory concepts allows the systems tracts of traditional sequence stratigraphy to be viewed as a continuous spectrum within which facies variations can be related, without presupposing the studied depositional system was exposed to a specific development in sea level change.

The trajectory approach presents a higher resolution tool compared to traditional sequence stratigraphy. For example, a succession which in traditional sequence stratigraphy would be classified as a normal regression in a highstand systems tract (Posamentier, H. W. *et al.*, 1988; Posamentier, H. W. & Vail, P. R., 1988; Van Wagoner, J. C. *et al.*, 1988; Van Wagoner, J. C. *et al.*, 1990) or a lowstand wedge systems tract (Hunt, D. & Tucker, M. E., 1992; Helland-Hansen, W. & Gjelberg, J. G., 1994) might be subdividable into several stratigraphic units based on different trajectory patterns. As will be shown in this dissertation, increasing steepness of a normal regressive shoreline and shelf edge trajectory angle is linked to different styles of stratigraphic architecture and palaeogeography.

Purpose of study and data base

The purpose of this dissertation is to attempt to recognise links between trajectory patterns and the evolution of overall regressive, wave-influenced delta systems. As such delta systems appear on different scales in the stratigraphic record, ranging from the construction of individual parasequences (typically up to a few 10's of m thick) to the construction of entire continental margins (100's-1000's metres thick), multi-scaled data sets are required to resolve this purpose. To be able to compare the responses of depositional systems to different rates and amounts of rise in relative sea level, data from basins which experienced different subsidence rates were studied. The data presented here therefore comprise: 1) *core and well data* from the Jurassic Brent delta, North Sea; 2) *outcrop data* from the Cretaceous Blackhawk Formation, Book Cliffs, Utah, USA; and 3) *seismic and well data* from the Pleistocene succession in Columbus Basin and Plataforma Deltana, offshore Venezuela (Table 1, Fig. 5).

Table 1 Overview of the settings of the different study areas and the data types included in this dissertation

Study	Geographical location	Structural setting	Basin	Age	Data type
Chapter 2	North Sea, Norway	Extensional basin	Viking Graben	Jurassic, Aalenian-Bajocian	Cores and well logs
Chapter 3	Book Cliffs, Utah, USA	Foreland basin	Western Interior Seaway	Cretaceous, Campanian	Outcrops
Chapter 4	Offshore	Foreland	Columbus Basin	Quaternary,	Seismic and

	Venezuela	basin	and Plataforma Deltana	Pleistocene-Holocene	well logs

Methodology

Logging of stratigraphic successions (chapters 2, 3 and 4): Sedimentary description of cores (**Chapter 2**) and outcropping field data (**Chapter 3**) in this study emphasised grain size and primary and secondary sedimentary structures. The descriptions formed the basis for separating the sedimentary rocks into facies and interpreting the depositional environments. During field work, key localities were correlated for the purpose of documenting larger scale geometries and lateral facies transitions. The correlations were performed by using published correlation diagrams from within the study area as well as laterally tracing strata in the field. For detailed sedimentary logs from cores and outcrops, see Appendix.

In addition, gamma wire line log descriptions provided additional data which supplemented the studies in **chapters 2 and 4**. Gamma logs record the radioactivity of a sedimentary succession. In general, sandstones display low amounts of radioactivity while clay-rich intervals display high amounts. The wire line gamma log response was integrated with core and seismic data to support the interpretation of lithology and depositional environments.

Seismic interpretation (Chapter 4): Mapping of seismic reflectors believed to represent approximate time lines was performed on 2D and 3D seismic data by using Landmark software suite (Seisworks and Geoprobe), and the resultant surfaces are referred to as horizons. In the 3D cube, the horizons were interpolated across the study area. These interpolated horizons provided surfaces upon which calculation of RMS (Root Mean Square) attribute maps were performed for the purpose of revealing the lateral changes in the absolute value of the amplitudes along the horizons. These map view characteristics were then integrated with the cross-sectional signature and founded the basis for the division of seismic facies, and interpretation of depositional environments.

Interpretation of the 2D seismic data emphasised the development of larger scale geometries with time, such as clinoform height and foreset length, and was also used to place the smaller area 3D data set into a regional perspective. For further comments on the seismic interpretation methodology used in this dissertation, see Berg and Woolverton (1985) and Yilmaz (1987).

Chapter 2

Genesis of an anomalously thick shoreface sandstone tongue: Rannoch-Etive formations (Middle Jurassic Brent delta), Gullfaks area, Northern North Sea

Kristian Helle and William Helland-Hansen

Abstract

Regressive, wave-dominated shoreface sandstones are typically reported to have thicknesses of less than 20 m, and only rarely to exceed 30 m. The prograding barrier bar complexes of the Rannoch-Etive formations in the North Sea Brent Group, however, comprise far greater thicknesses (in places exceeding 100 m). The genesis of these successions has not been well understood, and the purpose of this study is to investigate within the framework of facies geometries in both modern and ancient depositional systems how the Rannoch-Etive sandstones could have been formed.

Theoretically, a 100 m thick succession of shoreface sandstones may form in 3 different ways: 1) by regression during stable sea level with a deep (100 m) shoreface sand pinch-out depth, 2) as a normal regression during rising relative sea level, or 3) by stacking of regressive-transgressive cycles during rising relative sea level.

The former option is less likely as shoreface sands in modern wave-dominated deltas are reported to typically extend down to only 5-12 m of water depth, far too shallow to form the 100 m thick Rannoch-Etive sandstones. Regarding option (2), the present study did not find convincing evidence for regressive-transgressive cycles, and the progradation is therefore interpreted as normal regressive without being punctuated by transgressions (option 3). In such a scenario, the vertical sandstone thickness would be determined by: 1) shoreline trajectory angle, 2) the horizontal (dip-directed) length of shoreface sand, and 3) shoreface sand pinch-out depth.

Modern wave-dominated deltas typically have shoreface sand lengths of up to 2 km. Within this framework, a 100 m thick vertical shoreface sandstone succession could result from a regression characterised by a shoreline trajectory of 2.6-5.4° (implying 80-95 m rise in relative sea level), a 5-12 m deep shoreface sand pinch-out depth, and a 1-2 km shoreface sand length.

Introduction

Shallow marine sandstones are common hydrocarbon reservoirs around the world and are found in a wide range of dimensions and shapes and sizes, ranging from individual isolated offshore sand bars (100s of sq m) to extensive sheets (100,000s of sq km) of deltaic sandstones (Reynolds, A. D., 1999). A thorough understanding of the factors which control the porosity, permeability, geometry and connectivity of such sandstones and their associated flow heterogenities is a major prerequisite for understanding the petroleum system contained within them.

Integrating studies of modern and ancient depositional systems with geometrical modelling of facies migration (Cant, D. J., 1991) may contribute to increased knowledge of the controls affecting the lithological distribution in such systems. This in turn can help to optimise production strategies in existing producing reservoirs. Such an approach may also help in predicting the presence of hydrocarbon reservoirs beyond the extent of data coverage.

Regressive, wave-dominated shoreface sandstone tongues are typically up to 30 m thick (Fig. 1) (Reynolds, A. D., 1999). The Rannoch-Etive formations (Brent Group) in the North Sea, however, comprise shoreface sandstones that exceed 100 m in places (Graue, E. *et al.*, 1987). Such thicknesses of shallow marine sandstones have also been reported from other places in the stratigraphic record (e.g. Garn Formation on the mid Norwegian shelf (Corfield, S. *et al.*, 2001) and Fulmar Formation of the UK North Sea (Howell, J. A. *et al.*, 1996)).

The mechanisms responsible for the creation of such thick marine sandstones have not been well understood. The purpose of this study is to investigate the possible controls on the genesis of the thick shallow marine sandstones in the Brent Group within the depositional framework described in previously published Brent literature. The study attempts to use geometrical modelling of facies belts (Cant, D. J., 1991), based on facies belt geometries revealed by studies of selected cores penetrating the Brent delta and on published studies of modern depositional systems.

Regional setting of the Brent delta

In Aalenian to Bajocian times, increased sediment supply from the south led to the northwards progradation of the Rannoch, Etive and Ness formations in the North Sea Brent delta (Figs. 2, 3) (Graue, E. *et al.*, 1987; Helland-Hansen, W. *et al.*, 1992; Johannessen, E. P. *et al.*, 1995). The sediments were probably sourced from the uplift of the Central North Sea Dome (Underhill, J. R. & Partington, M. A., 1993; 1994), the Norwegian mainland area (van der Beck, P., 1994) and the Shetland mainland area (Dore, A. G. *et al.*, 1999). The Brent delta regressed as a ramp margin (sensu Ahr, W. M., 1973) for approximately 200 km (Graue, E. *et al.*, 1987) before it was transgressed and overlain by the Tarbert Formation (Fig. 3c) (Graue, E. *et al.*, 1987; Helland-Hansen, W. *et al.*, 1992; Johannessen, E. P. *et al.*, 1995).

Brent delta facies

A detailed sedimentological description of the Rannoch-Etive formations was undertaken on continuous and high quality cores from three selected wells (Fig. 3b) (34/8-1, Visund field; 34/7-19, Vigdis field; and 15/10-A5H, Gullfaks field). The description emphasised sedimentary structures and grain size (measured approximately every 20 cm using microscope and grain size comparator).

This study recognises three facies in the regressive part of Brent delta (Figs. 3, 4, Table 1): 1) the lower shoreface sandstones of the Rannoch facies, 2) the barrier related sandstones of the Etive facies, and 3) the continental Ness facies. The facies are stacked in a gradually shallowing upwards succession (Fig. 5) and display large lateral thickness variations (Fig. 3a,b). The thickest parts lie within the up to 50 km wide Viking Graben and Shetland Basin (Fig. 2), where the total thickness of Rannoch-Etive formations exceeds 100 m in parts of the study area (Fig. 3) (Graue, E. *et al.*, 1987).

Table 1 Facies recognised in the regressive part of the Brent delta. The facies are stacked as an upward shallowing succession (cf. Fig. 5).			
Facies	**Sedimentary structures**	**Depositional environment**	**References**
Ness	Beds with highly varying grain size ranging from mudstone to very coarse grained sandstone. Some root traces and in situ coals. Sandstones contain wave ripple, current ripple and trough cross-lamination. Mudstones commonly contain lenticular to flaser bedding.	The presence of coal and root traces implies deposition in a continental environment. The wave ripples suggest presence of standing water bodies such as lagoons/bays and/or lakes whereas the current-generated structures imply deposition from flowing water. The facies is therefore interpreted as a continental plain.	(Budding, M. C. & Inglin, H. F., 1981; Livera, S. E., 1989)
Etive	Amalgamated fine to very coarse grained sandstones containing planar cross, trough cross and current ripple lamination, as occasional wave ripple lamination. In places, the facies appears massive or as planar laminated. The sorting varies from well sorted to poorly sorted. The facies is 30-50 m thick and has a sharp contact to the overlying Ness facies.	The lack of continental markers, and the facies stratigraphic position below continental deposits and above marine deposits, suggests a marginal marine depositional environment. The well sorted sediments are believed to have been transported by longshore currents, whereas the poorly sorted ones are interpreted as having been dumped, by shore-normal currents. The facies is therefore interpreted as barrier bar sandstones comprising foreshore, upper shoreface, longshore bar, mouth bar, tidal deltas and wash over fans deposits.	(Budding, M. C. & Inglin, H. F., 1981; Morris, J. *et al.*, 2003)
Rannoch	Amalgamated beds of well sorted, very fine to fine grained sandstone. Sedimentary structures include planar lamination, occasionally low angle, and rare high angle truncation surfaces. The facies is approximately 50 m thick and has a sharp contact to the overlying Etive facies. The facies has a gradational lower contact to the underlying mud of the Dunlin Group. The transition grades upward from lenticular lamination to interbedded thin beds of lenticular laminated mudstone and planar laminated, very fine grained, sandstone with occasional low angle truncations, and finally to homogenous Rannoch facies sandstones.	The planar lamination with low angle trough cross-lamination is likely to represent hummocky cross-stratification. These structures are believed to be wave-generated and to have formed above storm wave base in sand-dominated zones along wave-dominated coasts. The lack of current-generated structures suggests only minor longshore directed transport of sand in this zone. The finer grain size and the stratigraphic context with the overlying Etive facies suggest the Rannoch facies was deposited seawards of the latter and represents lower shoreface sandstones interfingering seawards with the offshore mud of the Dunlin Group.	(Richards, P. C. & Brown, S., 1986; Scott, E. S., 1992; Jennette, D. C. & Riley, C. O., 1996)

Palaeogeography

The large thicknesses of hummocky cross-stratification in the Rannoch facies (Fig. 5, cf. Table 1) imply that the coast was strongly influenced by waves (Richards, P. C. & Brown, S., 1986; Scott, E. S., 1992; Jennette, D. C. & Riley, C. O., 1996). The overlying Etive facies is interpreted as representing facies related to a barrier system, such as barrier sandstones, wash-over fans, flood tidal deltas and tidally influenced shallow marine channels (Budding, M. C. & Inglin, H. F., 1981; Morris, J. *et al.*, 2003). The Ness facies is considered to mainly comprise marginal marine to non-marine deposits as brackish water lagoons (Budding, M. C. & Inglin, H. F., 1981), as well as lagoonal deltas and fluvial plains deposits that comprises evidence of repeated autogenic facies stacking (Livera, S. E., 1989).

The Rannoch-Etive facies are therefore likely to represent genetically linked facies in a progradational lagoon-barrier complex (Fig. 3), which is in accordance with previously published literature (e.g. Livera, S. E., 1989; Cannon, S. J. C. *et al.*, 1992; Helland-Hansen, W. *et al.*, 1992; Mitchener, B. C. *et al.*, 1992; Scott, E. S., 1992; Morris, J. *et al.*, 2003), although others have proposed deposition during fluvial influence (Brown, S. & Richards, P. C., 1989; Johannessen, E. P. *et al.*, 1995; Olsen, T. R. & Steel, R., 1995; Fjellanger, E. *et al.*, 1996), strandplain setting (Jennette, D. C. & Riley, C. O., 1996) and in the context of a more mixed fluvial/barrier models (Olaussen, S. *et al.*, 1992). For an overview of previous Brent delta studies the reader is referred to Richards (1992) and Olsen and Steel (2000).

Geometries in modern wave-dominated deltas

The terms used in this study are *"shoreface sand length"* referring to the horizontal distance extending seawards from the foreshore to where homogenous sand is replaced by heterolithic sand and mud, and *"shoreface sand pinch-out depth"* which refers to the water depth where the homogenous sand is replaced by heterolithic sand and mud (Fig. 6).

The length and pinch-out depth of shoreface sand in modern sandy delta systems is highly dependent on the coastal processes. Along wave-dominated (sub-linear) coasts, the shoreface sand length is commonly 1-2 km and the shoreface sand pinch-out depths typically 6-12 m (Table 2, Fig. 7). In areas with high sediment input from tidal outlets or converging longshore currents, the length may increase to 3 km (cf. Rodriguez, A. B. *et al.*, 2001). However, these lengths and depths increase dramatically as the fluvial and/or tidal influence increases, and the sand may extend 25 km seaward from the shoreline and have a 70 m pinch-out depth if tidal dominance is sufficient (e.g. Ganges-Brahmaputra, see Mallik, T. K., 1976; Kuehl, S. A. *et al.*, 1989). In front of abandoned or active river outlets in modern fluvio-wave-dominated deltas, the shoreface sands typically construct 2-8 km long tongues with pinch-out depths of 15-20 m (Table 2, Fig. 7). Between the river outlets, the length and pinch-out depth are approximately as for wave-dominated coasts (i.e. 1-3 km and 5-10 m, respectively).

The large difference in shoreface sand length along wave-dominated and fluvio/wave-dominated coasts (Table 2) suggests that sediment transport by wave-generated longshore currents is limited to the zone nearest the shoreline (i.e. <2 km from the foreshore). The tongues of shoreface sand occurring seawards of ancient river mouths in the Ebro delta (Fig. 7) (Diaz, J. I. *et al.*, 1996) are likely to have been formed as a result of that sand-rich hypopycnal flows extending from the river mouths being sufficiently strong to penetrate the littoral energy fence set up by wave-generated longshore currents. Initially, the tongues are likely to have been dominated by fluvially related currents; however, if storm wave base is deeper than the shoreface sand pinch-out depth (15-20 m), these structures may later be overprinted by storm wave generated structures (e.g. hummocky cross-stratification). The storm waves also probably interact with the sea floor in the mud dominated areas located between the tongues, but the lack of sand flux to these areas prevents the formation of wave-generated structures such as hummocky cross-stratification and more massive mud facies may develop through storm activity.

Table 2 Width and pinch-out depth of homogenous shoreface sand in modern sandy, wave-dominated and Fluvio/wave dominated delta systems.

Delta type	**Delta**	**Approximate shoreface sand length (km)**	**Shoreface sand pinch-out depth (m)**	**Reference**

Wave-dominated	Texas coast	1-2 (3 at converging alongshore currents)	6-12	(Rodriguez, A. B. *et al.*, 2001)
	Nayarit, Mexico	2	7-10	(Curray, J. R. *et al.*, 1969)
	Tiber, Italy	0.8-1.8	5-12	(Bellotti, P. *et al.*, 1994)
	Ventra-Port Hueneme, USA	1-2	9	(Howard, J. D. & Reineck, H.-E., 1981)
Fluvio/wave-dominated	Ebro, Spain	2 between river outlets. 8 near river outlets	10 between river outlets. 15 near river outlets	(Diaz, J. I. *et al.*, 1996)
	Po, Italy	2-3	15	(Colantoni, P. *et al.*, 1979)
	Rhone, France	1-2 between river outlets. 2-4 near river outlets	5-10 between river outlets. 10-20 near river outlets	(van Straaten, L. M. J. U., 1959)

Furthermore, as the tongue shape is preserved after channel avulsion and resultant shutting down of the sediment supply to the tongues (Fig. 7), it is unlikely that wave generated currents will be able to transport this sand along-strike for any significant distance in areas more than 1-2 km offshore, even during storms. The length and pinch-out depth of shoreface sand are also approximately the same for wave-dominated coasts highly affected by storms/hurricanes (e.g. Texas coast, cf. Table 2) and for coasts with more moderate storm activity (e.g. Tiber delta; cf. Table 2). This suggests that once a coast is wave/storm dominated, the length and pinch-out depth of (homogenous) shoreface sand are corresponding to fair weather wave base (5-15 m deep) (Elliott, T., 1986b; Friedman, G. M. *et al.*, 1992; Walker, R. G. & Plint, A. G., 1992), and is only affected to a limited degree by storm strength, storm frequency and depth of storm wave base.

The *physiographic shoreface* on modern sandy coastal depositional systems extends seawards from the surf zone until the first observable break in slope on the shoreface profile (Swift, D. J. P., 1976; Friedman, G. M. & Sanders, J. E., 1978; Niedoroda, A. W. *et al.*, 1984; Swift, D. J. P. *et al.*, 1985). Here, the shoreface merges with the gently dipping (0.03°) inner shelf, typically at about 10 m water depth along prograding parts of modern coasts (Clifton, E. H., 2000). The dip directed length of the shoreface is related to the mean bottom slope, sediment supply and amount of energy available to the depositional system (Niedoroda, A. W. *et al.*, 1984). Along wave-dominated coasts, the shoreface typically develops a concave-upward profile with slope angles varying between 0.1 and 0.3° (Niedoroda, A. W. *et al.*, 1985; Walker, R. G. & Plint, A. G., 1992) and with the profile steepening toward areas with higher wave influence (see Rodriguez, A. B. *et al.*, 2001). However, along coastlines with large fluvial sediment supply, the shoreface profile typically has a concave-downward profile that is generally steeper (varying between 0.3 and 2.9°) than found along more wave-dominated coastlines (Orton, G. J. & Reading, H. G., 1993).

Clearly, the physiographic shoreface definition is unrelated to grain size changes, and the toe of the physiographic shoreface do therefore not necessarily correspond to the water depth where the transition from homogenous sand to heterolithic sand and mud deposits occur (e.g. Rodriguez, A. B. *et al.*, 2001). Both the physiographic shoreface profile and the length and pinch-out depth of homogenous shoreface sand are, however, important input parameters for geometrical facies modelling of facies belt migration (below).

Genesis of the Rannoch-Etive formations

Theoretically, anomalous thick successions of shoreface sandstones may form as 3 different end members: 1) by regression during stable sea level with a deep shoreface sand pinch-out depth, 2) by normal regression during rising relative sea level, or 3) by stacking of regressive-transgressive cycles (Fig. 8a,b,c).

Regarding the former alternative, shoreface sand off modern sandy wave-influenced coasts is typically reported as not extending beyond water depths of 20 m of water depth (Table 2). Progradation of such a depositional system during stable sea level would ideally be expected to result in a no more than a 20 m thick sandstone succession. Consequently, this excludes a deep shoreface sand pinch-out depth (i.e. over 100 m) as the main mechanism for generating the thick shoreface sandstones in the Rannoch-Etive formations (Fig. 8a).

The original subdivision of the regressive part of the Brent delta coincided with the lithostratigraphic Rannoch-Etive-Ness formations and the progradation was regarded as a single event (alternative 2 above) (Fig. 9b) (e.g. Helland-Hansen, W. *et al.*, 1992). However, with the development of high resolution sequence stratigraphy, it was proposed that the formations are comprised of several 3rd order, 4th order and even higher order sequences, implying fluctuating relative sea levels and regressive-transgressive cycles during an overall progradation (alternative 3 above) (Fig. 9c) (e.g. Johannessen, E. P. *et al.*, 1995; Olsen, T. R. & Steel, R., 1995).

Clearly, regressive-trangressive cycles are associated with seaward and landward directed migration of facies belts and are likely to be preserved in the stratigraphic record as repeated intrusions of one facies belt into the up-dip or down-dip located adjoining facies belts. The dip-directed migration may, however, not be sufficient to prevent amalgamation resulting in local over-thickening of shoreface sandstones (Fig. 8c).

The shoreface sand length in wave-dominated deltas (1-2 km) (Table 2) is much shorter than the horizontal dip-directed distance between the studied wells (c. 20 km) (Fig. 3). Consequently, if regressive-transgressive cyclicity was the dominating progradational style of the Brent delta it is likely that an up-dip directed movement of the shoreline would be captured by facies changes in the studied cores, either as: 1) repeated stacking of offshore-offshore transition-lower shoreface facies in front of the delta, 2) repeated intrusion of Etive facies into Rannoch facies, or 3) intrusion of marine sandstones into the continental Ness facies. These three points are discussed below.

1) The transition from the offshore mud of the Dunlin Group to the overlying Rannoch facies is gradual and does not consist of repetitive stacking of facies that are attributable to regressive-transgressive cycles (Fig. 5).

2) The Rannoch facies itself is a gradually shallowing-up succession without obvious repetition of smaller scale shallowing-up successions. However, there is a thin interval of Etive facies encased in Rannoch facies a few metres below the Rannoch-Etive boundary in some wells penetrating the Brent Group (e.g. in well 34/7-19 at 2585 m, and in well 34/10-A5H at 1884 m, see Fig. 5). Due to the close stratigraphic relation to the Rannoch-Etive boundary, it is likely that this facies stacking represents bed set

interfingering, and should not be regarded as evidence for regressive-transgressive cycles.

Gamma logs of the well 34/8-1 display obviously repeated upwards decreases in gamma values for the Rannoch-Etive formations (Fig. 10). However, these gamma trends correspond to homogenous sandstones in the cores which do *not* display facies changes attributable to transgressions. The gamma trends are therefore likely to have another origin than representing regressive-transgressive cycles. Some change in mud content in the sandstones should be expected from variations in mud/sand ratio in the sediments supplied related e.g. to changes in position of channel outlets, without this being automatically related to relative sea level changes and parasequence stacking.

3) There is some evidence for repeatedly stacked upward fining of grain size in the cores from the lower delta plain deposits of the Ness Formation (Fig. 5). However, this is a depositional setting where autogenic processes are very common. As long as intrusions of Rannoch-Etive facies are not evident within the Ness facies, this repetitive stacking should not be interpreted to reflect dip-directed migration of the shoreline, but rather be attributed to autogenic processes in the delta plain realm. These autogenic processes are exemplified by progradation and abandonment of lagoonal deltas (Livera, S. E., 1989) or by shifting tidal inlets, both of which can lead to repeated shallowing of bays/lagoons and result in rhythmic stratigraphic stacking.

For the above reasons, it is concluded that there is no strong evidence for the shoreline moving landwards within the study area during progradation of the Rannoch-Etive formations shoreline, and that the depositional system developed as a normal regressive event (Fig. 8b).

Curved coastlines favour autogenic shifts and regressive-transgressive cylicity (e.g. Scruton, P. C., 1960; Elliott, T., 1986a). Consequently, the lack of evidence of regressive-transgressive cycles in the studied deposits is likely to reflect a low amount of curvature along the Brent coastlines. The facies analysis above favours a lagoon-barrier coastline, which is a common interpretation for the Brent delta (e.g. Livera, S. E., 1989; Cannon, S. J. C. *et al.*, 1992; Helland-Hansen, W. *et al.*, 1992; Mitchener, B. C. *et al.*, 1992; Scott, E. S., 1992; Morris, J. *et al.*, 2003). The shoreface sand length and pinch-out depth of the Brent delta are therefore likely to have been 1-2 km and 5-12 m, respectively (cf. Table 2), which would be the same as for a strandplain environment, as Jeannette and Riley (1996) suggested. Alternatively, a sub-linear coastline may have been constructed by channel belts entering the sea as a multiple source or line source (e.g. Johannessen, E. P. *et al.*, 1995), implying shoreface sand lengths and pinch-out depths of 2-8 km and 10-20 m, respectively. However, the latter model seems less likely due to the low amount of fluvial related facies evident in the Rannoch-Etive formations and the offshore mud of the Dunlin Group. Also, the abundance of lagoonal delta systems in the Ness Formation indicates that fluvial channels did not necessarily extend to the coastline (Livera, S. E., 1989).

The vertical shoreface sandstone thickness in such normal regressive deposits is determined by 1) shoreline trajectory angle, 2) shoreface sand pinch-out depth, and 3) shoreface sand length (Fig. 11a) (Cant, D. J., 1991). A 100 m thick shoreface sandstone succession may form from any combination of these three parameters (Fig.11, Table 3). Within the framework of modern wave-dominated coasts (Table 2), a 100 m thick succession of shoreface sandstone could have formed during progradation with a shoreline trajectory of 2.6-5.4° (implying 80-95 m rise in relative sea level), a 5-12 m deep shoreface sand pinch-out depth, and a 1-2 km shoreface sand length. This indicates that anomalous thick shoreface sandstones can result from normal regressions without having to be punctuated by transgressions. The main geometrical control on vertical sandstone thickness in the studied part of the Brent delta may therefore have been the amount of rise in relative sea level, and shoreface sand length.

The shoreface length and pinch-out depth ranges used in this study have been collected from the literature on modern delta systems (Table 2); however, no suitable modern analogues exist for the lagoons and the lagoonal delta systems of the Ness Formation that were located behind the Brent shoreline (Livera, S. E., 1989). This prevents comparison of the shoreline trajectory angles calculated in this study with trajectory angles obtained from modern delta systems.

Table 3: Minimum angle of shoreline trajectory, θsht=arc-tan(100m-d)/l, required to generate a 100 m thick package of homogenous shoreface sandstone, plotted against shoreface sand pinch-out depths (d), shoreface sand lengths (l) and relative sea level rise needed (r). Grey areas represent values common in modern, sandy, wave-dominated shorelines. The shoreface slope, θss=arc-tan(d/l), in modern fine sand dominated deltas is highly variable, but commonly lies between 5-50 mkm^{-1} (0.3-2.9°) along wave/fluvio dominated deltas (Orton, G. J. & Reading, H. G., 1993). Along wave-dominated coasts, the shoreface angle is typically 0.1°-0.3° (Niedoroda, A. W. *et al.*, 1985; Walker, R. G. & Plint, A. G., 1992). Calculations are based on formulas presented by Cant (1991).

Delta type	**Shoreface sand length (l)**	**Relative sea level rise (r)**													
		0m	10m	20m	30m	40m	50m	60m	70m	80m	90m	95m	99m	99.9m	
		Shoreface sand pinch-out depth (d)													
		100m	90m	80m	70m	60m	50m	40m	30m	20m	10m	5m	1m	0.1m	
Wave-dominated	1,000m	***0°***	***0.6°***	***1.1°***	***1.7°***	***2.3°***	***2.9°***	***3.4°***	***4.0°***	***4.6°***	***5.1°***	***5.4°***	***5.7°***	***5.7°***	***θsht***
		5.7°	5.1°	4.6°	4.0°	3.4°	2.9°	2.3°	1.7°	1.1°	0.6°	0.3°	0.06°	0.006°	θss
	2,000m	***0°***	***0.3°***	***0.6°***	***0.9°***	***1.1°***	***1.4°***	***1.7°***	***2.0°***	***2.3°***	***2.6°***	***2.7°***	***2.8°***	***2.9°***	***θsht***
		2.9°	2.6°	2.3°	2.0°	1.7°	1.4°	1.1°	0.9°	0.6°	0.3°	0.1°	0.03°	0.003°	θss
Fluvio/wave-dominated	4,000m	***0°***	***0.1°***	***0.3°***	***0.4°***	***0.6°***	***0.7°***	***0.9°***	***1.0°***	***1.1°***	***1.3°***	***1.4°***	***1.4°***	***1.4°***	***θsht***
		1.4°	1.3°	1.2°	1.0°	0.9°	0.7°	0.6°	0.4°	0.3°	0.1°	0.07°	0.01°	0.001°	θss
Fluvio/tide dominated	8,000m	***0°***	***0.1°***	***0.1°***	***0.2°***	***0.3°***	***0.4°***	***0.4°***	***0.5°***	***0.6°***	***0.6°***	***0.7°***	***0.7°***	***0.7°***	***θsht***
		0.7°	0.6°	0.6°	0.5°	0.4°	0.4°	0.3°	0.2°	0.1°	0.07°	0.04°	0.007°	0.0007°	θss
	16,000m	***0°***	***0.04°***	***0.07°***	***0.1°***	***0.1°***	***0.2°***	***0.2°***	***0.3°***	***0.3°***	***0.3°***	***0.3°***	***0.4°***	***0.4°***	***θsht***
		0.4°	0.3°	0.3°	0.3°	0.2°	0.2°	0.1°	0.1°	0.07°	0.04°	0.02°	0.004°	0.0004°	θss

Conclusions

- The wave-dominated, homogenous shoreface sandstone of the Rannoch-Etive formations comprises a gradual shallowing-up succession and is therefore likely to represent a single progradational event, not punctuated by transgressions.

- The controls on vertical shoreface sand thickness in such deposits are: 1) shoreline trajectory angle, 2) shoreface sand pinch-out depth, and 3) shoreface sand length.
- Using geometries from modern deltas believed to represent good analogues for the Rannoch-Etive formations, it is possible that the anomalously thick shoreface sandstones of the 100 m thick Rannoch-Etive formation could result from progradation with a shoreline trajectory of 2.6-5.4° (implying 80-95 m rise in relative sea level), a 5-12 m deep shoreface sand pinch-out depth, and a 1-2 km shoreface sand length.

Acknowledgement

Tor Sømme (Univ of Bergen) is acknowledged for discussions during preparation of the manuscript. Alf Ryseth, Scott Bullimore, Knut Inge Brendeland and Inge Kaas at Statoil are acknowledged for assisting with data selection and discussions regarding Brent delta stratigraphy.

Chapter 3

Palaeogeography and stratigraphic architecture of stacked shoreface sandstone tongues: Upper Cretaceous Kenilworth Member (Blackhawk Formation), Utah, USA

Kristian Helle and William Helland-Hansen

Abstract

The Campanian Blackhawk Formation (Western Interior foreland basin) was deposited in a ramp setting with wave-dominated shorelines located between the offshore Mancos Shale Formation and an eastwards progradational coastal plain, during a period of overall rising relative sea level.

The Kenilworth Member of the Blackhawk Formation consists of 5 parasequences (K1-K5) that can be divided into 2 main types: 1) long regressive parasequences (K1: 15 km, K4: 25 km) which have a direct down-dip transition from fluvial to open marine deposits (deltaic coasts), and 2) short regressive parasequences (K2: 5 km, K3: 7 km, K5: 4 km) which have lagoon-barrier complexes located between the fluvial and open marine deposits (lagoon-barrier coasts).

The deltaic and lagoon barrier coasts are interpreted as strike equivalent depositional environments. Along the deltaic coasts, the delivery of fluvial sediment was too large for lagoons to develop. Any accommodation created behind the shoreline would immediately have been filled by sediments supplied by the fluvial system. The magnitude of the sediment flux to these areas was also sufficiently large for the K1 and K4 shorelines to prograde 14 km and 25 km into the basin, respectively, implying a major proturberance along the coastline where fluvial channel belts entered. In contrast, along lagoon-barrier coasts, the fluvial sediment supply was not sufficient to fill the accommodation created behind the shoreline, and lagoons developed. The lagoonal barriers were formed and able to prograde a short distance due to deposition of longshore drifted sediments.

The stacking of deltaic and lagoon-barrier coasts suggests that two deltaic shifts, represented by the bases of K1 and K4, exerted a major control on stratigraphic architecture in the member. If applying this model to the Blackhawk Formation as a whole, it consists of six deltaic shifts.

Introduction

Ancient wave-influenced delta systems are common high quality reservoirs throughout the world due to the abundance of well sorted sandstones. An increased understanding of the 3D geometry and stacking pattern of such sandstone bodies and their associated flow barriers within these depositional systems is vital for optimising production strategies in existing hydrocarbon producing reservoirs. Also, enhanced understanding of these issues would improve the ability to predict sand-rich lithologies beyond the extent of data coverage.

The study area is lies within the US Western Cretaceous Seaway and extends for 100 km along the Book Cliffs from Helper to east of Green River in Utah (Fig. 1). These areas comprise one of the best exposed and investigated shallow marine deposits in the world and sequence stratigraphy was partly developed based on studies in these outcrops (e.g. Haq, B. U. *et al.*, 1987; various papers in Wilgus, C. K. *et al.*, 1988; Caldwell, W. G. E. & Kauffman, E. G., 1993; Van Wagoner, J. C. & Bertram, G. T., 1995; and Coe, A. L. *et al.*, 2003). Van Wagoner et al. (1990) used examples from the Book Cliffs stratigraphy to introduce the term 'parasequence' which they defined as a relatively conformable succession of genetically related beds or bedsets bounded by marine flooding surfaces and their correlative surfaces.

Within a parasequence, the cross-sectional migration path of the shoreline through time can be described by the shoreline trajectory (Fig. 2) (Helland-Hansen, W. & Martinsen, O. J., 1996). In regressive nearshore depositional systems, the shoreline trajectory is rising during relative sea level is rise, horizontal during stable relative sea level, and falling acretionary or non-accretionary during falling relative sea level conditions. During transgressions, the shoreline trajectory can either be accretionary or non-accretionary. The shoreline trajectory approach has previously been applied to the study area by Hampson (2000) who interpreted several trajectory trends within a parasequence exposed in the Book Cliffs.

This study mainly focuses on the Kenilworth Member of the Blackhawk Formation and aims to reconstruct the palaeogeography and controls on stratigraphic stacking in the member. The member has previously been described in detail by Balsley (1980), Taylor and Lovell (1995) and Pattison (1995), and their correlation diagrams for the area were used for identifying and tracing parasequences in the field.

Geological framework

The Blackhawk Formation (Campanian) was sourced from the rising Sevier highlands to the west and deposited in the Western Interior foreland basin to the east (Fig. 1a) (Roehler, H. W., 1990; Kauffman, E. G. & Caldwell, W. G. E., 1993). The formation comprises six lithostratigraphic units: Spring Canyon, Aberdeen, Kenilworth, Sunnyside, Grassy and Desert members (Fig 3) (Young, R. G., 1955; Young, R. G., 1957). The members were deposited in a ramp setting with wave-influenced shoreface sands being deposited between the offshore Mancos Shale Formation and an aggradational and progradational coastal plain (Young, R. G., 1955; Young, R. G., 1957; Balsley, J. K., 1980; Swift, D. J. P. *et al.*, 1987; Pattison, S. A. J., 1995; Taylor, D. R. & Lovell, R. W. W., 1995). Overall, the depositional system prograded roughly eastwards during a period of relative sea level rise, resulting in the accumulation of an up to 400 m thick stratigraphic succession (e.g. Pattison, S. A. J., 2005a). The Kenilworth Member was divided by Balsley (1980) and Taylor and Lovell (1995) into 5 littoral sandstone tongues or parasequences, a division which is adopted in this study.

Facies

Five facies and nine subfacies have been recognised on the basis of sedimentary logging of outcrops, where grain size, primary and secondary sedimentary structures, geometry of beds and bed sets have been emphasised, as well as stratigraphic context (Table 1, Figs. 4 and 5). Lateral facies transitions were mapped on foot and with binoculars. For more detailed facies descriptions and interpretations, the reader is referred to Balsley (1980), Kamola (1984) and Van Wagoner et al. (1990).

Table 1 Description and interpretation of facies and subfacies recognised in this study.

Facies	Subfacies	Description	Interpretation
Fluvial plain	Fluvial channel	5-8 m thick bodies of fine and occasionally lower medium grained sandstone with basal erosion evident in places. The sandstones thin out but may extend up to hundreds of metres laterally. Internally, scours and occasional channel geometries up to a few metres deep are evident. The sandstone bodies contain current structures (trough X-lamination, planar X-lamination and current ripples) but they may also be occasionally massive. Lateral accretion surfaces have not been demonstrated. The subfacies is encased in overbank subfacies. **(Figs. 4, 5a)**.	The lateral thinning of the sandstone bodies, the basal erosion evident in places, the presence of current-generated structures and the close relation to the encasing overbank subfacies suggests that this subfacies represents larger fluvial channel belts. The absence of lateral accretion structures, including bank-attached bars, indicates that the channels are largely straight and are likely to represent braided channel belts. These observations and interpretations are consistent with a detailed study of the continental part of the Blackhawk Formation by Adams and Bhattacharya (2005) in Rock Canyon, east of Salina, Utah.
	Overbank	The subfacies consists of carbonaceous sandstone bodies interbedded with 10-70 cm thick, dark coloured, massive, highly carbonaceous mudstone and coal beds. The sandstone bodies fall into 2 categories: 1) laterally accretionary surfaces (2 m high) terminating in channel geometries filled with mud; 2) 30-100 cm thick very fine to fine grained sandstones commonly pinching out in outcrop, bounded by sharp tops and planar to erosive bases. These bodies are mostly sheet like, however; occasionally local channel geometries up to 1 m deep and 10 m wide are present. Ripples and trough X-stratification are present in places. Root traces are common on top of beds. **(Figs. 4, 5b)**	The roots, coal, carbonaceous mudstone and absence of marine bioturbation imply deposition on a coastal plain with a persistent wet environment with standing water and/or mires (Davies, R. *et al.*, 2005). The two types of sand bodies are likely to represent different fluvial related sub-environments: 1) sandstones with lateral accretion terminating in a mud-filled channel imply that the coastal plain had occasional shallow, meandering channels with stable water discharge and associated oxbow lakes; 2) The sheet like sandstone bodies are likely to represent unchannelised and distal parts of crevasse splays. The channel geometries are likely to have been cut by crevasse channels with pulsed water discharge extending from larger fluvial channels and onto overbank areas where the sheet like sandstones were deposited (during floods).
Lagoon	Proximal tidal delta	4-5 m thick very fine to medium grained sandstones containing sedimentary structures as mud-draped current ripples, trough X-stratification, planar X-stratification, herring bone structures and dunes. Palaeo-currents are bi-directional and oriented roughly perpendicular to palaeo-shoreline (i.e. toward E and W). Erosive sedimentary structures as low angle, commonly mud-draped scours and channels are common. Bioturbation is not evident. The subfacies appear up-dip of foreshore subfacies. **(Figs. 4, 5c)**	The up-dip position from foreshore subfacies suggests deposition landwards of the coastline, and the bi-directional palaeocurrents oriented perpendicular to the palaeo-shoreline indicates deposition during both flood and ebb tidal currents. The scouring and channelisation imply high energy currents and the subfacies is interpreted as a proximal tidal delta located near the tidal inlet of a lagoon. The sand-rich intervals were deposited during tidal ebb and floods whereas the mudstone drapes were deposited during slack water.
	Distal tidal delta	3 m thick very fine to fine grained sandstone comprising current ripples, massive or weak planar lamination. Beds are commonly 20-100 cm thick, planar stratified and extend for 10s-100s of m. Palaeo-currents are unidirectional and oriented roughly palaeo-landwards (i.e. toward W). Occasional root traces and commonly high carbonaceous content. The subfacies can be traced laterally into proximal tidal delta subfacies and appears up-dip of foreshore subfacies. **(Figs. 4, 5d)**	The up-dip position from foreshore subfacies suggests deposition landward of the coastline and the landward-directed palaeocurrents imply deposition with flood tidal dominance. The planar stratified beds indicate deposition of sheet-shaped sands where energy level was too low for channelisation. The subfacies is interpreted as a distal tidal delta located immediately landward of the channelised proximal tidal delta subfacies and the associated tidal inlet of the lagoon.
Sandstone tongue	Foreshore	1-3 m thick, fine to medium grained sandstone. Dominating sedimentary structure is plane, parallel lamination. The subfacies appears stratigraphically above and up-dip of upper shoreface subfacies. **(Figs. 4, 5e)**	The plane parallel lamination is interpreted to result from deposition in the swash zone.
	Upper shoreface	1-7 m thick, fine to medium grained sandstone containing current structures (planar X-stratification and trough X-stratification). Palaeocurrents are bi-directional and orientated parallel to palaeocoastline (toward south and north). The subfacies appears stratigraphically above and up-dip from lower shoreface subfacies. **(Figs. 4, 5f)**	The current structures orientated parallel to the palaeocoastline are interpreted as generated by longshore currents set up by waves close to the shoreline.
	Lower shoreface	1-25 m thick, amalgamated very fine to fine grained sandstone dominated by hummocky X-stratification. Marine bioturbation common. The subfacies appear stratigraphically above and up-dip of offshore transition facies. **(Figs. 4, 5g).**	The stratigraphic position and finer grain size compared to upper shoreface subfacies imply a more distal environment for this subfacies. Hummocky X-stratification is generated by oscillating and/or combined flow currents during storms. The absence of fair weather mudstone suggests these were eroded by storms, indicating a depositional environment above storm wave base but below longshore currents.
Offshore transition		Interbedded mudstone and very fine grained sandstone. Mudstone is 1-20 cm thick, intensely bioturbated, dark to light grey and contains vague discontinuous undulating lamination. Sandstone is 1-20 cm thick, bioturbated, has poorly defined upper and lower boundaries and contains occasional current and wave ripples, planar lamination and hummocky X-stratification. **(Figs. 4, 5h)**	The intense bioturbation with alternating sandstone and mudstone suggest a normally quiet environment interrupted by largely non-erosive episodic deposition from combined flows and oscillating currents. The facies is interpreted to reflect a depositional environment with limited excess sand, below reach of storm wave erosion and up-dip of offshore environment.
Offshore		Mainly massive mudstone with faint parallel lamination. Bioturbation is common. **(Figs. 4, 5i)**	This facies is interpreted to have been deposited in areas without excess sand seawards of lower shoreface subfacies. The massiveness makes it difficult to decide if the sediments were affected by wave movement or not.

Parasequences

Two types of nearshore palaeogeographic setting are recognized in the five parasequences (K1-K5) that comprise the Kenilworth Member: 1) deltaic coasts implying a direct down-dip transition from fluvial plain facies to sandstone tongue facies, and 2) lagoon-barrier coasts implying that the fluvial plain facies is separated from the sandstone tongue facies by lagoonal facies.

Along modern sandy, wave-dominated coasts, homogenous shoreline sand is reported to extend down to 5-20 m of water depth (e.g. see van Straaten, L. M. J. U., 1959; Curray, J. R. *et al.*, 1969; Colantoni, P. *et al.*, 1979; Howard, J. D. & Reineck, H.-E., 1981; Bellotti, P. *et al.*, 1994; Diaz, J. I. *et al.*, 1996; Rodriguez, A. B. *et al.*, 2001). Thus within such a framework, sandstone tongue facies resulting from progradation with a horizontal shoreline trajectory (stable sea level), would ideally have a maximum thickness of 20 m. 17 out of 21 (80%) of the sandstone tongues in the Blackhawk Formation have a maximum thicknesses of 20 m or less (Desert Member excluded, data compiled from Kamola, D. L. & Van Wagoner, J. C., 1995; Taylor, D. R. & Lovell, R. W. W., 1995; Taylor, K. G. *et al.*, 2004; Davies, R. *et al.*, 2006). The remaining 20% that have thicknesses exceeding 20 m are therefore regarded as over-thickened and to have been deposited during progradation with a rising shoreline trajectory (rising relative sea level), resulting in vertical stretching of facies belts (Fig. 6).

Kenilworth 1 parasequence

Nearshore palaeogeography: The up-dip termination of the Kenilworth 1 sandstone tongue facies is located approximately 1-2 km west of Kenilworth village (Fig. 7). Here the outcrops are difficult to access, but can be mapped using binoculars; some 10 km up-dip, at the Road Cut locality, the Kenilworth 1 parasequence correlates into fluvial plain facies. Also, Balsley (1980) noted coastal plain deposits in this area, with no indication of lagoons or interdeltaic deposits. The dip facies stacking is therefore likely to be direct from fluvial plain facies to sandstone tongue facies, without the presence of lagoon facies. Consequently, the nearshore palaeogeography is interpreted as representing a deltaic coast, without lagoon-barrier complexes.

Sandstone tongue: The tongue thickens down-dip from its most palaeo-landward exposures, attaining its maximum thickness (29 m) in the Pace Canyon area (Fig. 7). Here, lower shoreface subfacies overlie offshore facies with a sharp, subplanar contact (Fig. 8). From this area, the tongue thins toward the south and pinches out into offshore transition and offshore facies a few kilometres south of Bear Canyon.

Shoreline trajectory: The transgression at the base of the Kenilworth 1 parasequence moved the shoreline palaeo-landward from Coal Canyon to Kenilworth village, a dip distance of 6 km. No landward-thickening continental deposits are present below the retreating shoreline, implying a non-accretionary transgression at the base of the Kenilworth 1 parasequence.

During the regressive phase of the parasequence, the shoreline moved from the Kenilworth village area to Pace Canyon, a dip distance of approximately 25 km. Further, the maximum thickness of the sandstone tongue (29 m) suggests vertical stretching of facies belts and deposition with a rising regressive shoreline trajectory.

Kenilworth 2 parasequence

Nearshore palaeogeography: The up-dip termination of the Kenilworth 2 sandstone tongue facies is located in the Pace Canyon area (Fig. 7) but the outcrop quality here does not allow the nearshore palaeogeography to be defined with confidence. However, in Soldier Canyon, some 9 km up-dip, a well exposed succession of proximal tidal delta subfacies (cf. Table 1) is present (Fig. 9) and the nearshore palaeogeography is therefore interpreted to represent a lagoon-barrier coast.

Sandstone tongue: The tongue thickens down-dip from its most palaeo-landward locations in Pace Canyon, to a maximum thickness of 14 m in the Rock Canyon area (Fig. 7). From here, the tongue thins down-dip and pinches out into offshore transition and offshore facies south of Horse Canyon. This sandstone tongue is time equivalent to the pro-delta deposits at Hatch Mesa (Pattison, S. A. J., 2005d, see below).

Shoreline trajectory: The transgression at the base of the Kenilworth 2 parasequence moved the shoreline less than 1 km landward, without deposition of a landward-thickening continental deposit below. This implies the transgression at the base of the Kenilworth 2 parasequence was non-accretionary.

During the regressive phase of the parasequence, the shoreline moved from south of Pace Canyon to Bear Canyon, a dip distance of approximately 4 km. The parasequence is not associated with incision attributable to falling relative sea level and the presence of lagoonal facies in the nearshore environment suggests a high water table during deposition. Furthermore, no vertical stretching of facies is apparent, either in the continental or the marine part of the parasequence. The Kenilworth 2 is therefore interpreted as having been deposited with a subhorizontal shoreline trajectory.

Kenilworth 3 parasequence

Nearshore palaeogeography: The up-dip termination of the Kenilworth 3 sandstone tongue facies is located in the Pace Canyon area (Fig. 7) but the outcrop quality here prevents certain recognition of the nearshore palaeogeography. However, in Soldier Canyon, a well exposed succession of distal tidal delta subfacies (cf. Table 1) is present (Fig. 9) and the nearshore palaeogeography is therefore interpreted as representing a lagoon-barrier coast.

Sandstone tongue: The tongue thickens down-dip from its most landward positions to a maximum thickness of 16 m at Whitemore Canyon (Fig. 7). From this locality, the tongue thin and pinches out into offshore transition and offshore facies south of Horse Canyon.

Shoreline trajectory: The transgression at the base of the Kenilworth 3 parasequence moved the shoreline approximately 4 km palaeolandward, without deposition of landward-thickening continental deposits below. This implies the transgression at the base of the Kenilworth 3 parasequence was non-accretionary.

During the regressive phase of the parasequence, the shoreline moved approximately 5 km basinward. As for the underlying Kenilworth 3, the Kenilworth 4 parasequence is not associated with incision attributable to falling relative sea level and the presence of a lagoon in the nearshore environment suggest a high water table during deposition. No vertical stretching of facies is apparent either in the continental or marine part of the parasequence, which is therefore interpreted as having been deposited with subhorizontal shoreline trajectory.

Kenilworth 4 parasequence

Nearshore palaeogeography: The up-dip termination of the Kenilworth 4 sandstone tongue facies is located approximately 3 km south of B-Canyon. Here, the facies change is direct from fluvial plain to sandstone tongue facies (cf. Table 1) and does not show evidence of lagoonal facies. The parasequence is therefore interpreted as representing a deltaic coast. The continental part of the parasequence displays topographical relief where areas with major channel belts have stratigraphic thicknesses of up to 13 m (Fig. 9), whereas inter-channel belt areas are typically only 2-3 m thick (Fig. 7). This implies that the sediment surface had some relief during deposition, represented by depressions in the inter-channel belt areas.

Sandstone tongue: The tongue is largely sharp-based and thickens down-dip from its most landward locations to a maximum thickness of 20 m in the Lila Canyon area (Fig. 7). From this locality, the tongue has a roughly even thickness to Middle Mountain (17 m), from where it pinches into offshore transition facies along Gunnison Butte.

Shoreline trajectory: The transgression at the base of the Kenilworth 4 parasequence moved the shoreline less than 1 km landward compared to the underlying parasequence, without deposition of landward thickening continental deposits below. This implies the transgression at the base of the Kenilworth 4 parasequence was non-accretionary.

During the regressive phase of the parasequence, the shoreline prograded approximately 15 km basinwards. The maximum thickness of the sandstone tongue

(20 m) and the preservation of continental strata (up to 13 m, Fig. 9) behind the coast line is interpreted as indicating deposition with a horizontal to slightly rising shoreline trajectory, as opposed to earlier interpretations (see below, Pattison, S. A. J., 1995; Taylor, D. R. & Lovell, R. W. W., 1995; Hampson, G. J., 2000; Howell, J. & Flint, S., 2003).

Kenilworth 5 parasequence

Nearshore palaeogeography: The up-dip termination of the Kenilworth 5 sandstone tongue facies is located between Pace Canyon and Soldier Canyon (Fig. 7). In Soldier Canyon, outcrops reveal proximal tidal delta subfacies (cf. Table 1) and the nearshore palaeogeography is therefore interpreted as representing a lagoon-barrier coast (Fig. 9).

Sandstone tongue: The tongue thickens down-dip from its most landward positions to a maximum thickness of 25 m in Bear Canyon (Fig. 7). From here, the tongue thin and pinches out into offshore transition and offshore deposits approximately 3 km south of B-Canyon. Interestingly, the thickest part of the sandstone tongue partly overlies the inter-channel depression in the Kenilworth 4. This may imply that thicker sandstone tongue development should be expected in areas overlying depressions associated with continental inter-channel belt areas, compared to locations overlying channel belt areas.

Shoreline trajectory: The transgression at the base of the Kenilworth 5 parasequence was accompanied by a landward migration of the shoreline of more than 23 km. The transgression flooded the topographical relief of the underlying sediment surface of the Kenilworth 4 deltaic coast. No landward-thickening continental deposits were observed below and the transgression is therefore believed to have been non-accretionary.

During the regressive phase of the Kenilworth 5 parasequence, the shoreline prograded approximately 5 km basinwards. The maximum thickness of the sandstone tongue (25 m) is likely a result of vertical stretching of facies belts and deposition with a rising regressive shoreline trajectory. Also, when the maximum flooding surface above the Kenilworth 5 is used as a horizontal datum, it is evident that the parasequence prograded with a rising shoreline trajectory (Fig. 11 in Taylor and Lovell (1995)).

Regional palaeogeography

Both Kenilworth 1 and 5 have inferred *rising* regressive shoreline trajectories (Table 2); however, of these it is only Kenilworth 5 which is associated with a lagoon-barrier complex. Further, both Kenilworth 2 and 4 have inferred *sub-horizontal* shoreline trajectories, but only Kenilworth 2 is associated with a lagoon-barrier complex. This suggests that the angle of the regressive shoreline trajectory is not necessarily related to the type of nearshore palaeogeography. Moreover, the Kenilworth 3 transgression moved the shoreline just 4 km up-dip whereas the Kenilworth 5 transgression moved the coastline 23 km up-dip, though both these parasequences are associated with a lagoon-barrier complex. This suggests that the transgressive distance was not associated with a particular type of nearshore palaeogeography.

However, the lagoon-barrier coasts are associated with parasequences displaying short regressive distances, whereas parasequences with long regressive distances are associated with deltaic coasts (Table 2). This may be interpreted in terms of the fluvial sediment flux to the areas with *long* regressive distances being too large for lagoons to develop. Any accommodation generated behind the shoreline due to a rise in relative sea level would immediately be filled by sediments supplied by the fluvial system. The sediment supply to these areas was actually sufficient for the shoreline to prograde 14 and 25 km during deposition of Kenilworth 1 and 4, respectively (Table 2).

Table 2 Overview of sandstone tongue properties. Two types of nearshore palaeogeographies are recognised: deltaic coasts and lagoon-barrier coasts. The type of palaeogeography seems to be related to the regressive distance. Short regressive distances are 4-5 km whereas long regressive distances are 15-25 km. This implies a seawards protuberance of approximately 10-20 km at deltaic coasts compared to lagoon-barrier coasts, when the delta is at its most regressive position (see text). Aberdeen and Sunnyside data taken from Balsley (1980) and Kamola and Huntoon (1995).

Parasequence	**Maximum thickness of sandstone tongue (m)**	**Inferred regressive trajectory angle**	**Observed distance of transgressive shoreline migration at parasequence base (km)**	**Distance of regressive shoreline migration (km)**	**Nearshore palaeogeography**	**Channel shift and associated shift in delta lobe position**	**Inferred delta lobe stacking (compared to underlying lobe)**	**Deltaic cycle**
Sunnyside 1	-	-	-	15	-	**V**	**Strike and back-stepping**	
Kenilworth 5	25	Rising	23	5	Lagoon-barrier	**IV**	**Strike-stepping**	**B**
Kenilworth 4	20	Horizontal to gently rising	<1	15	Deltaic	**III**	**Strike-stepping**	
Kenilworth 3	16	Sub-horizontal	4	5	Lagoon-barrier	**II**	**Strike and basin-stepping**	**A**
Kenilworth 2	14	Sub-horizontal	<1	4	Lagoon-barrier			
Kenilworth 1	29	Rising	6	25	Deltaic	**I**	**Strike-stepping**	
Aberdeen 4-5	-	-	-	c. 3-6	-	-	-	-

In contrast, for parasequences with *short* regressive distances and associated lagoon-barrier coasts, the fluvial sediment supply was insufficient to fill the accommodation created behind the shoreline which formed as a response to a local or regional rise in relative sea level, leaving these areas occupied by lagoons. Furthermore, the lagoonal barrier bars themselves were able to prograde a few kilometres, due to the sediments supplied by longshore drift. The source of these sediments was presumably the areas where major channel belt outlets supplied large amounts of sand to the marine realm (i.e. deltaic coasts).

This study therefore proposes that the deltaic coasts and lagoon-barrier coasts represent genetically linked and strike equivalent depositional sub-environments. Fluvial sediments supplied along the deltaic coasts were drifted by longshore currents to time equivalent lagoon-barrier coasts located some distance along depositional strike. Hence, the difference in continental and longshore sediment supply between deltaic and lagoon-barrier coasts was probably related to the distance from the major fluvial channel belts (Fig. 10a,b).

To connect the coastline between areas with short and long regressive distances, the coastline must have had major seaward protuberances along the deltaic coasts, where the outlets of the main channel belts were located. In the most regressive positions of the parasequences, these deltaic protuberances are likely to have extended seawards of the lagoon-barrier coasts for distances approximately equalling the difference in regressive distance of the two, i.e. 10-20 km (Table 2).

Unfortunately, lateral outcrop control does not allow direct observation of this inferred strike variability. The lagoon-barrier coast of Kenilworth 2, however, is time equivalent to the wave-influenced pro-delta deposits at Kenilworth 2 level exposed at Hatch Mesa (Pattison, S. A. J., 2005a). This is taken to indicate that the Kenilworth 2 shoreline had a major protuberance (10-20 km) in the area due to the presence of major channel belt outlets (not preserved) located some distance up-dip of Hatch Mesa.

Such a curved coastline can be indicative of an asymmetric or symmetric delta (sensu Bhattacharya, J. P. & Giosan, L., 2003). An *asymmetric delta* develops where the groin effect at the river mouth reduces the amount of longshore drift on the down-drift side of the river outlet compared to the up-drift side. The down-drift side therefore receives less sediments and progrades slower, causing the formation of a curved coastline. Lagoon-barrier complexes tend to form in these low sediment supply areas (Fig. 10a), as described from the Danube delta by Bhattacharya and Giosan (2003). An asymmetric delta construction has been proposed from other places in the Cretaceous Interior Seaway; a reinterpretation of McCubbin's (1982) work on the Gallup Sandstones by Bhattacharya and Giosan (2003) proposes an asymmetric delta with the strand plains formed on the up-drift side of main channel belt outlets (their Fig. 12).

In a *symmetric delta*, the lagoons would have been present on both sides and at some distance from the main channel belt (Fig. 10b). The sediments dumped at the river mouths would in such a model have been transported along the Kenilworth coastlines by longshore currents with successively lower rates of deposition away from the river outlet, resulting in a protuberance of the coastline. Due to the minor amount of fluvial related facies such as mouth bars and prodelta deposits evident in the sandstone tongues facies, it is likely that wave reworking largely overprinted the potential evidence of fluvially generated structures.

The top of the Kenilworth 4 sandstone tongue is frequently cut by fluvial channels along its exposure in Book Cliffs (Fig. 7) (Pattison, S. A. J., 1995; Taylor, D. R. & Lovell, R. W. W., 1995). This suggests that the main sediment transport to the coastline was *along the top* of sandstone tongues (Fig. 10b) with long regressive distances, and not immediately down drift of these as predicted in the asymmetric model (Fig. 10a). This is compatible with a symmetric model, but not with an asymmetric one, so a symmetric delta lobe model is therefore proposed in this study (Fig. 10b).

The palaeogeographic reconstruction of the Kenilworth coastlines can be illustrated by the modern Rosetta Lobe in the Nile delta (Fig. 11). This symmetric deltaic coast has prograded no less than 14 km the last 2 ka, but is now being transgressed, partly due to the building of the Aswan Dam in 1964 (Sestini, G., 1989). Also, the lagoon-barrier complex at Galveston island has prograded c. 4 km the last 3.5 ka (Friedman, G. M. *et al.*, 1992). The above implies that the progradational distances of the deltaic and lagoon-barrier coasts in the Kenilworth Member are realistic within a modern framework (cf. Table 2).

The delta lobe model outlined above contrasts with previous studies which interpret the Blackhawk Formation lagoons as transgressive features (Fig. 12) (Kamola, D. L. & Van Wagoner, J. C., 1995; Howell, J. & Flint, S., 2003; Hampson, G. J. & Howell, J. A., 2005): During stable relative sea level, they interpreted that the delta system moves seawards as a linear coastline without lagoons (Fig. 12a). When a rise in relative sea level commences and terminates the regression, the shoreline is transgressed and the nearshore environment is transformed into a linear lagoon-barrier coast. When rise in relative sea level slows down or stops, the lagoons start to infill with sediment delivered from the fluvial systems, tidal inlets and wash over fans (Fig. 12b). Once the lagoons are filled, they suggest that fluvial channels break through to the coastline, initiating a renewed phase of shoreline progradation (Fig. 12c). In their model, parasequences with different regressive distances would not be strike equivalent depositional environments, but indicative of how far the individual parasequences were able to prograde into the basin before being transgressed

(Kamola, D. L. & Van Wagoner, J. C., 1995; Howell, J. & Flint, S., 2003; Hampson, G. J. & Howell, J. A., 2005).

Stratigraphic architecture

The parasequences in the Kenilworth Member are bounded by flooding surfaces of varying dip-directed length which punctuated the overall regression of the delta system within the study area (Table 2). Three categories of flooding surfaces can be identified: type 1) minor flooding surfaces related to local scale variability in the accommodation/sediment supply ratio (top Kenilworth 2 and 3), e.g. formed as a result of changes in channel outlet position reducing the amount of longshore drift along lagoon-barrier coasts (cf. Hampson, G. J., 2000; Sømme, T. *et al.*, in press); type 2) flooding surfaces related to the abandonment and subsidence of individual delta lobes (top Kenilworth 1 and 4); and type 3) major flooding surfaces related to accommodation outpacing sediment supply on a regional scale causing backstepping of the entire delta system (top Kenilworth 5).

In total, four major strike-directed shifts (10s to 100s of km) in position of main channel belt outlets and associated delta lobe positions are inferred in the Kenilworth Member, and have been interpreted as two deltaic cycles (Table 2).

Deltaic cycle A (Figs. 13a,b): The Kenilworth 1 delta lobe is underlain by the short (<6 km) regressive parasequences of the upper Aberdeen Member (Kamola, D. L. & Huntoon, J. E., 1995). This implies that the onset of deposition of the Kenilworth Member was associated with the main channel belt outlets shifting into the study area from the north or south (channel shift I), in turn causing the strike-stepping of the Kenilworth 1 delta lobe (cf. Table 2).

As the Kenilworth 1 delta lobe is overlain by the lagoon-barrier complexes of Kenilworth 2-3, the main channel belts and the associated delta lobe must have shifted away to north and/or south of the study area at the onset Kenilworth 2 deposition (channel shift II, Table 2). Furthermore, the flooding surface which marks the abandonment of the Kenilworth 1 delta lobe is short, and since the delta lobes are inferred to have major seawards curvature, the Kenilworth 2-3 delta lobes are likely to be basinward-stepping, as well as strike-stepping with respect to the underlying Kenilworth 1 lobe (cf. Table 2). The Kenilworth 2-3 channel belts may have shifted in response to over-extension of the Kenilworth 1 fluvial system and have re-established in the embayment inferred to be located south of the Kenilworth 1 lobe as this area may have represented a shorter and steeper courses to the sea (e.g. see Scruton, P. C., 1960; Elliott, T., 1986a).

As the flooding surfaces at the base of Kenilworth 2 and 3 are short, the parasequences reflect the same nearshore palaeogeography (Table 2) and are stacked as a basinward stepping parasequences (Fig. 7), they are interpreted as type 1 flooding surfaces (see above).

Deltaic cycle B (Fig. 13c,d): The onset of Kenilworth 4 deposition represents a delta lobe shifting back into the Book Cliffs area (channel shift III), causing the shoreline to migrate 15 km basinwards. Possibly there were Kenilworth 4 lagoon-barrier complexes located to the north and south of Book Cliffs.

Following maximum regression, the Kenilworth 4 delta lobe was flooded and overlain by the Kenilworth 5 lagoon-barrier complex (Table 2). The length of the flooding surface (23 km) roughly equals the maximum expected curvature along the coastline (20 km), so the flooding is believed to relate to the abandonment and subsidence of the Kenilworth 4 lobe (channel shift IV, type 2 flooding surface). The abandonment was probably caused by a northwards or southwards shift of the channel belts, and the inferred Kenilworth 5 delta lobe is therefore likely to be strike-stepping. This is also supported by the fact that Kenilworth 2, 3 and 5 lagoon-barrier complexes are largely vertically stacked (Fig. 7), suggesting that at this stage (K2-K5) there was no major dip-directed movement of lagoonal depositional environments.

The Kenilworth 5 lagoon-barrier complex is separated from the overlying long regressive deltaic coast of the Sunnyside 1 parasequence (S1) delta lobe by a 15 km flooding surface (cf. Table 2) (Balsley, J. K., 1980). This indicates that Kenilworth Member (and deltaic cycle 2) deposition was terminated by a backstepping and strike-stepping delta shift (channel shift V). It is likely that this backstepping was caused by accommodation outpacing sediment supply on a regional scale (type 3 flooding surface).

Deltaic cycle stacking pattern (Fig 13e): As outlined above, the onset of deposition of Kenilworth Member is marked by the strike-stepping of the Kenilworth 1 delta lobe. The onset of Kenilworth 2 and 3 deposition represents strike and basinward-stepping delta lobes whereas the Kenilworth 4 and 5 delta lobes are solely strike-stepping. This further implies that the bay line (defined as the demarcation line between fluvial environments appearing above sea level and paralic/delta plain environments (Posamentier, H. W. *et al.*, 1988)) moved seawards from Kenilworth 1 to 2, but then was stationary during deposition of Kenilworth 2-5. This suggest that the lobes are stacked as compensation style architecture, where embayments located between deltaic lobes were successively created and filled by strike directed movement of deltaic proturberances (caused by channel avulsion). The Kenilworth Member deposition was terminated by a regional flooding causing the delta system to strike and back-step which marks the onset Sunnyside Member deposition.

Interestingly, the bases of the two deltaic cycles (i.e. base Kenilworth 1 and 4) are accompanied by sharp-based sandstone tongues (Fig. 8). This is interpreted as a result of delta lobes abruptly being starved by fluvial avulsion causing river outlets to re-establishin other areas and suddenly introduce sand into previously mud-dominated parts of the nearshore environment (such as embayments in inter-lobe areas), resulting in homogenous sand overlying offshore mud with a sharp contact. The fluvial avulsion may have been caused by the increasing curvature along the delta lobes leading to over-extension of the fluvial system which responded by choosing shorter and steeper courses to the sea (e.g. see Scruton, P. C., 1960; Elliott, T., 1986a) (see more detailed discussion below).

Previous sequence stratigraphic models

In the first sequence stratigraphic analysis of the Kenilworth Member, Taylor and Lovell (1991; 1995) indicated 5 parasequences (Fig. 14a). In their model, parasequences 1-4 comprise a highstand systems tract truncated by a sequence boundary associated with a lowstand system tract, whereas parasequence 5 represents a transgressive systems tract. This model predicts that detached lowstand deposits associated with the sequence boundary are present further basinward.

In contrast, Pattison's (1995) model comprises 9 parasequences for the same stratigraphic succession. He divided the Kenilworth 4 sandstone body of Taylor and Lovell (1995) into 3 units (his parasequences 6, 7 and 8), arguing that parasequence 6 comprises highstand deposits whereas the latter two are attached lowstand deposits. Pattison (1995) further indicated that 2 sequence boundaries, SB1 and SB2, run through the sandstone body and corresponds to the bases of parasequences 7 and 8, respectively, and furthermore that these parasequences were separated by a surface created during a sea level stillstand that punctuated an overall relative sea level fall (Fig. 14b). This model does not predict detached lowstand shorelines further basinwards and interprets the uppermost parasequence (parasequence 9) to represents a transgressive systems tract. The numbering of the parasequences and sequence boundaries was adjusted by Pattison (2005a) to fit a 5 fold division.

Later, Howell and Flint (2003) combined the above models and suggested that the Kenilworth Member should be divided into 6 parasequences (Fig. 14c). They argued that the Kenilworth 4 sandstone body of Taylor and Lovell (1995) should be divided into 2 (their parasequences 4 and 5) separated by a sequence boundary corresponding to SB1 of Pattison (1995). As with Taylor and Lovell's (1991; 1995) model, Howell and Flint (2003) predicts the presence of detached lowstand shorelines further out in the basin, and the uppermost parasequence is interpreted as representing a transgressive systems tract.

Revised sequence stratigraphic model

Based on the interpreted parasequence stacking pattern in this study (Table 2, Fig 13e), parasequence 5 is regarded as strike-stepping rather than back-stepping. The parasequence is therefore assigned to the highstand systems tract, instead of the transgressive systems tract as previous studies propose (Pattison, S. A. J., 1995; Taylor, D. R. & Lovell, R. W. W., 1995; Howell, J. & Flint, S., 2003). The revised model therefore regards the entire Kenilworth Member to represent highstand systems tract deposits, which is overlain by the transgressive systems tract of the Sunnyside 1 parasequence (Fig 14d). This implies that the sequence boundary and the associated lowstand systems tract previously proposed for the Kenilworth 4 parasequence (Ainsworth, R. B. & Pattison, S. A. J., 1994; Pattison, S. A. J., 1995; Taylor, D. R. & Lovell, R. W. W., 1995; Hampson, G. J., 2000; Howell, J. & Flint, S., 2003) are not recognised.

The rejection of the sequence boundary is based on the following observations: 1) the equally thick or thicker development of the continental part of the Kenilworth 4 parasequence compared to the Kenilworth 2, 3 and 5 parasequences, which indicate absence of incision relatable to falling relative sea level in the terrestrial environment during Kenilworth 4 deposition (cf. Figs. 7, 9). 2) The lack of continental red beds related to Kenilworth 4 parasequence which suggest high water-table during deposition. 3) The channel geometries in Kenilworth 4 belong to the fluvial plain facies (cf. Table 1) and do not display abnormal channel dimensions or sedimentary structures attributable to a fall in relative sea level. 4) Detailed field work along the Book Cliffs was unable to detect localities where Kenilworth 4 fluvial channels truncate the underlying Kenilworth 3 parasequence (in contrast to the studies by Pattison, S. A. J., 1995; Taylor, D. R. & Lovell, R. W. W., 1995; Howell, J. & Flint, S., 2003). 4) The vertically stacked successions of offshore-offshore transition facies evident in front of the delta (in the vincinity of Gunnison Butte), display gradually shallowing parasequences that lack evidence of basinward downstep in facies (Fig 7). 5) The sharp-based shoreface may be related to autogenic delta lobe shifts rather than falling relative sea level.

Regarding the latter point, this study propose that sharp-based sandstone tongues may result from channel belt avulsion that lead to a sudden introduction of large amounts of sand into a previously mud-dominated shallow marine environment. In modern wave/fluvial-dominated deltas, for example the Ebro delta in Spain, homogenous shoreline sand extends almost 8 km seaward in front of river outlets, whereas it only extends 2 km seaward between river outlets (Diaz, J. I. *et al.*, 1996). During channel belt avulsion and consequent shift in delta lobe position, the homogenous shoreline sand would therefore be expected to step basinward up to 6 km and introduce sand to areas previously dominated by deposition of offshore transition or offshore facies. Such a sequence of events could account for the genesis of the sharp-based sandstone tongues in Kenilworth Member. If the storm wave base is deeper than the pinch-out depth of homogenous shoreline sand, it is likely that the fluvially related sedimentary structures will be overprinted by wave-generated structures. This may result in lower shoreface subfacies being recorded in the stratigraphic succession as directly overlying offshore facies.

It follows from the above that using forced regression as the standard interpretation for basinward-stepping, sharp-based, shallow marine sandstone tongues might result in erroneous prediction of down-dip attached or detached lowstand shallow marine sandstones. Predicting the presence of another sand-rich deltaic lobe located some distance along strike might be equally valid. The present model demonstrates that sharp-based sandstone facies may appear in normal regressive deltas, in contrast with previous interpretations that indicates that they normally are related to falls in sea level (e.g. Plint, A. G., 1988; Van Wagoner, J. C. *et al.*, 1991; Posamentier, H. W. *et al.*, 1992; Ainsworth, R. B. & Pattison, S. A. J., 1994; Pattison, S. A. J., 1995)

Implication for Blackhawk Formation cyclicity

As outlined above, this study proposes that lagoon-barrier coasts are strike equivalent to deltaic coasts, and that the coastline had major protuberance. Even though this study only presents data from Kenilworth Member, some tentative suggestions may be made for the rest of the Blackhawk Formation. For example, Grassy Member and parts of Spring Canyon Member consist of stacked lagoon-barrier complexes with short regressive distances (Kamola, D. L. & Van Wagoner, J. C., 1995; O'Byrne, C. J. & Flint, S., 1995). Applying the model for Kenilworth Member, this may imply that these complexes are strike equivalent to deltaic coasts with long regressive distances (not preserved/exposed). On the other hand, the Sunnyside and Desert members display long regressive distances (Balsley, J. K., 1980), and might therefore be strike equivalent to lagoon-barrier complexes with short regressive distances (not preserved/exposed).

Overall, the Blackhawk Formation comprises 6 parasequences/progradationally stacked parasequence sets with long regressive distances that are separated by 5 parasequences/parasequence sets with short regressive distances (Table 3). Each of the stratigraphic intervals comprising long distance regressions are interpreted as the result of major channel belt outlets being located in the study area during those time intervals, forcing the shoreline to migrate seawards.

The deltaic progradations consisting of a *single* parasequence represent individual deltaic advances (not punctuated by type 1 flooding events), eventually terminated by river avulision and subsequent creation of a type 2 flooding surface (Table 3). In contrast, the deltaic progradations which comprise parasequence *sets* experienced multiple higher frequency transgressions (type 1) superimposed on the overall regression, without major shifts in position of the feeder fluvial channel belts. Eventually, the punctuated advance was ended by channel avulsion and a type 2 flooding surface was created. As for the Kenilworth Member, it is proposed for the entire Blackhawk Formation that the long regressive parasequences/parasequence sets are stacked in compensation style architecture due to overextension of the fluvial system (see above and Scruton, P. C., 1960; Elliott, T., 1986a).

Based on this, the Blackhawk Formation stratigraphy can be organised into 6 deltaic cycles which commence and terminate with a change from parasequences/parasequence sets with long regressive distance to ones with short regressive distances (Table 3). Each of these cycles represents major channel belt outlets shifting into, and then away from, the study area.

Superimposed on these shifts in position of channel belt outlets, relative sea level rise occasionally outpaced sediment supply and caused the delta system to be flooded (type 3 flooding surface) and to backstep (e.g. at top Kenilworth Member). Also superimposed on the deltaic cycles are some candidate and documented sequence boundaries. Interestingly, these sequence boundaries do not correlate well with the bases of the deltaic cycles (Table 3), indicating sediment supply was so high that it largely overruled falling relative sea level in controlling the timing of regression. However, it is uncertain whether the presented palaeogeographic model (Fig. 9b) can be applied to periods with falling relative sea level conditions as these are likely to be associated with low water table, possibly not favouring the development of lagoons.

As with the Kenilworth Member, lateral outcrop control does not allow direct observation of this inferred strike variability in the Blackhawk Formation. At the upper Aberdeen level in the vicinity of Gunnison Butte, however, Pattison (2005c; 2007) reported subaqueous channel geometries which he interpreted as representing conduits for high and low density turbulent underflows from the delta front into the prodelta region. The strike equivalent deposits of these underflow deposits are exposed in the Price area (Pattison, S. A. J., 2005b) some 60 km to the north, in an area where upper Aberdeen strata display short regressive parasequences (Table 3) (Kamola, D. L. & Huntoon, J. E., 1995). This may imply that there was a deltaic protuberance west of the Gunnison Butte vicinity. The areas to the north in the Price area would then represent an embayment with short regressive distances (observed) and an associated lagoon-barrier coast.

In contrast, Kamola and Huntoon (1995) interpreted the repetitive stacking pattern in the Blackhawk Formation to result from repeated thrusting cycles in the Sevier highlands and associated changing rates of rise in relative sea level in the foreland basin. The main transgressions, according to their model, would correlate with the episodes of greatest thrust-sheet movement, while tectonically quiescent periods would correlate with parasequence progradation (Kamola, D. L. & Huntoon, J. E., 1995). The larger transgressions in the Blackhawk Formation were probably caused by the rise in regional relative sea level outpacing sediment supply, since the shoreline moved landwards further than would be expected solely from strike directed shifts in channel belt outlets and associated lagoon-barrier coasts (i.e. c. 20 km). Flooding surfaces up to about 20 km long, however, may be attributed to autogenic deltaic lobe shifts rather than backstepping of the entire delta system.

Table 3 Model for Blackhawk Formation cyclicity. Each cycle commences and terminates with a change from parasequences/parasequence sets with short regressive distance to parasequences/parasequence sets with long regressive distances (grey shading). Sequence boundaries mostly do not correspond with these shifts in channel belt outlets, suggesting sediment supply overruled relative sea level ability to become the main control on stratigraphic architecture. Sandstone tongue thicknesses in bold indicate inferred over-thickened successions (i.e. >20m).

Member	Para-sequence	Sandstone tongue thickness (m)	Regressive distance (km)	**Deltaic cycle**	**Sequence (this study)**	Sequence (all studies)	Reference
Desert	D2	?	Long	**6**	**5**	9	(Balsley, J. K., 1980; Van Wagoner, J. C. *et al.*, 1991)
	D1	?	Long		**4**	8	
Grassy	G4	A few m	Short	**5**	**3**	7	(O'Byrne, C. J. & Flint, S., 1995)
	G3	A few m	Short				
	G2	12	8 (short)			6	
	G1	20	11 (?short)				
Sunnyside	S3	**22**	23 (long)		**2**	5	(Balsley, J. K., 1980; Howell, J. & Flint, S., 2003; Davies, R. *et al.*, 2006; Sømme, T. *et al.*, in press)
	S2	**30**	26 (long)		**1**	4	
	S1	12	17 (long)				
Kenilworth	K5	**25**	4 (short)	**4**			(This study, Pattison, S. A. J., 1995; Taylor, D. R. & Lovell, R. W. W., 1995)
	K4	20	15 (long)			3	
	K3	16	5 (short)	**3**			
	K2	14	5 (short)				
	K1	**29**	25 (long)				
Aberdeen	A5	8	?	**2**		2	(Balsley, J. K., 1980; Kamola, D. L. & Huntoon, J. E., 1995; Taylor, K. G. *et al.*, 2004)
	A4	3	3-6 (short)				
	A3	5	short				
	A2	8	12 (long)				
	A1	10	23 (long)			1	
Spring Canyon	SC7	13 (min)	2 (short)	**1**			(Kamola, D. L. & Van Wagoner, J. C., 1995); (Kamola, D. L. & Huntoon, J. E., 1995); *(Hampson, G. J. & Storms, J. E. A., 2003)
	SC6	5 (min)	1 (short)				
	SC5	9	4 (short)				
	SC4	11	13 (21*) (long)				

Conclusions

- The entire Kenilworth Member represents a highstand systems tract overlain by a transgressive systems tract.
- Correlation between shoreline trajectory angle and facies architecture could not be established. However, *long regressive distances* are associated with deltaic coasts, whereas *short regressive distances* are associated with lagoon-barrier coasts. These two nearshore sub-environments are interpreted as strike equivalent and the delta is likely to have had major protuberances, with lagoon-barrier coasts located some distance along strike on both sides.
- Kenilworth Member comprises two parasequences with long regressive distances corresponding to two major shifts in channel belt outlets and associated delta lobes. The lobes are stacked as compensation style architecture, where embayments located between deltaic lobes were successively created and filled by strike directed movement of deltaic proturberances (caused by channel avulsion).
- Overall, the Blackhawk Formation comprises 6 parasequences/parasequence sets with long regressive distances separated by parasequences/parasequence sets with short regressive distances. These correspond to 6 shifts in channel belt outlets. The shifts are not contemporaneous with the sequence boundaries in the Blackhawk Formation, which indicates that sea level falls were a less important control on stratigraphic architecture in the basin than has been assumed in the existing models.
- Sharp-based shorefaces do not necessarily need to be the result of fall in relative sea level but can be formed in normal regressive delta systems by channel avulsion causing sudden introduction of sand into a previously mud dominated environment.

Acknowledgements

This study has been funded by VISTA (www.vista.no) which is Statoil's basic research program conducted in close collaboration with the Norwegian Academy of Science and Letters. John Howell and Simon Pattison are thanked for introducing the field area. Ragnhild Granberg, Andreas Olsen, Britta Paasch, and in particular Tor Sømme are acknowledged for assistance in the field and discussions regarding the Blackhawk stratigraphy.

Chapter 4

The effect of clinoform growth pattern on shelf margin stability and palaeogeographic evolution: the Pleistocene Columbus Basin and Deltana Amacuro Platform, offshore Venezuela

Kristian Helle, Rune Kyrkjebø, Sverre Henriksen, William Helland-Hansen, and Britta Paasch.

Abstract

The palaeo-Orinoco delta and shelf edge regressed axially in the foredeep of the Eastern Venezuelan Basin and were associated with deposition influenced by a successively increasing rise in relative sea level toward the thrust front. The area therefore enables comparison between the sedimentary and tectonic processes active when prograding during a rapidly rising relative sea level (close to the thrust front, Columbus Basin), and a more slowly rising relative sea level (further south, Deltana Amacuro Platform). The two areas developed in very different ways as the Columbus Basin experienced abundant synsedimentary deformation (shelf edge failures cutting up to 100 m deep, and large scale growth faulting cutting 1000s of m deep) whereas the Deltana Amacuro Platform remained largely tectonically inactive.

The various types of synsedimentary deformation observed in the study area are interpreted as representing processes successively activated and/or terminated when prograding toward successively increasing rates and amounts of rise in relative sea level: 1) Progradation during slowly rising relative sea level is likely to be assocated with only minor shelf edge failures (graded-margin progradation), 2) as rate of rise in relative sea level increases, major shelf edge collapse-healing cycles are likely to develop due to the effect of increased loading along the upper slope (erosive-margin progradation), and 3) if amount of rise in relative sea level is sufficient, major growth faulting will develop in an attempt to lower the gravitational potential that was buildt up along with the successively increasing size of the shelf-slope-basin floor clinoform (collapse-margin progradation).

The growth faulting created large amounts of accommodation on the topset which trapped so much sediment that it prevented the margin from further progradation. This implies that prograding clinoforms have a maximum size that is limited by the sediment shear strength and the gravitational potential of a clinoform.

Introduction

Prograding continental margins that are located in areas where major delta systems enter the ocean are commonly associated with gravity-driven deformation, typically expressed by growth faults, folds, shelf edge failures and diapirism (e.g. Winker, C. D. & Edwards, M. B., 1981; Galloway, W. E., 1986; Rowan, M. G. *et al.*, 2004). Such areas are of considerable economic interest due to the significant amount of sand supplied by the fluvial system, and the abundance of potential hydrocarbon traps formed by the gravity tectonics.

The main control on stratigraphic architecture in these deposits is interplay between shorter term depositional processes occurring on a daily-10 ka basis, and longer term processes such as the build-up of regional stress regimes which may take several million years. Examples of the former are pelagic/hemipelagic fallout, episodic down-slope transport of sediments by turbidity currents or slumps, changing paths of ocean currents (e.g. Stow, D. A. V. *et al.*, 1996) or deltas shifting position between inner shelf and shelf edge (e.g. Steel, R. J. & Olsen, T., 2002). The latter can be the result of loading of offshore shales under the weight of 1000s of metres of deltaic sediments, resulting in diapirism (e.g. Wood, L. J., 2000), or the building of gravitational potential along a clinoform as it increases in size with time. As these different scaled mechanisms interact, the resulting stratigraphic architecture may be highly complex; hence it is vital to understand the interplay between sedimentary processes and gravity tectonics for the purpose of predicting the occurrences and volumes of hydrocarbon bearing lithological units.

In general, gravity tectonics can be divided into three principle types: gravity gliding, gravity spreading and diapirism (Ramberg, H., 1981). *Diapirism* results from movement of a buoyant layer into an overlying relatively higher density overburden. *Gravity gliding* (Fig. 1a) is strictly defined as the rigid translation of a body down a slope, with displacement vectors parallel to the detachment plane, whereas *gravity spreading* is the vertical collapse and lateral spreading of a rock mass under gravity because of a sloping upper surface (Fig. 1b) (DeJong, K. A. & Scholten, R., 1973; Ramberg, H., 1981). Even if gravity gliding and gravity spreading represent different mechanisms they may be difficult to distinguish (Schultz-Ela, D. D., 2001), and gravity failure commonly occurs as a combination of the two (Fig. 1c) (Rowan, M. G. *et al.*, 2004).

In the stratigraphic record, prograding deltas and continental margins can be described by using trajectory analysis (see below) (Helland-Hansen, W. & Martinsen, O. J., 1996; Steel, R. J. *et al.*, 2000). Individual deltaic advances across the shelf to the shelf edge can be identified by using the shoreline trajectory; the progradation of the entire margin can be revealed by applying the shelf edge trajectory. Combining the shelf edge and base-of-slope trajectories (below) allows one to describe the overall geometric evolution of a continental margin clinoform (i.e. if the clinoform is increasing or decreasing in size with time). Based on the latter it is further possible to describe the build-up or reduction of gravitational potential along the clinoform with time. The trajectory approach therefore provides a useful tool to investigate the relations between depositional processes and gravity tectonics along a prograding margin.

Trajectory Analysis

Shoreline trajectory: The shoreline trajectory is defined as the cross-sectional migration path of the shoreline through time (Fig. 2) (Helland-Hansen, W. & Gjelberg, J. G., 1994; Helland-Hansen, W., 1995; Helland-Hansen, W. & Martinsen, O. J., 1996). The angle of the trajectory is controlled by sediment supply, relative sea level change and basin physiography, and the concept allows the sum of these variables to be viewed as a continuous spectrum. There are two main categories of shoreline trajectory: transgressive and regressive. The transgressive trajectories can further be divided into accretionary and non-accretionary, whereas the regressive trajectories can be divided into normal regressive, sub-horizontal, accretionary forced regressive, and non-accretionary forced regressive (Fig. 2). Since the introduction of the concept it has been applied to depositional systems by several authors (e.g. Mellere, D. & Steel, R., 1995b; Hampson, G. J., 2000; Bhattacharya, J. P. & Willis, B. J., 2001; Crabaugh, J. P., 2003; Hampson, G. J. & Storms, J. E. A., 2003; Løseth, T. M. *et al.*, 2006).

Shelf edge trajectory: The shelf edge trajectory concept (Steel, R. J. *et al.*, 2000) is based on the same principles as outlined by Helland-Hansen and Gjelberg (1994), but is defined as the cross-sectional migration path of the shelf edge through time (Fig. 3). A notable difference between the shoreline trajectory and shelf edge trajectory concepts is that the former is applied to shoreface clinoforms (metres to 10s of metres high) whereas the latter is applied to shelf-slope-basin floor scale clinoforms (100-a couple of 1000s of metres high). The shelf edge trajectory can be used as a reliable indicator for long term relative sea level fluctuations; falling, flat and rising shelf edge trajectories represent periods with falling, stable and rising relative sea level, respectively (Fig. 3). The shelf edge trajectory trends can then provide a framework to which different depositional environments can be related.

Subsequent to the introduction of the shelf edge trajectory concept, Steel and Olsen (2002) used it to suggest that the formation of significant basin floor fans is associated with flat or falling shelf edge trajectories, while Porebski and Steel (2003) related varying shelf edge delta architectures to different shelf edge trajectory trends (their Fig. 11). The concept has also been applied in other studies (e.g. Mellere, D. *et al.*, 2002; Plink-Björklund, P. & Steel, R., 2002; Carvajal, C. R. & Steel, R. J., 2006).

Base of slope trajectory: The shelf edge trajectory concept does not directly include the depositional system's response to processes located seaward of the shelf edge (Fig 3). We can thus capture these effects by means of the base-of-slope trajectory (partly based on Helland-Hansen, W. & Martinsen, O. J., 1996), which is defined as the cross-sectional migration path of the base-of-slope through time. This path is controlled by the sediment supply to the base-of-slope, and the basin physiography and subsidence. However, the base-of-slope trajectory is intimately linked to the processes at the shelf edge as these largely control the sediment supply to the basin floor.

The base-of-slope trajectory can be coupled with the shelf edge trajectory to describe the geometric development of clinoforms through time, and can further be used to decide if the accommodation seaward of the shelf edge was increasing or decreasing during progradation (Fig. 3). If the accommodation was increasing with time (diverging trajectories) the basin can be classified as underfilled (sensu Carroll, A. R.

& Bohacs, K. M., 1999) (i.e. basin floor water depth was increasing with time), whereas if the accommodation was decreasing with time (converging trajectories) the basin can be classified as overfilled (sensu Carroll, A. R. & Bohacs, K. M., 1999) (i.e. basin floor water depth was decreasing with time). Diverging trajectories indicate that the gravitational potential is increasing along a clinoform with time, whereas converging trajectories indicate the opposite (see below).

Geological setting

The Orinoco platform (or Plataforma Deltana) represents the offshore extension of the Eastern Venezuelan Basin (Di Croce, J. *et al.*, 1999) and can be further divided into the largely tectonically inactive Delta Amacuro Platform to the south, and the growth-faulted Columbus Basin to the north (Figs. 4,5) (Leonard, R., 1983). The latter is bounded to the north by the offshore extension of Trinidad's Central Range thrust belt and to the east by the present shelf edge (Leonard, R., 1983). The Columbus Basin comprises thick (>100 m), laterally extensive and continuous, deltaic reservoirs (Sydow, J. C. *et al.*, 2003) with substantial amounts gas and oil reserves (e.g. Di Croce, J. *et al.*, 1999; Finneran, J. M. & Bally, K., 1999).

During Cretaceous and Palaeogene times, Venezuela developed as a passive margin dipping roughly toward the north and northeast (Di Croce, J. *et al.*, 1999). The onset of the Neogene transpression and subsequent overthrusting of the Caribbean Plate above the South American Plate terminated the passive margin phase, and the foredeep called Eastern Venezuela Basin started to develop (Fig. 4). In the stratigraphic record, this transition is recorded by the basal foredeep unconformity (25 Ma) which separates the passive margin strata from the active margin strata (Di Croce, J. *et al.*, 1999).

The uplift changed the discharge pattern of the northern part of South America and led to the establishment of the palaeo-Orinoco River along the axial part of the foreland basin (Fig. 4). The sediments supplied by the river exceeded the accommodation in the foredeep and resulted in an east north-eastward progradation of the delta system and the palaeo-shelf edge during Miocene times (Di Croce, J. *et al.*, 1999; Wood, L. J., 2000). In Plio-Pleistocene times, the palaeo-Orinoco delta prograded across a storm and current-influenced shelf (Wood, L. J., 2000), with the resulting sedimentary succession thickening northwards toward the thrust front (Fig. 5). During this period, more than 12,200 m of Plio-Pleistocene clastic sediments accumulated in Columbus Basin (Wood, L. J., 2000).

The middle Pliocene palaeo-Orinoco delta is today exposed in the Mayaro Formation along Mayaro Beach in the southeast Trinidad (Bowman, A., P, 2003). Even if these successions are older than the studied Pleistocene age deposits, they probably represent the same overall depositional system and may be viewed as an outcrop analogue.

Purpose of study

The successively increasing rates of rise in relative sea level northwards toward the thrust front (e.g. Di Croce, J. *et al.*, 1999) resulted in the construction of a margin where the shelf-slope-basin floor clinoforms successively increased in size with time, and along-strike toward the thrust front. The foreland basin therefore enables comparison of the sedimentary and tectonic responses to varying clinoform growth patterns along a prograding shelf edge (Fig. 6). Hence, the purpose of this study is to investigate how clinoform growth patterns are linked to sedimentary processes, synsedimentary deformation and palaeogeographic evolution in an attempt to understand why the Columbus Basin and Deltana Amacuro Platform developed so differently.

Study area and database

The study area is located offshore Venezuela in the vicinity of licence blocks 1-4 and comprises the southern part of the Columbus Basin and the southerly adjacent Deltana Amacuro Platform area (Fig. 7). The data presented mainly comprises 2D/3D seismic reflection data, but is to some degree supplemented with data from well Lau-1 and by literature concerning the modern Orinoco delta system.

The 3D cube is a merge of two surveys and provides high resolution seismic stratigraphic data covering a 2000 sq km in block 1-4 (Fig. 7). In this area, correlations across fault tips show that the seismic resolution at 1000 ms two-way time (TWT) or 1000 m depth is about 30 m (Table 1). In general, the resolution decreases toward the subsurface, and 1 ms TWT in the studied seismic data roughly equals 1 m vertical distance.

The 2D seismic lines overlap the 3D data set and extend toward the south into the Deltana Amacuro Platform area (Figs. 4, 7) and enables regional correlation and comparison of larger scale, time equivalent elements such as lateral variations in clinoform growth pattern.

Table 1 Key information on the 3D seismic data presented in this study

Survey name	**Seismic class**	**Sample interval**	**Shot point interval**	**Seismic resolution**	**Map area coverage**	**Stacking**	**Seismic acquisition year**	**Seismic vessel**	**Phase**	**Acoustic impedance increase**	**Acoustic impedance decrease**
GO1999, and GO2001	2 merged 3D surveys	4 ms	25 m	30 m	2000 sq km	Full stack	1999 and 2001	Geco Longva and Western Legend	Normal	Peak (dark reflectors)	Trough (bright reflectors)

Seismic facies and analogues

Seismic facies analysis: In the 3D seismic data set, reflectors believed to represent approximate time lines were mapped out as horizons within a detailed study area of 800 sq km, limited by data coverage and faulting (Fig. 7). Seismic facies analysis was performed along interpolated horizons in the Pleistocene to Recent stratigraphic succession for the purpose of reconstructing the palaeogeography of the depositional system.

The seismic facies were differentiated on the basis of their signature in seismic cross-sections, appearance in attribute RMS (Root Mean Square) maps and their gamma log signature (if applicable). Four seismic facies have been recognised along clinoform surfaces: 1) fluvial seismic facies, 2) shallow marine seismic facies; 3) slope seismic facies, and 4) basin floor seismic facies. The boundaries between the seismic facies belts are not always sharp; some of them are gradational or interfingering. A more detailed description and interpretation of the seismic facies are provided in Table 2 and in Fig 8.

Palaeogeography: The seismic facies stacking pattern with fluvial seismic facies changing down dip into the wave-influenced shallow marine seismic facies suggests the depositional system represents a delta prograding across a wave-dominated continental shelf (cf. Table 2), which is in accordance with previous studies in the area (Wood, L. J., 2000; Sydow, J. C. *et al.*, 2003). Furthermore, shallow marine seismic facies commonly terminate in scours resulting from shelf edge failures indicating that shallow marine sand at least periodically reached the shelf-edge (cf. Table 2, Fig. 8). However, the general lack of observed fluvial incision along the shelf edge (this study; Wood 2000) suggests that sea level never dropped below the shelf edge and that the depositional system represented a shelf edge delta without incision (cf. Steel, R. J. *et al.*, 2003) when being in its most regressive position.

Regressive-transgressive cyclicity: The interpreted landward shift in depositional inferred in shallow marine seismic facies and in well LAU-1 (cf. Table 2) (cf. Wood, L. J., 2000; Sydow, J. C. *et al.*, 2003) implies that the shelf edge deltas were repeatedly transgressed and replaced by inner or mid shelf deltas, resulting in stacking of regressive-transgressive cycles (Fig. 10), as previously proposed by Wood (2000) and Sydow et al. (2003). This is also supported by a study of the Mayaro Formation, where the “delta topset interval” consists of upward-coarsening shallow marine parasequences, each terminated by flooding events (Bowman, A., P, 2003), which are probably analogous to the landward shift in facies detailed in this study. Faulting and poor well control makes it difficult to relate the entire studied sedimentary succession to regressive-transgressive cyclicity. However, it is believed that the cycles prevailed throughout the overall progradation studied stratigraphic interval (progradationally stacked parasequence set (sensu Van Wagoner, J. C. *et al.*, 1990)).

The time represented by each cycle is difficult to estimate as the high sediment input resulted in stretching of bio zones and poor biostratigraphic resolution. However, some tentative calculations can be made: typical sediment accumulation rates across the basin were 5-6 (or even 8) m per thousand years (Wood, L. J., 2000). The 50 ms/50 m thick inferred shallow marine sandstones in LAU-1 (cf. Table 2, Fig. 9) could then represent approximately 10 ka (using sediment rates of 5 m/ka) or less. Furthermore, for the present Orinoco delta, Burgess and Hovius (1998) and Muto and Steel (2002b) calculated the shelf transit time to be 12 thousand years using 0.001°

shelf slope and no change in relative sea level. This tentatively suggests that each regressive- transgressive cycle was about 12 ka.

Modern Orinoco delta system: At the seismic scale, the shelf edge deltas and the inner/mid shelf deltas can not be differentiated as their thickness is less than possible to distinguish in the seismic data. The inner shelf of palaeo-Orinoco delta may, however, have been similar to the modern Orinoco delta, which is located landward of submerged sandy coastal plains (McClelland Engineers, 1979), 130 km from the shelf edge (Fig. 11). The modern delta is divided into a tidal/fluvial dominated southern sector and a littoral current dominated northern sector (Warne, A. G. *et al.*, 2002).

Warne et al. (2002) reported that approximately 50 % of the sediments deposited at the modern Orinoco coast have been transported northwards from the Amazon River by the muddy Guayana Current. Furthermore, on a regional scale, Belderson et al. (1984) reported modern channelised basin floor deposits from side-scan sonar data along the Barbados deformation front (Orinoco Fan in Fig. 11), 350 km from the present day Orinoco Delta. In addition, a regional study of the present day margin foresets by Ercilla et al. (2002) proposes unconfined turbidity currents generated by slope failure, as well as channelised turbidity currents such as down slope mass wasting processes.

Table 2 Description and interpretation of seismic facies recognised in this study	
Description	**Interpretation**
FLUVIAL SEISMIC FACIES (Figs. 8B, 9): The seismic facies appears as topset reflectors and may be up to 1000 ms (TWT) thick (about 1000 m). Laterally, it either occurs across the whole study area or changes down dip into shallow marine seismic facies. The facies is associated with variable types of seismic responses coexisting beside each other, ranging from one end member with parallel, sub-planar, continuous reflectors to another with nonparallel, undulating-hummocky and discontinuous reflectors. In RMS maps, the facies appears disorganised; however, vague to occasional well-defined channel belt geometries and individual well-defined channel geometries are occasionally present at repeated stratigraphic intervals. Both channels associated with point bars indicating lateral migration, and channels without point bars indicating no lateral migration, are present. The fluvial seismic facies can be correlated to well LAU-1 where it appears as thick packages (50-100 ms/50-100 m) of upwards decreasing, increasing or stable gamma values.	The seismic facies topset position suggests a depositional environment extending either across the coastal plain to the shore or across the shelf to the shelf edge. However, the seismic facies complexity and occasional well-defined channel belts are features associated with alluvial or coastal plains rather than the shoreline-offshore profile, and the facies is therefore interpreted to represent a fluvial plain. The lack of deep and laterally continuous channel geometries implies frequent shifts in channel positions, and the large vertical extent suggests an aggradational fluvial plain. The alternating upwards coarsening and fining trends in the gamma logs are interpreted to reflect progradation and retrogradation of the fluvial system.
SHALLOW MARINE SEISMIC FACIES (Figs. 8C, 9): This seismic facies also appears as topset reflectors and the thickness may be up to 700 ms TWT (about 700 m). It occurs immediately seaward of fluvial seismic facies and down-dip, it is commonly steeply truncated by scours which mark the up-dip termination of slope seismic facies. The facies is characterised by parallel, subplanar, continuous, high amplitude reflectors and has sheet-like geometry extending about 10 km in a dip-direction, and more than 30 km along-strike. The seismic facies can be correlated to the LAU-1 well, where it typically consists of 35-55 ms (35-55 m) thick interval with upwards decreasing gamma values separated by abrupt increases in gamma value which are believed to reflect the presence of coarsening up sandstone units capped by mud. The mudstone intervals correspond to a soft kick (red amplitude) in the seismic data and seem to have more or less the same areal extent as the hard kick which corresponds to the sandstones (blue amplitude).	The seismic facies position on the topset, lack of seismic scaled channels and its position down dip of the channelised fluvial seismic facies suggest a shoreline-offshore origin for this seismic facies. The large areally distribution of both hard kicks and soft kicks indicates areal extensive lithological units. The correlation of hard and soft kicks to sandstones capped by mudstone in the LAU-1 well suggests deposition of alternating relatively high and low energy depositional environments, respectively. In the high energy depositional environment, the large areal extent and sheet like geometry of the inferred sandstones suggests that the sand was distributed along the coast by waves and longshore currents. The inferred sand-rich part of the seismic facies is therefore interpreted to represent wave-dominated shallow marine sandstones. The inferred mud-rich part of the seismic facies is likely to represent the extensive low energy depositional environment of offshore deposition. As these deposits are underlain by interpreted shallow marine sandstones they represent a landward shift in facies, which is in accordance with previous studies (Wood, 2000; Sydow et al., 2003). Consequently, the inferred mudstones represent transgressive sediments during periods when the palaeo-Orinoco delta was at inner or mid shelf positions.
SLOPE SEISMIC FACIES (Fig. 8D): The seismic facies represents foreset reflectors that dip seawards with a relief that increases from 5-600 ms/5-600 m height and 1° slope at near-base Pleistocene to 1500 ms/1500 m and 0.9° slope at the modern foreset. Up-dip, the seismic facies commonly truncates shallow marine seismic facies, whereas in a down dip direction it transforms into basin floor seismic facies. The seismic facies is characterised by nonparallel, chaotic to undulating and semicontinuous to discontinuous reflectors. In RMS maps, the seismic facies appear chaotic and scoured, with only a few continuous sinuous channel geometries observed in shallow seismic. The LAU-1 well does not intersect this seismic facies.	Based on the seaward depositional-dip and the high relief, slope seismic facies is interpreted as a continental slope environment extending from the shelf edge to the basin floor. The upward increase in clinoform height reflects successively deeper basin floor water depth during progradation, resulting from regional subsidence in the foreland basin and the eastwards dipping seafloor of the Atlantic Ocean. The erosive character of the shelf edge, the general scoured character of slope seismic facies and the lack of larger continuous slope channel systems suggest that down-slope transport of sediments results from mass wasting processes *along* the outer shelf/upper slope, rather than from longer lived single/multiple point sources. The sediments were reworked and distributed on the shoreface-shelf until the high sediment input eventually led to oversteepening and shelf edge failure. However, some channelised transport of sediments to the basin floor occurred, as evident from seismic attribute maps.
BASIN FLOOR SEISMIC FACIES (Fig. 8E): The seismic facies represents gently seawards dipping bottomset reflectors transforming up dip into the relatively steeper dipping slope seismic facies. The seismic facies are characterised by nonparallel, undulating and semicontinuous reflectors. In places the reflectors are distorted. In plan view, the seismic facies appear disorganised and mounded, but the large scale expression is difficult to map due to faulting. The LAU-1 well does not intersect this seismic facies.	Based on the down dip position of the slope seismic facies, the facies is interpreted to represent the basin floor environment. The mounded, undulating and semicontinous and, in places distorted, reflectors are likely to reflect deposition of down-slope mass wasted sediments, such as slumps.

Shoreline trajectory

The boundary between fluvial seismic facies and shallow marine seismic facies is interpreted as representing a depositional down-dip shift from fluvial to wave-dominated processes and can therefore be used as an approximate position for the palaeoshoreline. In cross-sections, the boundary can be picked at successively higher stratigraphic levels and when interpolated, they display a rising shoreline trajectory (Fig. 8) prograding roughly toward the northeast. As a result, thick sedimentary packages belonging to fluvial seismic facies accumulated landward of the inferred shoreline, whereas an equally thick sedimentary succession belonging to shallow marine seismic facies accumulated in seaward positions. On RMS maps, the progradation is illustrated by fluvial seismic facies becoming increasingly areally dominant as its down dip boundary to shallow marine seismic facies moves seaward with time (Figs. 8 f,g,h). The shoreline trajectory can therefore be classified as overall rising regressive implying a rising relative sea level during progradation, punctuated by floodings. As this trajectory is present outside areas with synsedimentary faulting, the relative sea level rise was mainly of regional extent, linked to the development of the foreland basin. The transgressive deposits are largely below seismic resolution and it is likely that the transgressive shoreline trajectories were largely non-accretionary, or else the transgressive deposits were eroded during the subsequent regression.

Shelf edge and base-of-slope trajectories

The shelf edge trajectories are not well displayed within the 3D data set due to growth faulting. However, the mapped seismic horizons can be correlated southwards to the well-displayed shelf edge trajectories in the Deltana Amacuro Platform area. Here, there is a break and lowering of the shelf edge trajectory angle at near-base Pleistocene (Fig. 12). This suggests sediment supply overwhelmed available accommodation at this time and caused the depositional system to step basinward. In plan view, it is evident that individual shelf edges are undulating to concave along-strike and prograded roughly toward the northeast (Fig. 13). Where concave, successive shelf edges tend to smooth the original concavity and thereby cause the shelf edge trajectory to deviate horizontally in comparison with neighbouring areas.

In the Columbus Basin, the near-base Pleistocene shelf edge is located at 1400 ms/1400 m below the seafloor (Fig. 8a) whereas in the Delta Amacuro Platform area it is located at 900 ms/900 m below the seafloor (Fig. 12). This northwards thickening of the studied stratigraphic interval across the Delta Amacuro Platform area through to the Columbus Basin (Fig. 5) indicates that subsidence and sediment accumulation were greater in the latter (Di Croce, J. *et al.*, 1999; Wood, L. J., 2000). Despite the higher subsidence rate, the present day shelf edge in Columbus Basin is located as far out in the basin (toward the northeast) as the shelf edge in the Delta Amacuro Platform area (Fig. 13). This implies that the shelf edge trajectory angle is overall steeping when moving along the depositional strike toward the area with the largest sediment accumulation (i.e. toward the thrust from the Delta Amacuro Platform to the Columbus Basin, Figs. 6, 14).

In the Columbus Basin, the clinoform relief increases by 1150 ms/1150 m from near-base Pleistocene (350 ms/350 m; Fig. 8a) to Recent (1500 ms/1500 m), indicating that the shelf edge and the base-of-slope trajectories were diverging. In contrast, in the Delta Amacuro Platform area, the clinoform relief increases by only 600 ms/600 m from near-base Pleistocene (900 ms/900 m; Fig. 12) to Recent (1700 ms/1700 m; Fig. 12). This implies increasing divergence between the shelf edge and base-of-slope trajectories toward the thrust front. The increase is mainly caused by the northwards steeping of the shelf edge trajectory (not by an increasing seaward dip in base-of-slope trajectory) and may therefore be classified as having a rising divergent trajectory pattern and to represent an underfilled basin (Fig. 2) (sensu Carroll, A. R. & Bohacs, K. M., 1999).

Shelf edge failures

Immediately above the near-base Pleistocene horizon in the Columbus Basin, the shallow marine seismic facies is separated from the slope seismic facies by c. 100 ms/100 m deep truncations, and the down-dip section is highly deformed (Figs. 15a,b,c). The truncations are likely to have resulted from episodic shelf edge failures that were caused by the shear stress component of gravity exceeding the shear strength along a seaward dipping geological surface (e.g. an older palaeo-continental slope), resulting in gravity gliding. However, as the shelf edge is associated with the seaward dipping seafloor of the continental slope, gravity spreading is also likely to have made a contribution to the stress regime that caused the shelf edge failures (cf. Fig. 1) (cf. Rowan, M. G. *et al.*, 2004). As the basin floor deposits are distorted, the sediments are likely to have been deformed during transport and probably mostly represent slump deposits (cf. Table 2).

Seismic reflectors are commonly observed to onlap the truncations, indicating healing of the slump scars (Figs. 15a,b,c). It is also evident that the healing and renewed progradation following a shelf edge failure is terminated by a successive shelf edge failure. This suggests that cycles of failure-healing-renewed progradation were a common process that occurred repeatedly during shelf edge migration within this seismic stratigraphic interval. This mode of progradation follows Ross et al.'s (1994) principle of slope readjustment and the margin can in the Columbus Basin margin can be classified as an *erosive margin.* In their model, they build on Hedberg's (1972) concepts of graded and erosional margins, where the former largely progrades in equilibrium with depositional and erosional processes (Fig. 16a), whereas the latter is recognised by oversteepening of the basin margin with sediments being bypassed to a base-of-slope position (Fig. 16b). It is difficult to decide if this process continued in the section above due to intense growth-faulting in the 3D study area. Possibly, the oversteepening and associated shelf edge failures terminated when growth-faulting commenced due to the lowering of the depositional profile which accompanied the basinward transport of fault blocks (see below).

In contrast to the Columbus Basin, the inferred relatively lower angle of the shelf edge trajectory in the Delta Amacuro Platform area is associated with clinoforms displaying only minor slope failures and without obviously repeated cycles of shelf edge failure-healing-renewed progradation (Fig. 12). Instead, the continental slope is constructed by discontinuous to chaotic reflectors with high to low amplitudes likely to reflect smaller scale slope processes (Fig 16a). This suggests that the clinoforms in the Deltana Amacuro Platform area prograded as a *graded margin* (sensu Hedberg (1972); Ross et al. (1994)).

A causal connection between increasing steepness of a rising shelf edge trajectory and increasing scale of shelf edge failures is therefore suggested; i.e. that increasing accommodation on the shelf edge during progradation favours oversteeping and the establishment of Ross et al.'s (1994) model of slope readjustment, whereas less accommodation on the shelf edge favours a more stable progradation (Fig. 15e). There are two factors that makes shelf edge failures more probable to occur with a rising shelf edge trajectory than with a horizontal trajectory: 1) the rise in relative sea level will cause the clinoform foreset to become longer, and to steepen along the upper slope (Ross, W. C. *et al.*, 1994), and 2) the effect of loading along the shelf edge will increase (Fig 15d). These two contributions to the stress regime associated with potential shelf edge failure make it more likely that the critical shear strength along a seaward dipping surface is reached, with episodic shelf edge collapse as the result.

Growth faulting

In addition to the relative minor scale (cutting 100 ms/100 m deep) and episodic shelf edge failures described above, larger scale (cutting 1000s of ms/1000s of m deep) and longer term (2 Ma) synsedimentary deformation represented by growth faulting also occurred during progradation in the Columbus Basin (Fig 17a). The growth faulted structural domains indicate a basinwards (eastwards) transport direction. The growth faults are listric and merge with the basal foredeep unconformity detachment surface (25 Ma), suggesting the collapse was not directly related to an external stress regime but is a result of gravitational tectonics. Careful mapping of the oldest appearing growth wedges in the hanging wall across to areas with well control indicates that the onset of the main deformation commenced at the near-base Pleistocene time. This dating is also supported by section balancing which helped to tie the pre-deformation succession back into the footwall where well information exists.

The deformation probably started out as a series of collapses in the delta front, perhaps as normal planar fault segments developing into listric faults that eventually linked up laterally due to the geometry of the underlying detachment. Rollover structures were formed above the subhorizontal part of the fault; continued movement and rotation of strata caused a series of growth basins to develop in the hanging wall.

The system is interpreted to be of back-stepping nature following the first major collapse.

Six synsedimentary structural domains resulted from the gravity failure in the Columbus Basin: a) footwall; b) detached normal faults; c) strongly rotated fault blocks; d) major listric faults and associated growth basins; e) rollover anticline; and f) basinwards syn- and anticlining (Fig. 17b).

1) Footwall domain: The *footwall* is regarded as the structurally undeformed part of the system (Figs. 17b,c) with only minor faulting and slump scar features being observed in the seismic data.

2) Detached normal faults domain

Structuring: Basinward and down-dip from the footwall, a series of en-echelon, planar normal faults are interpreted as *detached normal faults* (Figs. 17b,c). No major rotation of the fault blocks is observed, suggesting little horizontal displacement during fault movement. Throws on individual faults are minor and seems to decrease with depth. Consequently, several local detachment horizons may have controlled the formation of these faults. In plan view, the detached normal faults describe a narrow band and the domain is believed to represent an immature collapse feature which might have formed as a result of the major gravitational failure located further to the east.

Palaeoflow: The easternmost faults in this domain nearly intersect the seabed, implying that the area is still subsiding. This is also illustrated in shallow seismic attribute maps where synsedimentary fault blocks commonly trap sediments of the fluvial seismic facies. However, palaeoflows are only affected to a limited degree, suggesting sediment supply was commonly larger than creation of accommodation at this stage (Fig. 16c). Trapping of sediments within fault blocks is also evident from deeper seismic although channelisation is less obvious, probably due to loss of seismic resolution with depth.

3) Strongly rotated fault blocks domain

Structuring: It is suggested that this domain initially formed as planar normal faults over a larger area than today's domain. However, as gravity failure prevailed, the basinward areas developed into the major listric fault and associated growth fault domain (below) due to larger horizontal displacement along the basal foredeep unconformity in this area (Fig. 17b). The areas landward of the strongly rotated fault blocks were prohibited from developing into listric faults by lack of horizontal accommodation space caused by the fault separating the domains, and therefore continued to develop as planar fault blocks in the detached normal faults domain (Figs. 17b,c).

Palaeoflow: The domain trapped large amounts of sediment, but sediment supply still exceeded the rate of creation of accommodation. However, in contrast to the detached normal faults domain, meandering channels are observed to have overall palaeoflow directions parallel to the structural strike of the fault blocks (Fig. 16c).

4) Major listric faults and associated growth basins domain

Structuring: This domain is the most prominent structural style in the Columbus Basin (Figs. 17b,c). As with the strongly rotated fault blocks domain, it is suggested that this domain also initially formed as planar normal faults. However, as gravitational failure prevailed, the domain was separated from the strongly rotated fault blocks domain due to larger horizontal displacement along the basal foredeep unconformity in this domain. The horizontal and down dip displacement was ultimately controlled by the shape of the detachment surface which caused movement along the major fault that ultimately separated the two domains.

Geometries within this domain were also largely controlled by the differential amount of horizontal displacement, leading to complex linkage of major faults, (laterally and with depth), separation of fault blocks, hanging wall collapse and toe compression. In plan view, the domain has a fan-shaped geometry where the number and complexity of listric faults increases toward the north with each fault accommodating a growth basin (Fig. 17c). This northward increase in complexity can be explained by a northward increase in horizontal displacement along the detachments.

Palaeoflow: The onset of subsidence within the domain caused a rise in relative sea level within the fault domain, with the accommodation created being immediately filled by sediments from the Orinoco Delta system and probably also from the Guayana Current (Fig. 11). As the domain mainly comprises shallow marine seismic facies, it is suggested the sediments mostly consist of shallow marine sands and offshore deposits. The modern shelf edge is located within this fault domain, and its inability to prograde further seaward should be attributed to the enormous amount of sediment trapped within the growth basins (Figs. 16c , 17). Consequently, within the domain, the depositional system must have changed from being mainly progradational prior to faulting, to becoming mainly aggradational after the onset of faulting, which implies a steepening of the shelf edge trajectory. The sediment loading caused continuation of the gravitational collapse down to the east-northeast.

The strike of the modern shelf edge is oriented in roughly the same direction (i.e. roughly northwest-southeast) and is located approximately the same distance basinwards (Fig. 13), both within and outside the fault domain. This suggests the growth faulting trapped so much sediment that it prevented the entire *margin* extending from the Delta Amacuro Platform area through to the Columbus Basin from further seawards progradation.

5) Rollover anticlines domain

Structuring: Several rollover anticline segments are present within the Columbus Basin. Some of these are broken up and have evolved into individual growth basins and translational horst blocks within the growth basin domain. The presently “intact” rollover anticlines are found in association with the subhorizontal part of the outermost major listric fault (Fig. 17b). The shape of the rollovers varies from monoclinal in the south, cylindrical anticline in the central area to an up- and out-of-the-basin vergent thrust anticlinal shape in the north. Such variations are attributed to local changes in extension/accommodation space and the shape of the detachment that controls the rollover structure. Seawards, the rollover is bounded by normal faults representing the basinward limit of extensional related structures. This limit coincides with the Cretaceous boundary fault, and reactivation of this fault may have played an important role in *triggering* the gravitational collapse.

Palaeoflow: At times, the rollover obstructed sediments from bypassing to the basin floor, and resulted in trapping sediment in the growth basins. No significant deposition is likely to have occurred on the anticlinal crest. Deposition took place preferentially in the subsiding basins located landward and basinward of the crest (Fig. 17).

6) Basinwards syn- and anticline domain

Structuring: The basinward synclines and anticlines represent the compressional part of the collapse system and were most likely formed contemporaneously with the gravity collapse. The position and shape of these structures may have been controlled by the shape of the underlying detachment; an outer ramp in the detachment formed a syncline, whereas another flat formed the outer anticline. Further to the east, it is expected that syn- and anticlines are thrust-cored and not necessarily geometrically linked to the foredeep unconformity detachment.

Palaeoflow: The basinward thinning of the seismic stratigraphic package across the rollover anticlinal followed by basinward thickening in the synclinal indicate that some sediment bypassed the rollover anticlinal (Fig. 17). As the sediments in the synclinal basin consist of slope seismic facies, they are likely to represent continental slope sedimentation.

Controls on growth faulting

The gravitational collapse was accommodated by seawards movement of the fault domains, and activated detachment surfaces (Figs. 17a,b) at several stratigraphic levels. The collapse is therefore likely to have been initiated when the shear stress from the loading sedimentary package exceeded the shear strength threshold along these incompetent horizons. Through time, the angle of the continental slope seems to have roughly remained constant at about 0.9-1.0°, independent of the height and length of the foreset of the clinoforms. It is therefore unlikely that this angle itself affected the stability of the margin with respect to *growth faulting*. As progradation prevailed, however, the clinoform increased in size (i.e. the foreset length and relief increased) due to diverging shelf edge and base-of-slope trajectories. This was caused by the accommodation created by the regional rise in relative sea level which allowed aggradation in the topset position, and by the amount of sediment being supplied to the basin floor being too insignificant to maintain the initial clinoform depositional profile. While the latter was partly a result of the accommodation added by the regional rise relative sea level, it was mainly a result of the basin floor physiography with the eastwards dipping seafloor of the Atlantic Ocean which provided virtually infinite accommodation space in front of the depositional system.

The density contrast between the sediments below a seafloor clinoform and the water above is accompanied by a major decrease in overburden and associated horizontal overburden stress when going from the shelf edge to the base-of-slope (Fig. 18a). Moreover, if a margin is prograding with gradually increasing clinoform size, this difference will also gradually increase, as the sediments have a steeper density profile with depth than sea water (Fig. 18b). Eventually, the difference in landward and seaward directed horizontal overburden stress will exceed the shear strength along one or several incompetent horizons, causing the margin to experience gravitational failure and evolve into a collapse margin (or unstable margin of Winker, C. D. & Edwards, M. B., 1983). This implies that clinoforms have a maximum size (i.e. foreset length and relief) and that progradational margins will eventually be halted due to accommodation created by growth faulting, provided the shelf edge and base-of-slope trajectories are diverging.

Growth faulting associated with basinward dipping detachments is commonly interpreted as representing gravity gliding (e.g. Bruce, C. H., 1973; Crans, W. *et al.*, 1980; Winker, C. D. & Edwards, M. B., 1981; Galloway, W. E., 1986; Cobbold, P. R. & Szatmari, P., 1991; Demercian, S. *et al.*, 1993; Mauduit, T. *et al.*, 1997; Silva, S. R. P. *et al.*, 1999). The presence of a basinward dipping detachment in the study area (Fig. 17a,b) implies the gravity failure was partly a result of gravity gliding; however, the large amount of fault block rotation suggests that gravity spreading was the dominant driving component in a mixed mode gravity failure (sensu Rowan, M. G. *et al.*, 2004)(Fig. 1c). Though, the dominant driving component may change through time during a gravity failure (e.g. Rowan, M. G. *et al.*, 2004); and possibly in the study area, the failure may have been initiated as gravity gliding and later transformed into being more gravity spreading dominated. As fault movement is still occurring, this implies that the seaward transport of fault blocks has not lowered the relief of the foreset sufficiently to terminate gravity failure. Consequently, shear stress still exceeds shear strength along the detachment surfaces and basinward transport of fault blocks prevails today.

The break in shelf edge trajectory angle and the basinward stepping of the Deltana Amacuro Platform depositional system at near-base Pleistocene (Fig. 12) coincide roughly in time with the onset of growth fault collapse in the Columbus Basin. It is therefore suggested the growth fault gravitational collapse was a result of the depositional system stepping basinward with diverging shelf edge and base-of-slope trajectories at these times. The differential horizontal overburden stress eventually exceeded shear strength along the basal foredeep unconformity, and the collapse commenced (Fig. 19).

In a spatial context, the onset of faulting is probably related to the northwards increase in differential horizontal overburden stress caused by the inferred increase in divergence between the shelf edge and the base-of-slope trajectories toward this area. For the sake of argument, one can assume a homogenous sedimentary package extending from the Delta Amacuro Platform to the Columbus Basin. In such a framework, one may speculate as to whether faulting was commencing in the area where the angle of divergence passed through a threshold value causing the differential horizontal overburden stress on the sedimentary succession to exceed its shear strength. However, even if the increasing difference in horizontal stress controlled where onset faulting commenced on a regional scale, it may be more likely that local variations in shear strength within the sedimentary package controlled both the *timing* and where the onset of faulting commenced on a more *local scale*.

Triggering mechanisms could have been the sediment loading, or an external stress regime (episodic or long term) causing reactivation of the Cretaceous boundary fault (Fig. 17b) resulting in lowering of the shear strength/shear stress ratio along the basal foredeep unconformity. Alternatively, the greater amount of subsidence towards the east in the basin resulted in an increase in the gravitational shear stress component along the potential detachment surface as it steepened, and may have been the dominating factor triggering gravity failure.

Discussion

In the Columbus Basin, the depositional system initially prograded as an erosive margin in the manner of Ross et al.'s (1994) model of slope readjustment, but eventually collapsed, resulting in the establishment of the six synsedimentary fault domains. The shelf edge failures were related to the oversteepening along the shelf edge, whereas the growth faulting was related to the increasing clinoform relief and length of the foreset with time (diverging shelf edge and base-of-slope trajectory pattern). Hence, the shelf edge failures and the growth faulting occurred on different scales and had different causes. However, the collapse and basinward transport of fault blocks in the Columbus Basin was accompanied by lowering of the depositional profile across the margin. The onset of growth faulting may therefore have stopped the oversteeping leading to major shelf edge failures. No shelf edge failures have been observed in the major listric faults and associated growth basins domain which may indicate this change took place. The sedimentary succession, however, is so deformed by the faulting that this observation should be regarded as a tentative.

The various types of synsedimentary deformation observed in the study area may be interpreted as representing a spectrum of different scale sedimentary/tectonic processes activated/terminated during progradation with increasing rates of rise in relative sea level (Fig. 20): 1) Progradation with a horizontal to gently rising shelf edge trajectory is associated with only minor slope failure and the progradation of a graded margin (sensu Hedberg 1972; Ross 1994). 2) Progradation with a steeper rising shelf edge trajectory favours shelf edge failures resulting from oversteepening, and Ross et al.'s (1994) model of slope readjustment for erosive margin will then apply (sensu Hedberg 1972; Ross 1994). 3) Provided progradation involves diverging shelf edge and base-of-slope trajectories, the margin will eventually experience large scale gravitational failure and continue to evolve as a collapse margin (or unstable margin of Winker, C. D. & Edwards, M. B., 1983) associated with major growth faulting.

Conclusions

- During Pleistocene times, the Orinoco delta alternated between shelf edge and inner-shelf positions during rising relative sea level, resulting in the construction of a margin where clinoforms successively increased in size with time, and along-strike toward the thrust front.
- The growth faulted collapse in Columbus Basin was caused by the foreset length becoming too long (due to diverging shelf edge and base of slope trajectories) to support the overall seaward directed horizontal overburden stress. This implies that prograding clinoforms have a maximum size that can not be exceeded, since growth faulting will commence and create large accommodation on the topset, preventing the margin from further progradation.
- The gravitational collapse was accompanied by lowering of the depositional profile and changed the progradational mode from an erosive to a graded margin. Also, the collapse changed the terrestrial palaeogeography, in part forcing fluvial channels to trend parallel to fault blocks.
- The various types of synsedimentary deformation observed in the study are interpreted as representing processes successively activated and/or terminated when the angle of a shelf edge trajectory increased from horizontal/gently rising to more steeply rising: 1) minor slope failure and progradation as a graded margin, 2) major shelf edge collapses and progradation following Ross et al.'s (1994) model of slope readjustment along an erosive margin, and 3) major growth faulted gravitational failure of the entire margin and the development of a collapse margin.

Acknowledgement

This study has been fully funded by VISTA (www.vista.no), which is Statoil's basic research programme conducted in collaboration with the Norwegian Academy of Science and Letters. Statoil INT in Stavanger, Norway, is acknowledged for providing the data set and Eilert Hilde at Statoil's Research Centre in Trondheim is thanked for assisting with interpretational tools.

Chapter 5

Palaeogeography and stratigraphic architecture of normal regressive, wave-dominated deltas: Many scales but one causative link?

Kristian Helle

Abstract

Sequence stratigraphic studies have mainly been concerned with recognising links between fluctuating relative sea level and its effect on depositional systems. Little attention has been given to the effects of threshold values in the accommodation/sediment supply ratio which are *not* caused by fluctuating relative sea level. This study focuses on the response of prograding wave-dominated delta systems to successively increasing amounts and rates of rise in relative sea level (ranging from a few m to 1000s of m), and shows that such deposits can ideally be divided into 6 progradational modes (**a-f**):

a) Sub-linear coast along a strandplain; **b)** sub-linear lagoon-barrier coast with associated lagoonal deltas; **c)** sinuous coasts with deltaic lobes and lagoons located in topographical lows between main fluvial channel belts and landwards of the inter-deltaic embayments; **d)** autogenic deltaic lobe shifting resulting in delta plain aggradation at a rate by far exceeding the aggradational rate in more offshore positions, eventually leading to the development of clinoforms of shelf-margin scale (up to a couple of 1000 m high). As long as the depositional system progrades without major shelf edge failures, it represents a graded margin; **e)** oversteepening and episodic shelf edge failures during progradation due to increased loading along the upper slope, typical for an erosive margin; **f)** As the clinoform size increases with time, the gravitational potential also increases and the margin will respond by initiating growth faulting in an attempt to lower its potential. The accommodation created at the topset by growth faulting will trap so much sediment that it will prevent the margin from further progradation.

How far a depositional system reaches on this scale (a-f) will depend on if the sediment supply is sufficient to maintain the progradation and if rise in relative sea level is sufficient to accommodate the next step.

Introduction

The preceding chapters comprise different types of data sets collected from different stratigraphic successions of various ages and have shown that the trajectory terminology is useful on various scales, ranging from individual shoreface sandstone tongue geometries (**Chapter 2**), through architecture of stacked shoreface sandstone tongues (**Chapter 3**) to the evolution of entire margins (**Chapter 4**). According to Helland-Hansen and Martinsen (1996) and Steel et al. (2000), the shoreline and shelf edge trajectory angles are controlled by rates of change in relative sea level, sediment supply rates and basin physiography. In addition to showing the importance of the angle of the trajectory in controlling stratigraphic architecture, this dissertation also points to other parameters being vital, such as facies belt dip lengths at the time of deposition (**Chapter 2**) and the distance of progradation (**Chapter 3**). The coupling of trajectories (e.g. shelf edge and base-of-slope trajectory) is important for understanding the deformational history and its affect on stratigraphic architecture along continental margins build by delta systems (**Chapter 4**). **Chapters 2-4** consider the evolution of three different wave-influenced delta systems, and the results of each of the studies are summarised below.

Chapter 2 investigates the Brent delta in the North Sea, which regressed toward the north along the axial part of the extensional Viking Graben. The progradation resulted in deposition of shallow marine sandstones that in places exceed 100 m in thickness, far greater than what has typically been reported (<30 m) for ancient shallow marine sandstone tongues. It is concluded that the progradational part of the Brent delta in the study area could have been formed by a single normal regressive event, and not necessarily result from stacking of regressive-transgressive cycles.

The vertical sandstone tongue thickness in such normal regressive deposits is controlled by: 1) shoreline trajectory angle, 2) shoreface sand pinch-out water depth, and 3) shoreface sand horizontal length at the time of deposition (Cant, D. J., 1991). Within the framework of facies geometries in modern wave-influenced deltas, a 100 m thick amalgamated succession of shallow marine sandstones would result from regression with: a shoreline trajectory of 2.6-

5.4° (implying 80-95 m rise in relative sea level), a 5-12 m deep shoreface sand pinch-out depth, and a 1-2 km shoreface sand length.

In **Chapter 3**, the deltaic Blackhawk Formation in Utah, USA is studied. The delta was deposited in a foreland basin with palaeocurrent directions oriented perpendicular to the structural strike of the uplifted areas. The depositional system developed as overall progradational stacked parasequences during a period of overall rise in relative sea level resulting in an up to 400 m thick succession (e.g. Pattison, S. A. J., 2005a).

Trajectory analysis of the studied succession did not recognise any link between trajectory angle and the types of depositional environments present; however, the study concludes there is a link between regressive distance and the types of depositional environments present: 1) parasequences displaying *long* regressive distances are associated with a direct transition from fluvial plain to the marine realm, and 2) parasequences displaying *short* regressive distances are associated with lagoons located between the fluvial plain and the marine realm. These environments are interpreted as representing lateral and time equivalent depositional environments. This further implies that the coastline had major curvature (10-20 km deltaic headlands) and that shifts in position of main channel belt outlets were the main control on stratigraphic architecture. The sequence boundaries in these stratigraphic successions do not correspond to these shifts, and it is therefore suggested that fluctuating relative sea level was of less importance in controlling stratigraphic architecture than the shifts in position of channel belt outlets and associated delta lobes.

Chapter 4 treats the wave-influenced palaeo-Orinoco delta and shelf edge which regressed axially in the Eastern Venezuelan Basin foredeep and was therefore associated with a successively increasing relative sea level rise toward the thrust front. Consequently, the area enables a comparison to be made between the sedimentary and tectonic processes located some distance from the thrust front (Deltana Amacuro Platform) with processes located close to the thrust front (Columbus Basin). In particular, progradation with a gentle normal regressive shelf edge trajectory (Deltana Amacuro Platform) can be compared to progradation with a steep normal regressive shelf edge trajectory (Columbus Basin). The two areas developed in very different ways as the Columbus Basin experienced episodic shelf edge failures and long term growth faulting whereas the Deltana Amacuro Platform remained largely tectonically inactive.

This comparative study concludes that only minor shelf edge failures occurs during progradation with sub-horizontal shelf edge trajectory, whereas repeated shelf edge collapse-healing cycles occur where prograding with a steeper shelf edge trajectory. In the Columbus Basin, progradation prevailed with rising shelf edge trajectory and eventually growth faulting commenced as a result of the foresets became too long to be stable. The growth faulting resulted in lowering of the shelf-to-basin floor profile which further terminated the repeated shelf edge collapse-healing cycles. The growth faulting created accommodation on the topset which changed the subaerial palaeogeography and trapped sediments, causing loading and continued subsidence.

Progradational modes and rising relative sea level

The studied successions represent different overall normal regressive depositional systems located within different structural frameworks: **Chapter 2** treats a delta system prograding axially in an extensional setting; **Chapter 3** treats a delta system prograding perpendicular to the axis of a foreland basin, whereas **Chapter 4** treats a delta system prograding axially in a foreland basin. These basins experienced different rates of subsidence, which makes it possible to compare the stratigraphic architecture associated with progradation with increasing amount and rates of overall rise in relative sea level. A synthesis of the above studies suggests that normal regressions ideally can be divided into six modes which are successively initiated when prograding against increasing rates of rise relative sea level. These progradational modes can be divided into two main stages: the ramp margin progradation stage, and the shelf-edge construction and progradation stage (Figs. 1, 2).

The model is highly idealised and assume a wave-dominated (overall) prograding coastline, and that long term rise in relative sea level is increasing with time, but with sediment supply always exceeding accommodation. However, with time, the sediment supply/accommodation ratio is constantly to be lowered and approaching equality. How far the development proceeds in each depositional system will mainly depend on whether the rise in relative sea level is sufficient to accommodate the next step on the scale, and if sediment supply is sufficient to continue progradation. However, the development may terminate at any progradational mode or may fluctuate between modes, or a mode may be skipped (e.g. going directly from mode A to mode C progradation, without entering mode B progradational mode) (below).

Stage I: Ramp-margin progradation

Mode A (Figs. 1, 2): Ramp-margin (Ahr, W. M., 1973) progradation commences once the water depth is sufficient to enable the formation of a high-energy coast where fluvial output and wave-energy interact to shape a wave-dominated delta that progrades during sea level stillstand (horizontal shoreline trajectory). In this model, it is assumed that the wave-influence is sufficient to prevent development of a high-curvature coastline with extensive deltatic headlands. Such a progradation would result in a shoreface sandstone thicknesses that is ideally as thick as the shoreface sand pinch-out water depth (up to 20 m) (Fig. 1a). The base shoreface sand and the toe of the shoreface-clinoform are likely to be located at approximately the same bathymetric position, and provided constant sediment supply, such a progradation will continue until the delta reaches deeper water. Further, the lack of accommodation created on the coastal plain would be expected to prevent the formation of lagoons in the continental environment, and a strandplain is likely to be formed instead (Fig. 1).

Mode B (Figs. 1, 2): If a rise in relative sea level commences during regression, the progradation will be transformed from mode A to mode B, and be accompanied by vertical stretching (over-thickening) of facies belts (Fig. 1b) (**Chapter 2**). The amount of stretching is mainly dependent on the dip-directed length of the shoreface sand and the amount of rise in relative sea level. The increasing accommodation created on the continental plain during the rise in relative sea level is likely to be associated with development of a lagoon-barrier coast (Fig. 1). This type of regression can be exemplified by the over-thickened shoreface sandstones of the Rannoch-Etive formations resulting from the progradation of the Brent delta lagoon-barrier coast (**Chapter 2**).

At the onset of the rise in relative sea level, the base shoreface sand and toe of the shoreface-clinoform are likely to be located at approximately the same water depth (Fig. 1). This implies the toe of the shoreface-clinoform is associated with a sedimentological contrast from (homogenous) shoreface sand to offshore transition mud-sand heterolithics. Progradation during a rise in relative sea level is commonly associated with increasing clinoform size (increasing foreset length and height) (e.g. Driscoll, N. W. & Karner, G. D., 1999) due to greater aggradation at the topset compared to the bottomset (Fig. 1). However, shoreface sands along wave-dominated coastlines are commonly reported to extend no deeper than to 20 m water depth (**Chapter 2**) (cf. van Straaten, L. M. J. U., 1959; Curray, J. R. *et al.*, 1969; Colantoni, P. *et al.*, 1979; Howard, J. D. & Reineck, H.-E., 1981; Bellotti, P. *et al.*, 1994; Diaz, J. I. *et al.*, 1996; Rodriguez, A. B. *et al.*, 2001), even if the clinoform height may be considerably larger (80 m or more) (Scruton, P. C., 1960; Friedman, G. M. *et al.*, 1992). Consequently, when a rise in relative sea level commences, the toe of shoreface-clinoform trajectory is likely to diverge with the base shoreface sand trajectory and the associated shoreline trajectory, resulting in a successively increasing clinoform size (Fig. 1). The toe of the shoreface-clinoform will then no longer represent a sedimentological transition from (homogenous) shoreface sand to an offshore transition environment, but a change from e.g. sand-dominated to mud-dominated heterolitics, or separate areas with different sediment accumulation rates (cf. Friedman, G. M. *et al.*, 1992; Rodriguez, A. B. *et al.*, 2001).

Mode C (Figs. 1, 2): During continued rise in relative sea level, the mode B delta will not be able to regress the coastline along its full extent. Due to the rise in relative sea level, supply of sediment and accompanying strike feeding will be too low to maintain progradation. Consequently, barriers that may have existed will move landwards in a gradual or stepped manner (Nummedal, D. *et al.*, 1987; Friedman, G. M. *et al.*, 1992; Reading, H. & Collinson, J., 1996, and references within these). Still, the high sediment supply close to the fluvial channel belt and at the river mouth will enable the channel-overbank areas to aggrade and mouth bars to prograde at the same time as the barriers move landwards. The lagoons will eventually be located in topographical lows between main channel belts on the continental plain, and some distance landwards from the river outlets.

Associated with this rearrangement of the nearshore depositional environments, the coastline transforms from a relatively linear to a high curvature coastline. As a consequence, regressive-transgressive cycles, or parasequences (sensu Van Wagoner, J. C. *et al.*, 1990) are likely to develop as result of repeated over-extension of the fluvial system causing the rivers to choose shorter and steeper gradients to the sea **(Chapter 3**) (e.g. van Straaten, L. M. J. U., 1959; Scruton, P. C., 1960; Elliott, T., 1986a). However, as long as the bay line (defined as the demarcation line between fluvial environments appearing above sea level and paralic/delta plain environments (Posamentier, H. W. *et al.*, 1988)) moves overall seawards, the delta system will be prograding. If the accommodation/sediment supply ratio is gradually increasing with time, the delta system may evolve from initially having a: *progradational* bay line, through a *stationary* bay line, into finally a *retrogradational* bay line (Posamentier, H. W. *et al.*, 1988). This evolution can be exemplified by the development of the Kenilworth Member in the Blackhawk Formation (Fig 13e in **Chapter 3**) and possibly also by the transition from the regressive Rannoch-Etive formations (mode B) to the overall landward-stepping, regressive-transgressive cycles of the Tarbert Formation (mode C) (e.g. Graue, E. *et al.*, 1987; Rønning, K. & Steel, R. J., 1987; Fält, L. M. *et al.*, 1989) (**Chapter 2).**

Stage II: Shelf-margin construction and progradation

Mode D (Figs. 1, 2): The termination of the ramp-margin stage, and the construction of a shelf-margin represented by clinoforms that are more than 100 to a couple of 100's metres high (e.g. Hedberg, H. D., 1972; Steckler, M. S. *et al.*, 1999) depends on several factors. Firstly, the long term rise in relative sea level (effectuated by basinal subsidence) must be sufficient to accommodate such high relief features, and secondly, sediment supply must be sufficient to fill the accommodation and accrete the margin. Once progradation of a high-curvature coastline (mode C) has been established, the fluvial system is likely to be locally and periodically over-extended, causing fluvial avulsion and rivers taking shorter and steeper routes to the interdeltaic embayments (e.g. Scruton, P. C., 1960; Elliott, T., 1986a). With time, the flooding of starved and subsiding delta lobes results in the focus of sedimentation being repeatedly moved landward, in turn causing the delta plain environment to aggrade at a rate by far exceeding aggradation in more offshore mud dominated distal positions. Such a differential aggradation will result in the superposition of successive shoreline breaks, eventually developing high-relief clinoforms of shelf-margin scale (up to a couple of 1000 metres high) (cf. Steckler, M. S. *et al.*, 1999) (Fig. 1).

Once established, the shelf-margin clinoforms start to grow in size, with a migratory path that can be described in terms of the shelf edge trajectory (Steel, R. J. *et al.*, 2000; Steel, R. J. & Olsen, T., 2002). As long as the shelf-margin clinoform progrades with more or less constant foreset geometry (i.e. sedimentation aggradation being equal along the foreset), the margin is likely to migrate as a graded margin (sensu Hedberg, H. D., 1972; Ross, W. C. *et al.*, 1994). Such a margin-type progrades in equilibrium with depositional and erosional processes and is not associated with larger shelf edge failures as these are likely to be caused by oversteepening along the upper foreset (see below).

Neither the mode B Brent delta nor the parasequences in the Blackhawk depositional system (**Chapter 3)** developed shelf-margin clinoforms because the rise in relative sea level in the basin was not sufficient to accommodate such large scale geometries. In contrast, in the Deltana Amacuro Platform area (**Chapter 4)**, the rise in relative sea level was sufficient to develop a shelf-margin clinoform (graded margin) with an associated deep marine depositional system.

Mode E (Figs. 1, 2): Shelf edge failures form as a result of the shear stress component of gravity exceeding the shear strength along seaward dipping surfaces of weakness (e.g. Rowan, M. G. *et al.*, 2004) (e.g. a seawards dipping submerged palaeo-continental slope). When increasing the angle of a shelf edge trajectory, there are two factors that makes shelf edge failures more probable to occur than with a horizontal trajectory: 1) the rise in relative sea level will cause the clinoform foreset to become longer, and to steepen along the upper slope (Ross, W. C. *et al.*, 1994), and 2) the effect of loading along the shelf edge will increase (cf. Fig 15d in **Chapter 4**). These two contributions to the stress regime associated with potential shelf edge failure make it more likely that the critical shear strength along a seaward dipping surface is reached, with episodic shelf edge failures as the result. The failure is followed by a healing phase where the erosional concavity (typically cutting up to 100 m deep) resulting from the shelf edge failure is smoothened. After this healing phase, continued regression may lead to the critical shear strength along a surface of weakness again being reached, causing renewed shelf edge failure. If such collapse-healing cycles are being repeated, the progradation will be in accordance with Ross et al.'s (1994) model of slope readjustments for erosive margins (Fig. 1, 2) (sensu Hedberg, H. D., 1972; Ross, W. C. *et al.*, 1994).

Mode F (Figs. 1, 2): As noted above, if a shelf-margin is prograding during rise in relative sea level or into deeper waters the clinoform size (foreset length and height) is likely to increase due to diverging shelf edge and base-of-slope trajectories. This is associated with the build-up of differential seaward and landward horizontal overburden stress which eventually will cause the margin to experience long term (100s ka-several Ma) growth faulting (cutting 1000s of metres deep) (Fig. 1, 2) (cf. Fig 18 in **Chapter 4**) that will prevent further seaward progradation.

This progradational mode was reached tn the Columbus Basin where the collapse affected the terrestrial environment in that fluvial channel belts were deviated to trend parallel to strike of faults. The collapse also lowered the depositional profile across the margin and thereby decreasing the amount of episodic shelf edge failures. On a regional scale, the accommodation created by the growth faulting provided a sediment trap which caused the margin to be halted from further seaward progradation. If the growth faulting will continue until sufficiently extensional to trigger diapiric growth, the margin will develop into a diapiric over-ride phase (Winker, C. D. & Edwards, M. B., 1983) where the stratigraphic architecture is dominated by deformation driven by rising diapirs.

Discussion

The above shows that progradation during rising relative sea level ideally can be divided into 6 modes which are successively initiated with increasing rise in relative sea level. The termination of one progradational mode and the onset of another is related to threshold values in the accommodation/sediment supply ratio (all modes represent long term regressions which imply that the overall sediment supply exceeds accommodation).

Trajectory analysis has previously been applied in sequence stratigraphic studies where sediment partitioning has been coupled to oscillating relative sea level, but not to threshold values within the sediment supply/accommodation budget (*without* oscillating sea-level). Steel and Olsen (2002) suggested basin floor sedimentation to be more likely during horizontal to falling shelf edge trajectories, as falling relative sea level enables the establishment of slope channel systems conducting sediments to bottomset positions. Further, Plink-Björklund and Steel (2002) stressed the *amount* of fall in relative sea level and its effect on deposition. In outcrops in Spitsbergen, Norway, they found that falling shoreline trajectories extending below the shelf edge are associated *with* incision of fluvial channels into the shelf edge and concomitant development of basin floor fans. In contrast, shorelines prograding to below the shelf edge *without* incision were associated with upper slope fans.

If the accommodation/sediment supply ratio fluctuates sufficiently with time, the progradation may also alternate between different modes. For example, the alternation between modes A and B has been documented in modern deltas where the presence of lagoons is related to rapidly rising sea level, whereas slowly rising or stable sea level is associated with strandplains (Dominguez, J. M. L. *et al.*, 1987; Bellotti, P. *et al.*, 1994). A second example is the reinterpretation of the classical seismic section originally presented by Mitchum and Vail

(1977) and Todd and Mitchum (1977) (Payton, C. E., 1977, p. 137 and 157) by Winker and Edwards (1983 their Fig. 1). This cross-section may be interpreted as a change from a mode D graded margin to a mode F collapse margin, and then back into a mode D graded margin progradation (subsequent to a fall in relative sea level).

Clearly, the threshold values that separate the above progradational modes do not correspond to the boundaries of systems tracts of traditional sequence stratigraphy, which are largely based on position within a predefined fluctuating sea level curve. Traditional sequence stratigraphy would classify all of the above modes as either the highstand systems tract (Posamentier, H. W. *et al.*, 1988; Posamentier, H. W. & Vail, P. R., 1988; Van Wagoner, J. C. *et al.*, 1988; Van Wagoner, J. C. *et al.*, 1990) or lowstand wedge systems tract (Hunt, D. & Tucker, M. E., 1992; Nummedal, D., 1992; Helland-Hansen, W. & Gjelberg, J. G., 1994). Hence, trajectory analysis together with the appreciation of the importance of basin physiography embraces other controls on sedimentation than traditional systems tract analysis, such as the identification of threshold levels through varying accommodation/sediment supply scenarios as exemplified by the modes A-F outlined above.

Conclusions

- This dissertation present data from the Middle Jurassic Brent delta, the Upper Cretaceous Blackhawk Formation, and the Pleistocene successions in the Columbus Basin and Deltana Amacuro PLatform, offshore Venezuela. The studied successions all represent overall normal regressive depositional systems located within different structural settings. The basins experienced different rates of subsidence, which enabled comparison of the stratigraphic architecture associated with progradation under conditions of variable amounts and rates of rise in relative sea level.
- A comparison of the study areas concludes that long term normal regressive deposits comprising wave-dominated delta systems can ideally be divided into 6 progradational modes which are successively initiated during progradation with increasing rise in relative sea level. The termination of one progradational mode and the onset of another are related to threshold values in the accommodation/sediment supply ratio.
- Within a traditional sequence stratigraphic framework, the progradational modes would be classified as a highstand or a lowstand wedge system tract. Hence, this dissertation

emphasises that trajectory analysis is able to point to other important controls on sedimentation than fluctuations in sea level.

References

ADAMS, M.M. & BHATTACHARYA, J.P. (2005) No Change in Fluvial Style across a Sequence Boundary, Cretaceous Blackhawk and Castlegate Formations of Central Utah, U.S.A. *Journal of Sedimentary Research*, **75,** 1038-1051.

AHR, W.M. (1973) The Carbonate Ramp: An Alternative to the Shelf Model. *Transactions, Gulf Coast Association of Geological Societies*, **57,** 221–225.

AINSWORTH, R.B. & PATTISON, S.A.J. (1994) Where Have All the Lowstands Gone? Evidence for Attached Lowstand Systems Tracts in the Western Interior of North America. *Geology*, **22,** 415-418.

BALSLEY, J.K. (1980) Cretaceous Wave-Dominated Delta Systems, Book Cliffs, Eastern Central Utah. Continuing Education Course Field Guide., AAPG**,** 161.

BELDERSON, R.H., KENYON, N.H., STRIDE, A.H. & PELTON, C.D. (1984) A "Braided" Distributary System on the Orinoco Deep-Sea Fan. *Marine Geology*, **56,** 195-206.

BELLOTTI, P., CHIOCCI, F.L., MILLI, S., TORTORA, P. & VALERI, P. (1994) Sequence Stratigraphy and Depositional Setting of the Tiber Delta; Integration of High-Resolution Seismics, Well Logs, and Archaeological Data. *Journal of Sedimentary Research*, **64,** 416-432.

BERG, O.R. & WOOLVERTON, D.G. (1985) *Seismic Stratigraphy Ii; an Integrated Approach to Hydrocarbon Exploration*. AAPG.

BHATTACHARYA, J.P. & WILLIS, B.J. (2001) Lowstand Deltas in the Frontier Formation, Powder River Basin, Wyoming: Implications for Sequence Stratigraphic Models. *AAPG Bulletin*, **85,** 261-294.

BHATTACHARYA, J.P. & GIOSAN, L. (2003) Wave-Influenced Deltas; Geomorphological Implications for Facies Reconstruction. *Sedimentology*, **50,** 187-210.

BOWMAN, A., P (2003) Sequence Stratigraphy and Reservoir Characterization in the Columbus Basin, Trinidad. *PhD Thesis, Imperial College of Science, Technology & Medicine, Univ. of London, UK.*

BROWN, S. & RICHARDS, P.C. (1989) Facies and Development of the Middle Jurassic Brent Delta near the Northern Limit of Its Progradation, Uk North Sea. In: *Deltas: Sites and Traps for for Fossile Fuel* (Ed. by M. K. G. Whateley & K. T. Pickering), **Special Publication 41**, 253-267. Blackwell Scientific Publications. Geological Society, London.

BROWN, S. (1990) The Jurassic. In: *Introduction to the Petroleum Geology of the North Sea* (Ed. by K. W. Glennie), 219-254. Blackwell Scientific Publications, Oxford.

BRUCE, C.H. (1973) Pressured Shale and Related Sediment Deformation; Mechanism for Development of Regional Contemporaneous Faults. *AAPG Bulletin*, **57,** 878-886.

BUDDING, M.C. & INGLIN, H.F. (1981) A Reservoir Geological Model of the Brent Sands in Southern Cormorant. In: *Petroleum Geology of the Continental Shelf of North-West Europe; Proceedings of the Second Conference* (Ed. by L. V. Illing & G. D. Hobson), 326-334. Heyden and Son, London.

BULLIMORE, S.A. & HELLAND-HANSEN, W. (2002) Coastal Plain Facies and Shoreface Thickness; a Predictive Relationship? *Annual Meeting Expanded Abstracts - AAPG*, **2002,** 25.

BURGESS, P.M. & HOVIUS, N. (1998) Rates of Delta Progradation During Highstands; Consequences for Timing of Deposition in Deep-Marine Systems. *Journal of the Geological Society*, **155,** 217-222.

CALDWELL, W.G.E. & KAUFFMAN, E.G. (1993) *Evolution of the Western Interior Basin*. Geological Association of Canada, Newfoundland.

CANNON, S.J.C., GILES, M.R., WHITAKER, M.F., PLEASE, P.M. & MARTIN, S.V. (1992) A Regional Reassessment of the Brent Group, Uk Sector, North Sea. In: *Geology of the Brent Group* (Ed. by A. C. Morton, R. S. Haszeldine, M. R. Giles & S. Brown), **Special Publications 61**, 81-107. Geological Society London.

CANT, D.J. (1991) Geometric Modelling of Facies Migration; Theoretical Development of Facies Successions and Local Unconformities. *Basin Research*, **3,** 51-62.

CARROLL, A.R. & BOHACS, K.M. (1999) Stratigraphic Classification of Ancient Lakes: Balancing Tectonic and Climatic Controls. *Geology*, **27,** 99-102.

CARVAJAL, C.R. & STEEL, R.J. (2006) Thick Turbidite Successions from Supply-Dominated Shelves During Sea-Level Highstand. *Geology*, **34,** 665-668.

CLIFTON, E.H. (2000) Shoreface Myths and Misconceptions. *Annual Meeting Expanded Abstracts - AAPG*, 29.

COBBOLD, P.R. & SZATMARI, P. (1991) Radial Gravitational Gliding on Passive Margins. *Tectonophysics*, **188,** 249-289.

COE, A.L., BOSENCE, D.W.J., CHURCH, K.D., FLINT, S.S., HOWELL, J.A. & WILSON, R.C.L. (2003) *The Sedimentary Record of Sea-Level Change*. Cambridge University Press., Cambridge.

COLANTONI, P., GALLIGNANI, P. & LENAZ, R. (1979) Late Pleistocene and Holocene Evolution of the North Adriatic Continental Shelf (Italy). *Marine Geology*, **33,** 41-50.

CORFIELD, S., SHARP, I., HÄGER, K., DREYER, T. & UNDERHILL, J.R. (2001) An Integrated Study of Garn and Melke Formations (Middle to Upper Jurassic) of the Smørbukk Area, Halten Terrace, Mid-Norway. In: *Sedimentary Environments Offshore Norway - Paleozoic to Recent* (Ed. by O. J. Martinsen & T. Dreyer), **Special Publication 10**, 199-210. Norwegian Petroleum Society (NPF) Elseivier Science Amsterdam.

CRABAUGH, J.P. (2003) Facies Architecture and Shoreline Trajectory in the Sandstone Tongues of the Lower Iles Formation, Mesaverde Group (Campanian), Northwest Colorado. *Annual Meeting Expanded Abstracts - AAPG*, **12,** 34.

CRANS, W., MANDL, G. & HAREMBOURE, J. (1980) On the Theory of Growth Faulting; a Geomechanical Delta Model Based on Gravity Sliding. *Journal of Petroleum Geology*, **2,** 265-307.

CURRAY, J.R., EMMEL, F.J. & CRAMPTON, P.J.S. (1969) Holocene History of a Strand Plain, Lagoonal Coast, Nayarit, Mexico. *Lagunas Costeras, UN Simposio, Memorias del Simposio Internacional Lagunas Costeras. UNAM-UNESCO, Noviembre 28-30, 1967, México D.F*, 63-100.

DAVIES, R., DIESSEL, C., HOWELL, J., FLINT, S. & BOYD, R. (2005) Vertical and Lateral Variation in the Petrography of the Upper Cretaceous Sunnyside Coal of Eastern Utah, USA; Implications for the Recognition of High-Resolution Accommodation Changes in Paralic Coal Seams. *International Journal of Coal Geology*, **61,** 13-33.

DAVIES, R., HOWELL, J., BOYD, R., FLINT, S. & DIESSEL, C. (2006) High-Resolution Sequence-Stratigraphic Correlation between Shallow-Marine and Terrestrial Strata: Examples from the Sunnyside Member of the Cretaceous Blackhawk Formation Book Cliffs Eastern Utah. *AAPG Bulletin*, **90,** 1121-1140.

DEJONG, K.A. & SCHOLTEN, R. (1973) *Gravity and Tectonics*. John Wiley & Sons., New York.

DEMERCIAN, S., SZATMARI, P. & COBBOLD, P.R. (1993) Style and Pattern of Salt Diapirs Due to Thin-Skinned Gravitational Gliding, Campos and Santos Basins, Offshore Brazil. *Tectonophysics*, **228,** 393-433.

DI CROCE, J., BALLY, A.W. & VAIL, P. (1999) Sequence Stratigraphy of the Eastern Venezuelan Basin. In: *Sedimentary Basins of the World* (Ed. by P. Mann), **4**, 419-476. Elsevier.

DIAZ, J.I., PALANQUES, A., NELSON, C.H. & GUILLEN, J. (1996) Morpho-Structure and Sedimentology of the Holocene Ebro Prodelta Mud Belt, Northwestern Mediterranean Sea. *Continental Shelf Research*, **16,** 435-456.

DOMINGUEZ, J.M.L., MARTIN, L. & BITTENCOURT, A.C.S.P. (1987) Sea-Level History and Quaternary Evolution of River Mouth-Associated Beach-Ridge Plains Along the East-Southeast Brazilian Coast; a Summary. In: *Sea-Level Fluctuation and Coastal Evolution* (Ed. by D. Nummedal, O. Pilkey & J. Howard), **Special Publication 41**, 115-127. Society of Economic Paleontologists and Mineralogists

DORE, A.G., LUNDIN, E.R., JENSEN, L.N., BIRKELAND, O., ELIASSEN, P.E. & FICHLER, C. (1999) Principal Tectonic Events in the Evolution of the Northwest European Atlantic Margin. In: *Petroleum Geology of Northwest Europe: Proceedings of the 5th Conference* (Ed. by A. J. Fleet & S. A. R. Boldy), **5**, 41-61. Geological Society, London.

DRISCOLL, N.W. & KARNER, G.D. (1999) Three-Dimensional Quantitative Modeling of Clinoform Development. *Marine Geology*, **154,** 383-398.

ELLIOTT, T. (1986a) Deltas. In: *Sedimentary Environments and Facies* (Ed. by H. G. Reading), 113-154. Blackwell Scientific Publications, Oxford.

ELLIOTT, T. (1986b) Siliciclastic Shorelines. In: *Sedimentary Environments and Facies* (Ed. by H. Reading), 155-188. Blackwell Scientific Publications, Oxford.

EMBRY, A.F. (1993) Transgressive-Regressive (T-R) Sequence Analysis of the Jurassic Succession of the Sverdrup Basin, Canadian Arctic Archipelago. *Canadian Journal of Earth Sciences = Journal Canadien des Sciences de la Terre*, **30,** 301-320.

ERCILLA, G., ALONSO, B., WYNN, R.B. & BARAZA, J. (2002) Turbidity Current Sediment Waves on Irregular Slopes; Observations from the Orinoco Sediment-Wave Field. *Marine Geology*, **192,** 171-187.

FINNERAN, J.M. & BALLY, K. (1999) Petrophysical Characteristics of an Emerging Giant Gas Province: The Columbus Basin, Southeast Coast of Trinidad. *AAPG International Conference held in Birmingham England*

FJELLANGER, E., OLSEN, T. & RUBINO, J.L. (1996) Sequence Stratigraphy and Regional Paleogeography of the Middle Jurassic Brent Delta System, Northern North Sea. *Norsk Geologisk Tidsskrift*, **76,** 75-106.

FRIEDMAN, G.M. & SANDERS, J.E. (1978) *Principles of Sedimentology*. New York, John Wiley & Sons.

FRIEDMAN, G.M., SANDERS, J.E. & KOPASKA-MERKEL, D.C. (1992) *Principles of Sedimentary Deposits; Stratigraphy and Sedimentology*. Macmillan Publ. Co., New York, NY.

FÄLT, L.M., HELLAND, R., JACOBSEN, V.W. & RENSHAW, D. (1989) Correlation of Transgressive-Regressive Depositional Sequences in the Middle Jurassic Brent/Vestland Group Megacycle, Viking Graben, Norwegian North Sea. In: *Correlation in Hydrocarbon Exploration* (Ed. by J. D. Collinson), 191-201. Graham & Trotman, London.

GALLOWAY, W.E. (1986) Growth Faults and Fault-Related Structures of Prograding Terrigenous Clastic Continental Margins. *Gulf Coast Association of Geological Societies Transactions*, **36,** 121-128.

GALLOWAY, W.E. (1989) Genetic Stratigraphic Sequences in Basin Analysis 1. Architecture and Genesis of Flooding-Surface Bounded Depositional Units. *AAPG Bulletin*, **73,** 125-142.

GRAUE, E., HELLAND-HANSEN, W., JOHNSON, J., LØMO, L., NØTTVEDT, A., RØNNING, K., RYSETH, A. & STEEL, R. (1987) Advance and Retreat of Brent Delta System, Norwegian North Sea. In: *Petroleum Geology of North West Europe* (Ed. by J. Brooks & K. W. Glennie), 915-937. Graham & Trotman, London.

HAMPSON, G.J. (2000) Discontinuity Surfaces, Clinoforms, and Facies Architecture in a Wave-Dominated, Shoreface-Shelf Parasequence. *Journal of Sedimentary Research*, **70,** 325-340.

HAMPSON, G.J. & STORMS, J.E.A. (2003) Geomorphological and Sequence Stratigraphic Variability in Wave-Dominated, Shoreface-Shelf Parasequences. *Sedimentology*, **50,** 667-701.

HAMPSON, G.J. & HOWELL, J.A. (2005) Sedimentologic and Geomorphic Characterization of Ancient Wave-Dominated Deltaic Shorelines; Upper Cretaceous Blackhawk Formation, Book Cliffs, Utah, U. S. A. In: *New Directions in Deltaic Studies* (Ed. by L. Giosan & J. P. Bhattacharya), **Special Publication 83**, 133-154. Society for Sedimentary Geology.

HAQ, B.U., HARDENBOL, J. & VAIL, P.R. (1987) Chronology of Fluctuating Sea Levels since the Triassic. *Science*, **235,** 1156-1167.

HEDBERG, H.D. (1972) Continental Margins from Viewpoint of the Petroleum Geologist. In: *Reprint Series* (Ed. by, **3**, 154-194. AAPG Tulsa.

HELLAND-HANSEN, W., ASHTON, M., LØMO, L. & STEEL, R. (1992) Advance and Retreat of the Brent Delta; Recent Contributions to the Depositional Model. In: *Geology of the Brent Group* (Ed. by A. C. Morton, R. S. Haszeldine, M. R. Giles & S. Brown), **Special Publications 61**, 109-127. Geological Society, London.

HELLAND-HANSEN, W. & GJELBERG, J.G. (1994) Conceptual Basis and Variability in Sequence Stratigraphy; a Different Perspective. *Sedimentary Geology*, **92,** 31-52.

HELLAND-HANSEN, W. (1995) Sequence Stratigraphy: Remarks and Recommendations. In: *Sequence Stratigraphy on the Northwest European Margin* (Ed. by R. Steel, V. L. Fält, E. P. Johannessen & C. Matieu), **Special Publication 5**. Norwegian Petroleum Society (NPF) Elsevier, Amsterdam.

HELLAND-HANSEN, W. & MARTINSEN, O.J. (1996) Shoreline Trajectories and Sequences; Description of Variable Depositional-Dip Scenarios. *Journal of Sedimentary Research*, **66,** 670-688.

HELLAND-HANSEN, W. (2007). *Trajectory Analysis: Concepts, Cases and Challenges*. SEST, the first conference on shelf edge and shoreline trajectories, a dynamic approach to stratigraphic analysis, Tromsø, Norway.

HOWARD, J.D. & REINECK, H.-E. (1981) Depositional Facies of High-Energy Beach-to-Offshore Sequence; Comparison with Low-Energy Sequence. *AAPG Bulletin*, **65,** 807-830.

HOWELL, J. & FLINT, S. (2003) Siliciclastic Case Study: The Book Cliffs. In: *The Sedimentary Record of Sea-Level Change* (Ed. by A. Coe, D. Bosence, K. Church, S. Flint, J. Howell & C. Wilson), 135-208.

HOWELL, J.A., FLINT, S. & HUNT, C. (1996) Sedimentological Aspects of the Humber Group (Upper Jurassic) of the South Central Graben, Uk North Sea. *Sedimentology*, **43,** 89-114.

HUBBARD, R.J. (1988) Age and Significance of Sequence Boundaries on Jurassic and Early Cretaceous Rifted Continental Margins. *AAPG Bulletin*, **72,** 49-72.

HUNT, D. & TUCKER, M.E. (1992) Stranded Parasequences and the Forced Regressive Wedge Systems Tract; Deposition During Base-Level Fall. *Sedimentary Geology*, **81,** 1-9.

JENNETTE, D.C. & RILEY, C.O. (1996) Influence of Relative Sea-Level on Facies and Reservoir Geometry of the Middle Jurassic Lower Brent Group, Uk North Viking

Graben. In: *Geological Society* (Ed. by J. A. Howell & J. F. Aitken), **Special Publications 104**, 87-113.
JOHANNESSEN, E.P., MJØS, R., RENSHAW, D., DALLAND, A. & JACOBSEN, B. (1995) Northern Limit of The "Brent Delta" On the Tampen Spur - a Sequence Stratigraphic Approach to Sandstone Prediction. In: *Sequences Stratigraphy on the Northwest European Margin* (Ed. by R. Steel, V. L. Fält, E. P. Johannessen & C. Mathieu), **Special Publication 5**, 361-372. Norwegian Petroleum Society (NPF), Elsevier, Amsterdam.
KAMOLA, D.L. (1984) Trace Fossils from Marginal-Marine Facies of the Spring Canyon Member, Blackhawk Formation (Upper Cretaceous), East-Central Utah. *Journal of Paleontology*, **58,** 529-541.
KAMOLA, D.L. & HUNTOON, J.E. (1995) Repetitive Stratal Patterns in a Foreland Basin Sandstone and Their Possible Tectonic Significance. *Geology*, **23,** 177-180.
KAMOLA, D.L. & VAN WAGONER, J.C. (1995) Stratigraphy and Facies Architecture of Parasequences with Examples from the Spring Canyon Member, Blackhawk Formation, Utah. In: *Sequence Stratigraphy of Foreland Basin Deposits; Outcrop and Subsurface Examples from the Cretaceous of North America* (Ed. by J. C. Van Wagoner & G. T. Bertram), **Memoir 64**, 27-54. AAPG.
KAUFFMAN, E.G. & CALDWELL, W.G.E. (1993) The Western Interior Basin in Space and Time. In: *Evolution of the Western Interior Basin* (Ed. by W. G. E. Caldwell & E. G. Kauffman), **Special Publication 39**, 1-30. Geological Association of Canada.
KUEHL, S.A., HARIU, T.M. & MOORE, W.S. (1989) Shelf Sedimentation Off the Ganges-Brahmaputra River System; Evidence for Sediment Bypassing to the Bengal Fan. *Geology*, **17,** 1132-1135.
LARUE, D.K. & MARTINEZ, P.A. (1989) Use of Bed-Form Models to Analyze Geometry and Preservation Potential of Clastic Facies and Erosional Surfaces. *AAPG Bulletin*, **73,** 40-53.
LEONARD, R. (1983) Geology and Hydrocarbon Accumulations, Columbus Basin, Offshore Trinidad. *AAPG Bulletin*, **67,** 1081-1093.
LIVERA, S.E. (1989) Facies Associations and Sand-Body Geometries in the Ness Formation of the Brent Group, Brent Field. In: *Deltas: Sites and Traps for for Fossile Fuel* (Ed. by M. K. G. Whateley & K. T. Pickering), **Special Publication 41**, 269-286. Geological Society London.
LØSETH, T.M. & HELLAND-HANSEN, W. (2001) Predicting the Pinchout Distance of Shoreline Tongues. *Terra Nova*, **13,** 241-248.
LØSETH, T.M., STEEL, R.J., CRABAUGH, J.P. & SCHELLPEPER, M. (2006) Interplay between Shoreline Migration Paths, Architecture and Pinchout Distance for Siliciclastic Shoreline Tongues: Evidence from the Rock Record. *Sedimentology*, **53,** 735-U736.
MALLIK, T.K. (1976) Shelf Sediments of the Ganges Delta with Special Emphasis on the Mineralogy of the Western Part, Bay of Bengal, Indian Ocean. *Marine Geology,* **22,** 1-32.
MAUDUIT, T., GUERIN, G., BRUN, J.P. & LECANU, H. (1997) Raft Tectonics; the Effects of Basal Slope Angle and Sedimentation Rate on Progressive Extension. *Journal of Structural Geology*, **19,** 1219-1230.
MCCLELLAND ENGINEERS (1979) Interpretation and Assessment of Shallow Geological and Geotechnical Conditions, Orinoco Regional Survey Areas, Offshore Orinoco Delta, Venezuela. . *Unpublished report to Instituto Tecnologico Venezolano del Petróleó, Job no 13051, Caracas, Venezuela,***,** 55.
MCCUBBIN, D.G. (1982) Barrier-Island and Strand-Plain Facies. In: *Sandstone Depositional Environments* (Ed. by P. A. Scholle & D. R. Spearing), **Memoir 31**, 247-279. AAPG.

MELLERE, D. & STEEL, R.J. (1995) Facies Architecture and Sequentiality of Nearshore and Shelf Sandbodies; Haystack Mountains Formation, Wyoming, USA. *Sedimentology*, **42,** 551-574.
MELLERE, D. & STEEL, R. (1995b) Variability of Lowstand Wedges and Their Distinction from Forced-Regressive Wedges in the Mesaverde Group, Southeast Wyoming. *Geology*, **23,** 803-806.
MELLERE, D., PLINK-BJÖRKLUND, P. & STEEL, R. (2002) Anatomy of Shelf Deltas at the Edge of a Prograding Eocene Shelf Margin, Spitsbergen. *Sedimentology*, **49,** 1181-1206.
MIALL, A.D. (1986) Eustatic Sea Level Changes Interpreted from Seismic Stratigraphy; a Critique of the Methodology with Particular Reference to the North Sea Jurassic Record. *AAPG Bulletin*, **70,** 131-137.
MILANKOVITCH, M. (1941) Kanon Der Erdbestrahlung Und Seine Andwendenung Auf Das Eiszeitenproblem (Ed. by, **Special Publication 132, Vol 33**. Royal Serbian Sciences, Section of Mathematical and Natural Sciences, Belgrade.
MITCHENER, B.C., LAWRENCE, D.A., PARTINGTON, M.A., BOWMAN, M.B.J. & GLUYAS, J. (1992) Brent Group; Sequence Stratigraphy and Regional Implications. In: *Geology of the Brent Group* (Ed. by A. C. Morton, R. S. Haszeldine, M. R. Giles & S. Brown), **Special Publication 61**, 45-80. Geological Society
MITCHUM, R.M. & VAIL, P.R. (1977) Part 7, Seismic Stratigraphic Interpretation Procedure. In: *Seismic Stratigraphy and Global Changes of Sea Level* (Ed. by C. E. Payton), **Memoir 26**, 135-143. AAPG.
MORRIS, J., HAMPSON, G.J. & MAXWELL, G. (2003) Controls on Facies Architecture in the Brent Group, Strathspey Field, Uk North Sea; Implications for Reservoir Characterization. *Petroleum Geoscience,* **9,** 209-220.
MUTO, T. & STEEL, R.J. (1992) Retreat of the Front in a Prograding Delta. *Geology*, **20,** 967-970.
MUTO, T. & STEEL, R.J. (1997) Principles of Regression and Transgression; the Nature of the Interplay between Accommodation and Sediment Supply. *Journal of Sedimentary Research*, **67,** 994-1000.
MUTO, T. & STEEL, R.J. (2002a) Role of Autoretreat and a/S Changes in the Understanding of Deltaic Shoreline Trajectory; a Semi-Quantitative Approach. *Basin Research*, **14,** 303-318.
MUTO, T. & STEEL, R.J. (2002b) In Defense of Shelf-Edge Delta Development During Falling and Lowstand of Relative Sea Level. *Journal of Geology*, **110,** 421-436.
NIEDORODA, A.W., SWIFT, D.J.P., HOPKINS, T.S. & MA, C.-M. (1984) Shoreface Morphodynamics on Wave-Dominated Coasts. *Marine Geology*, **60,** 331-354.
NIEDORODA, A.W., SWIFT, D.J.P. & HOPKINS, T.S. (1985) The Shoreface. In: *Coastal Sedimentary Environments* (Ed. by R. A. Davis), 533-624. Springer-Verlag, New York, NY.
NUMMEDAL, D., PILKEY, O.H. & HOWARD, J.D. (1987) *Sea Level Fluctuation and Coastal Evolution*. Society of Economic Paleontologists and Mineralogists.
NUMMEDAL, D. (1992) The Falling Sea Level Systems Tract in Ramp Settings. *SEPM 1992 theme meeting; Mesozoic of the Western Interior; abstracts*, Society for Sedimentary Geology. Tulsa, OK**,** 50.
NYSTUEN, J.P. (1998) History and Development of Sequence Stratigraphy. In: *Sequence Stratigraphy, Concepts and Applications* (Ed. by F. M. Gradstein, K. O. Sandsvik & N. J. Milton), **Special Publication 8**. Norwegian Petroleum Society (NPF).
O'BYRNE, C.J. & FLINT, S. (1995) Sequence, Parasequence, and Intraparasequence Architecture of the Grassy Member, Blackhawk Formation, Book Cliffs, Utah, U.S.A. In: *Sequence Stratigraphy of Foreland Basin Deposits; Outcrop and Subsurface*

Examples from the Cretaceous of North America. (Ed. by J. C. Van Wagoner & G. T. Bertram), **Memoir 64**, 225-255. AAPG.

OLAUSSEN, S., BECK, L., FÄLT, L.M., GRAUE, E., JACOBSEN, K.G., MALM, O.A. & SOUTH, D. (1992) Gullfaks Field; Norway, East Shetland Basin, Northern North Sea. In: *Structural Traps Vi* (Ed. by N. H. Foster & E. A. Beaumont), **A-24**, 55-83. AAPG Treatise of Petroleum Geology, Atlas of Oil and Gas Fields.

OLSEN, T.R. & STEEL, R. (1995) Shoreface Pinch-out Style on the Front of the Brent Delta in the Easterly Tampen Spur Area. In: *Sequences Stratigraphy on the Northwest European Margin* (Ed. by R. Steel, V. L. Fält, E. P. Johannessen & C. Mathieu), **Special Publication No 5**, 273-290. Norwegian Petroleum Society (NPF) Elsevier, Amsterdam.

OLSEN, T.R. & STEEL, R.J. (2000) The Significance of the Etive Formation in the Development of the Brent System; Distinction of Normal and Forced Regressions. In: *Sedimentary Responses to Forced Regressions* (Ed. by D. Hunt & R. L. Gawthorpe), **Special Publication 172**, 91-112. Geological Society London.

ORTON, G.J. & READING, H.G. (1993) Variability of Deltaic Processes in Terms of Sediment Supply, with Particular Emphasis on Grain Size. *Sedimentology*, **40,** 475-512.

PATTISON, S.A.J. (1995) Sequence Stratigraphic Significance of Sharp-Based Lowstand Shoreface Deposits, Kenilworth Member, Book-Cliffs, Utah. *AAPG Bulletin*, **79,** 444-462.

PATTISON, S.A.J. (2005a) Isolated Highstand Shelf Sandstone Body of Turbiditic Origin, Lower Kenilworth Member, Cretaceous Western Interior, Book Cliffs, Utah, USA. *Sedimentary Geology*, **177,** 131-144.

PATTISON, S.A.J. (2005b) Significance of Inner Shelf Turbiditic-Rich Channel-Fill Deposits, Gunnison Butte to Tusher Canyon Region, Book Cliffs, Eastern Utah. *Abstracts with Programs - Geological Society of America*, **37,** 310.

PATTISON, S.A.J. (2005c) Recognition and Interpretation of Isolated Shelf Turbidite Bodies in the Cretaceous Western Interior, Book Cliffs, Utah. *GSA Field Guide*, **6,** 479-504.

PATTISON, S.A.J. (2005d) Storm-Influenced Prodelta Turbidite Complex in the Lower Kenilworth Member at Hatch Mesa, Book Cliffs, Utah, U.S.A.: Implications for Shallow Marine Facies Models. *Journal of Sedimentary Research*, **75,** 420-439.

PATTISON, S.A.J., AINSWORTH, R.B. & HOFFMAN, T.A. (2007) Evidence of across-Shelf Transport of Fine-Grained Sediments; Turbidite-Filled Shelf Channels in the Campanian Aberdeen Member, Book Cliffs, Utah, USA. *Sedimentology*, **54,** 1033-1063.

PAYTON, C.E. (1977) *Seismic Stratigraphy - Application to Hydrocarbon Exploration*. AAPG.

PLINK-BJÖRKLUND, P. & STEEL, R. (2002) Sea-Level Fall Below the Shelf Edge, without Basin-Floor Fans. *Geology*, **30,** 115-118.

PLINT, A.G. (1988) Sharp-Based Shoreface Sequences And "Offshore Bars" In the Cardium Formation of Alberta; Their Relationship to Relative Changes in Sea Level. In: *Sea-Level Changes: An Integrated Approach* (Ed. by C. K. Wilgus, B. S. Hastings, C. A. Ross, H. Posamentier, J. Van Wagoner & C. G. S. C. Kendall), **Special Publication 42**, 357-370. Society of Economic Paleontologists and Mineralogists.

POREBSKI, S.J. & STEEL, R.J. (2003) Shelf-Margin Deltas: Their Stratigraphic Significance and Relation to Deepwater Sands. *Earth-Science Reviews*, **62,** 283-326.

POSAMENTIER, H.W., JERVEY, M.T. & VAIL, P.R. (1988) Eustatic Controls on Clastic Deposition I, Conceptual Framework. In: *Sea-Level Changes: An Integrated Approach* (Ed. by C. K. Wilgus, B. S. Hastings, C. A. Ross, H. W. Posamentier, J. Van Wagoner & C. G. S. C. Kendall), **Special Publication 42**, 109-124. Society of Economic Paleontologists and Mineralogists.

POSAMENTIER, H.W. & VAIL, P.R. (1988) Eustatic Controls on Clastic Deposition Ii, Sequence and Systems Tract Models. In: *Sea-Level Changes: An Integrated Approach* (Ed. by C. K. Wilgus, B. S. Hastings, C. A. Ross, H. W. Posamentier, J. Van Wagoner & C. G. S. C. Kendall), **Special Publication 42**, 125-154. Society of Economic Paleontologists and Mineralogists.

POSAMENTIER, H.W., ALLEN, G.P., JAMES, D.P. & TESSON, M. (1992) Forced Regressions in a Sequence Stratigraphic Framework; Concepts, Examples, and Exploration Significance. *AAPG Bulletin*, **76,** 1687-1709.

RAMBERG, H. (1981) Gravity, Deformation and the Earth's Crust in Theory, Experiments and Geological Application (2nd Edition) (Ed. by, 452. Academic Press, London.

READING, H. (1978). In: *Sedimentary Environments and Facies* (Ed. by, 569. Blackwell Scientific Publications, Oxford.

READING, H. & COLLINSON, J. (1996) Clastic Coasts. In: *Sedimentary Environments: Processes, Facies and Stratigraphy.* (Ed. by H. Reading), 154-231. Blackwell Science.

REINECK, H.E. & SINGH, I.B. (1973) Depositional Sedimentary Environments; with Reference to Terrigenous Clastics (Ed. by. Springer-Verlag.

REYNOLDS, A.D. (1999) Dimensions of Paralic Sandstone Bodies. *AAPG Bulletin*, **83,** 211-229.

RICHARDS, P.C. & BROWN, S. (1986) Shoreface Storm Deposits in the Rannoch Formation (Middle Jurassic), North West Hutton Oilfield. *Scottish Journal of Geology*, **22,** 367-375.

RICHARDS, P.C. (1992) An Introduction to the Brent Group; a Literature Review. In: *Geology of the Brent Group* (Ed. by A. C. Morton, R. S. Haszeldine, M. R. Giles & S. Brown), **Special Publications 61**, 15-26. Geological Society, London.

RODRIGUEZ, A.B., FASSELL, M.L. & ANDERSON, J.B. (2001) Variations in Shoreface Progradation and Ravinement Along the Texas Coast, Gulf of Mexico. *Sedimentology*, **48,** 837-853.

ROEHLER, H.W. (1990) *Stratigraphy of the Mesaverde Group in the Central and Eastern Greater Green River Basin, Wyoming, Colorado, and Utah*. U. S. Geological Survey Professional Paper

ROSS, W.C., HALLIWELL, B.A., MAY, J.A., WATTS, D.E. & SYVITSKI, J.P.M. (1994) Slope Readjustment; a New Model for the Development of Submarine Fans and Aprons. *Geology*, **22,** 511-514.

ROWAN, M.G., PEEL, F.J. & VENDEVILLE, B.C. (2004) Gravity-Driven Fold Belts on Passive Margins. In: *Thrust Tectonics and Hydrocarbon Systems* (Ed. by K. McClay), **Memoir 82**, 157-182. AAPG.

RØNNING, K. & STEEL, R.J. (1987) Depositional Sequences within A "Transgressive" Reservoir Sandstone Unit; the Middle Jurassic Tarbert Formation, Hild Area, Northern North Sea. In: *Proceedings of the North Sea Oil and Gas Reservoirs Seminar* (Ed. by J. Kleppe, E. W. Berg, A. T. Buller, O. Hjelmeland & O. Torsaeter), 169-176. Graham & Trotman, London.

SCHULTZ-ELA, D.D. (2001) Excursus on Gravity Gliding and Gravity Spreading. *Journal of Structural Geology*, **23,** 725-731.

SCOTT, E.S. (1992) The Palaeoenvironments and Dynamics of the Rannoch-Etive Nearshore and Coastal Succession, Brent Group, Northern North Sea. In: *Geology of the Brent Group* (Ed. by A. C. Morton, R. S. Haszeldine, M. R. Giles & S. Brown), **Special Publications 61**, 129-147. Geological Society London.

SCRUTON, P.C. (1960) Delta Building and the Deltaic Sequence, Northwest Gulf of Mexico. In: *Recent Sediments, Northwest Gulf of Mexico* (Ed. by F. P. Shepard, P. F.B & T. H. Van Andel), 82-102. AAPG, Tulsa, OK

SESTINI, G. (1989) Nile Delta; a Review of Depositional Environments and Geological History. In: *Deltas: Sites and Traps for for Fossile Fuel* (Ed. by M. K. G. Whateley & K. T. Pickering), **Special Publications 41**, 99-127. Geological Society

SILVA, S.R.P., MACIEL , R.R. & SEVERINO, M.C.G. (1999) Cenozoic Tectonics of Amazon Mouth Basin. *Geo-Marine Letters* **18,** 256-262.

STECKLER, M.S., MOUNTAIN, G.S., MILLER, K.G. & CHRISTIE-BLICK, N. (1999) Reconstruction of Tertiary Progradation and Clinoform Development on the New Jersey Passive Margin by 2-D Backstripping. *Marine Geology*, **154,** 399-420.

STEEL, R.J., CRABAUGH, J.P., SCHELLPEPER, M., MELLERE, D., PLINK-BJÖRKLUND, P., DEIBERT, J. & LØSETH, T.M. (2000) Deltas Versus Rivers on the Shelf Edge: Their Relative Contributions to the Growth of Shelf Margins and Basin-Floor Fans (Barremian and Eocene, Spitsbergen). In: *Gcs-Sepm Foundation 20th Annual Research Conferance, Deepwater Reservoirs of the World* (Ed. by, 981-1009, Houston.

STEEL, R.J. & OLSEN, T. (2002) Clinoforms, Clinoform Trajectory and Deepwater Sands. In: *Sequence Stratigraphic Models for Exploration and Production: Evolving Methodology, Emerging Models and Application Histories* (Ed. by J. M. Armentrout & N. C. Rosen), **Special Publication**, 367-381. GCS-SEPM.

STEEL, R.J., PORĘBSKI, S., J, PLINK-BJÖRKLUND, P., MELLERE, D. & SCHELLPEPER, M. (2003) Shelf-Edge Delta Types and Their Sequence-Stratigraphic Relationships. In: *Shelf-Margin Deltas and Linked Downslope Petroleum Systems, Global Significance and Future Exploration Potential Gcs-Sepm Foundation 23rd Annual Research Conference, Houston (Cd-Rom)* (Ed. by H. Roberts, N. Rosen, R. Fillon & J. Anderson).

STOW, D.A.V., READING, H.G. & COLLINSON, J.D. (1996) Deep Seas. In: *Sedimentary Environments; Processes, Facies and Stratigraphy* (Ed. by H. G. Reading), 395-453. Blackwell Science, Oxford.

SWIFT, D.J.P. (1976) Coastal Sedimentation. In: *Marine Sediment Transport and Environmental Management* (Ed. by D. J. Stanley & D. J. P. Swift), 255-310. John Wiley & Sons., New York, NY.

SWIFT, D.J.P., NIEDORODA, A.W., CHISTOPHER, E.V. & HOPKINS, T.S. (1985) Barrier Island Evolution, Middle Atlantic Shelf, U.S.A; Part I, Shoreface Dynamics. *Marine Geology*, **63,** 331-361.

SWIFT, D.J.P., HUDELSON, P.M., BRENNER, R.L. & THOMPSON, P. (1987) Shelf Construction in a Foreland Basin; Storm Beds, Shelf Sandbodies, and Shelf-Slope Depositional Sequences in the Upper Cretaceous Mesaverde Group, Book Cliffs, Utah. *Sedimentology*, **34,** 423-457.

SYDOW, J.C., FINNERAN, J. & BOWMAN, A., P (2003) Stacked Shelf-Edge Delta Reservoirs of the Columbus Basin, Trinidad West Indies. In: *Shelf-Margin Deltas and Linked Downslope Petroleum Systems, Global Significance and Future Exploration Potential Gcs-Sepm Foundation 23rd Annual Research Conference, Houston (Cd-Rom)* (Ed. by H. Roberts, R. NC, F. RH & A. JB).

SØMME, T., HOWELL, J., HAMPSON, G.J. & STORMS, J.E.A. (in press) Genesis, Architecture and Numerical Modeling of Intra-Parasequence Discontinuity Surfaces in Wave-Dominated Deltaic Deposits: Upper Cretaceous Sunnyside Member, Blackhawk Formation, Book Cliffs, Utah, USA. In: *Recent Advances in Models of Siliciclastic*

Shallow-Marine Stratigraphy (Ed. by G. J. Hampson, R. J. Steel, P. M. Burgess & R. W. Dalrymple), **Special Publication 90**. SEPM.
TAYLOR, D.R. & LOVELL, R.W.W. (1991) Recognition of High-Frequency Sequences in the Kenilworth Member of the Blackhawk Formation, Book Cliffs, Utah. In: *Sequence Stratigraphy Applications to Shelf Sandstone Reservoirs; Outcrop to Subsurface Examples;* (Ed. by J. C. Van Wagoner, C. R. Jones, D. R. Taylor, D. Nummedal, D. C. Jennette & G. W. Riley). AAPG field conference guidebook, Tulsa, OK.
TAYLOR, D.R. & LOVELL, R.W.W. (1995) High-Frequency Sequence Stratigraphy and Paleogeography of the Kenilworth Member, Blackhawk Formation, Book Cliffs, Utah, U.S.A. In: *Sequence Stratigraphy of Foreland Basin Deposits; Outcrop and Subsurface Examples from the Cretaceous of North America.* (Ed. by J. C. Van Wagoner & G. T. Bertram), **Memoir 64**, 257-275. AAPG.
TAYLOR, K.G., GAWTHORPE, R.L. & FANNON-HOWELL, S. (2004) Basin-Scale Diagenetic Alteration of Shoreface Sandstones in the Upper Cretaceous Spring Canyon and Aberdeen Members, Blackhawk Formation, Book Cliffs, Utah. *Sedimentary Geology,* **172,** 99-115.
TODD, R.G. & MITCHUM, R.M. (1977) Part 8, Identification of Upper Triassic, Jurassic, and Lower Cretaceous Seismic Sequences in Gulf of Mexico and Offshore West Africa. In: *Seismic Stratigraphy and Global Changes of Sea Level* (Ed. by C. E. Payton), **Memoir 26**, 145-163. AAPG.
UNDERHILL, J.R. & PARTINGTON, M.A. (1993) Jurassic Thermal Doming and Deflation in the North Sea; Implications of the Sequence Stratigraphic Evidence. In: *Petroleum Geology of Northwest Europe: Proceedings of the 4th Conference* (Ed. by J. R. Parker), 337-345.
UNDERHILL, J.R. & PARTINGTON, M.A. (1994) Use of Maximum Flooding Surfaces in Determining a Regional Control on the Intra-Aalenian Mid-Cimmerian Sequence Boundary: Implications of North Sea Basin Development and Exxon's Sea Level Chart. In: *Recent Advances in Siliciclastic Sequence Stratigraphy* (Ed. by H. W. Posamentier & P. J. Weimer), **Memoir 58**, 449-484. AAPG.
VAN DER BECK, P. (1994) Mechanisms of Post-Rift Margin Uplift: The Case of Southern Norway. In: *Tectonic Evolution of Continental Rifts. Inferences from Numerical Modelling and Fission Track Thermochronology* (Ed. by P. van der Beck), 107-140. Thesis, Free University.
VAN STRAATEN, L.M.J.U. (1959) Littoral and Submarine Morphology of the Rhone Delta. In: *2nd Coastal Geog. Conf.* (Ed. by R. Russel), 233-264. Natl research Counsil, Baton Rouge, Louisiana State University.
VAN WAGONER, J.C. (1985) Reservoir Facies Distribution as Controlled by Sea-Level Change. *Soc. Econ. Geol. Mineral. Petrol. Annual Midyear Meeting, Golden, Colorado, Abstr. Prog., 2:91*.
VAN WAGONER, J.C., POSAMENTIER, H.W., MITCHUM, R.M., VAIL, P.R., SARG, J.F., LOUTIT, T.S. & HARDENBOL, J. (1988) An Overview of the Fundamentals of Sequence Stratigraphy and Key Definitions. In: *Sea-Level Changes: An Integrated Approach* (Ed. by C. K. Wilgus, B. S. Hastings, C. A. Ross, H. W. Posamentier, J. Van Wagoner & C. G. S. C. Kendall), **Special Publication 42**, 39-45. Society of Economic Paleontologists and Mineralogists.
VAN WAGONER, J.C., MITCHUM, R.M., CAMPION, K.M. & RAHMANIAN, V.D. (1990) *Siliciclastic Sequence Stratigraphy in Well Logs, Cores, and Outcrops: Concepts for High Resolution Correlation of Time and Facies.* AAPG.
VAN WAGONER, J.C., JONES, C.R., TAYLOR, D.R., NUMMEDAL, D., JENNETTE, D.C. & RILEY, G.W. (1991) *Sequence Stratigraphy and Facies Architecture of the Desert Member of*

the Blackhawk Formation and the Castlegate Formation in the Book Cliffs of Western Colorado and Eastern Utah. AAPG, Tulsa, OK.

VAN WAGONER, J.C. & BERTRAM, G.T. (1995) *Sequence Stratigraphy of Foreland Basin Deposits; Outcrop and Subsurface Examples from the Cretaceous of North America*. AAPG.

WALKER, R.G. (1979) *Facies Models*. Geological Association of Canada., Toronto.

WALKER, R.G. & PLINT, A.G. (1992) Wave- and Storm-Dominated Shallow Marine Systems. In: *Facies Models; Response to Sea Level Change* (Ed. by R. G. Walker & N. P. James), 219-238. Geological Association of Canada, St. Johns, NL.

WARNE, A.G., MEADE, R.H., WHITE, W.A., GUEVARA, E.H., GIBEAUT, J., SMYTH, R.C., ASLAN, A. & TREMBLAY, T. (2002) Regional Controls on Geomorphology, Hydrology, and Ecosystem Integrity in the Orinoco Delta, Venezuela. *Geomorphology*, **44,** 273-307.

WILGUS, C.K., HASTINGS, B.S., ROSS, C.A., POSAMENTIER, H.W., VAN WAGONER, J. & KENDALL, C.G.S.C. (1988) *Sea Level Changes: An Integrated Approach*. Society of Economic Paleontologists and Mineralogists.

WINKER, C.D. & EDWARDS, M.B. (1981) Unstable Progradational Clastic Shelf Margins. *AAPG Bulletin*, **65,** 1008.

WINKER, C.D. & EDWARDS, M.B. (1983) Unstable Progradational Clastic Shelf Margins. In: *The Shelf Break: Critical Interface on Continental Margins* (Ed. by D. J. Stanley & G. T. Moore), **Special Publication 33**, 139-157. Society of Economic Paleontologists and Mineralogists.

WOOD, L.J. (2000) Chronostratigraphy and Tectonostratigraphy of the Columbus Basin, Eastern Offshore Trinidad. *AAPG Bulletin*, **84,** 1905-1928.

YILMAZ, O. (1987) *Seismic Data Processing*. Soc. Explor. Geophys., Tulsa, OK.

YOUNG, R.G. (1955) Sedimentary Facies and Intertonguing in the Upper Cretaceous of the Book Cliffs, Utah-Colorado. *Geological Society of America Bulletin*, **66,** 177-202.

YOUNG, R.G. (1957) Late Cretaceous Cyclic Deposits, Book Cliffs, Eastern Utah. *AAPG Bulletin*, **41,** 1760-1774.

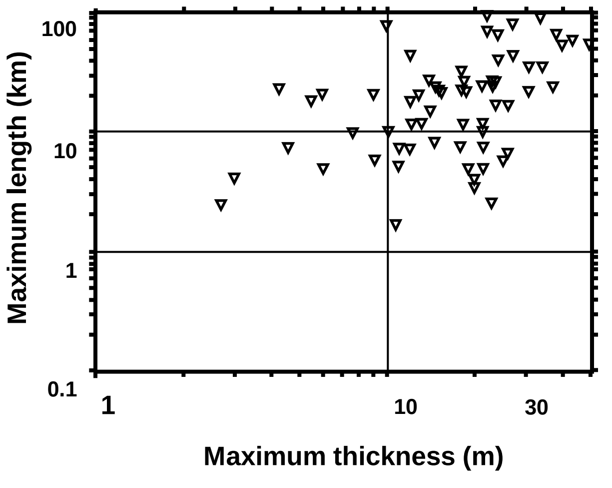

Fig. 1 Log-log plot of maximum thickness for ancient wave-dominated shoreface sandstones plotted against maximum dip directed length. 90% of the sandstones are 30 m in thickness or less. Adapted from Reynolds (1999).

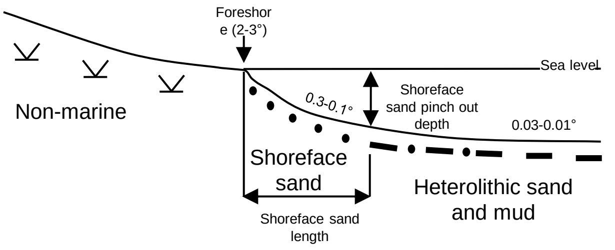

Fig. 2 Sketch of the dip stacking of facies in modern sandy wave-dominated coasts. Modified from Cant (1991). Angles of sediment surface from Walker and Plint (1992); Niedoroda et al. (1985).

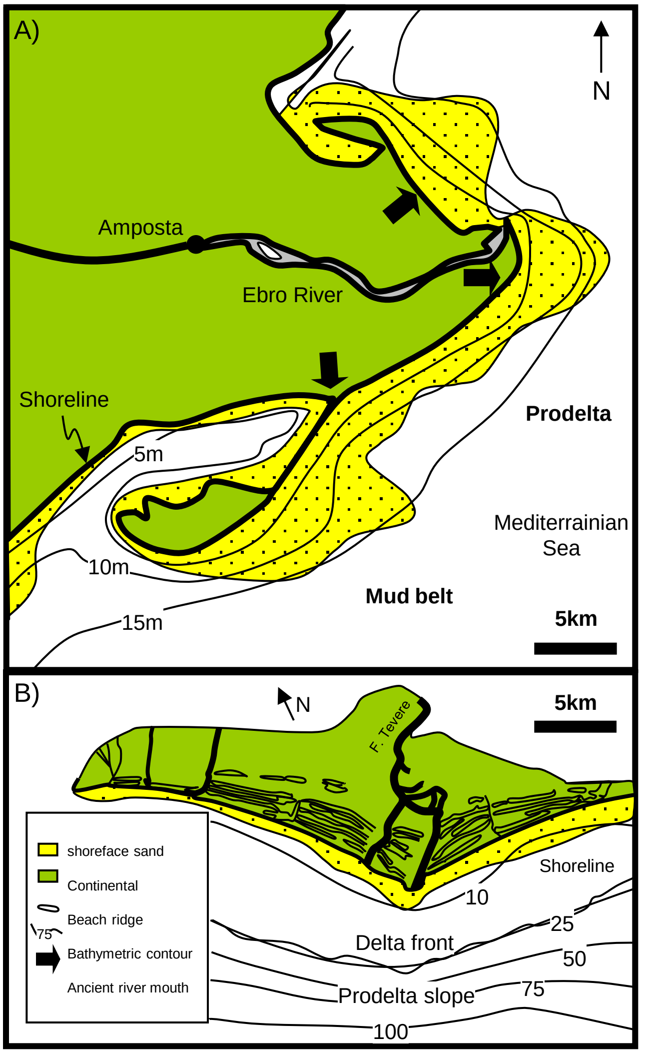

Fig. 3 Distribution of shoreface sand in the modern wave-influenced deltas. A) The Ebro delta, Spain. Shoreface sand length and pinch out depth varies from 10 km and 15 m near abandoned river outlets, to 2 km and 10 m between the outlets. In protected areas, shoreface sand length is a few 100 m and has a pinch out depth of less than to 5 m. Figure modified from Diaz (1996). B) The Tiber delta in Italy has shoreface sand extending 1-2 km seawards from the shoreline, and typically down to less than 10 m water depth. Modified from Belotti et al. (1994).

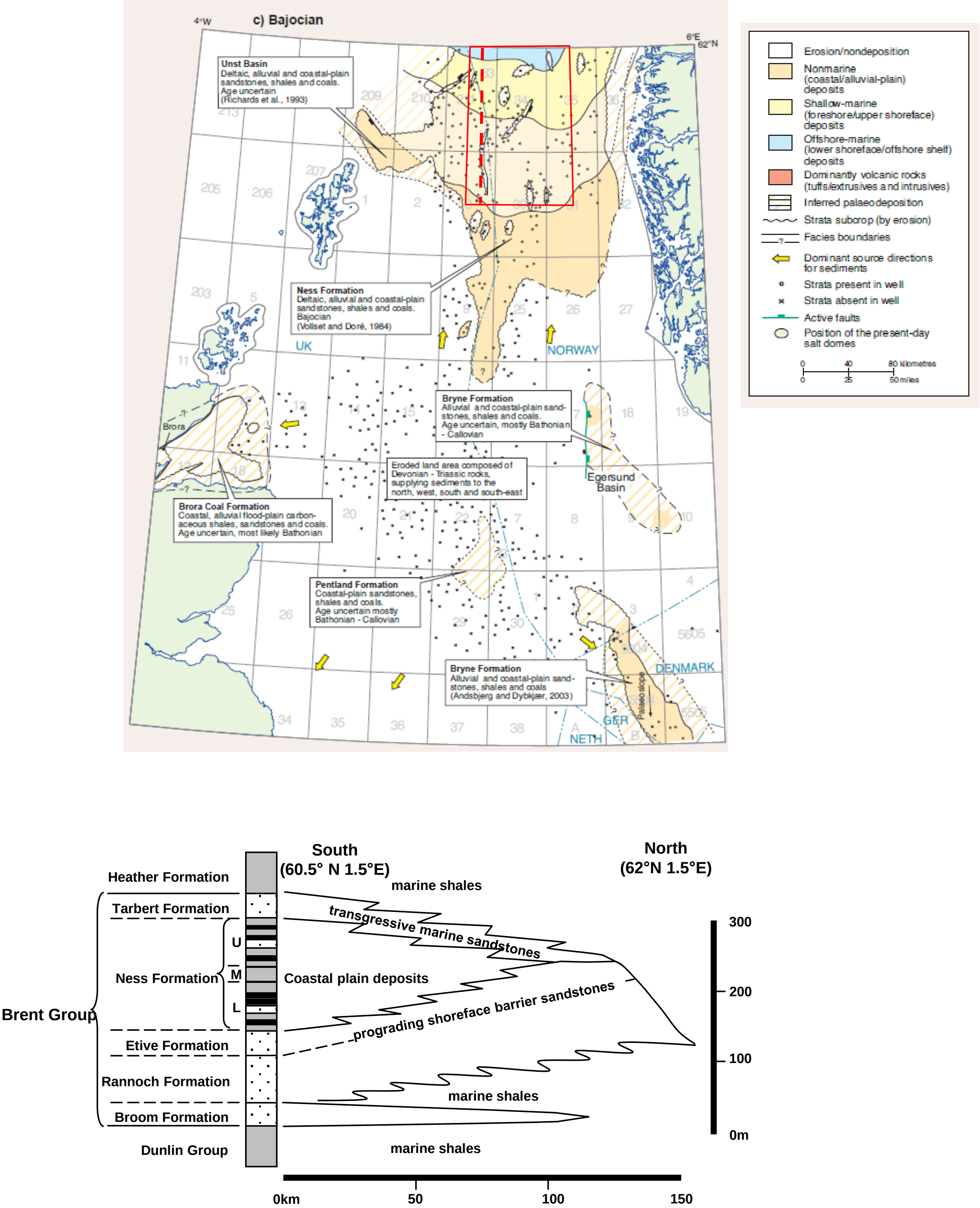

Fig. 4 Regional framework of the Brent Group in the North Sea. Red square indicate position of study area in Fig. 5. Red stippled line indicates profile in b. Adapted from Husmo et al. 2003. **B)** Generalized stratigraphic column and north–south section through the Brent Group in the East Shetland basin, illustrating lithostratigraphy and depositional environments (modified from Brown (1990) and Richards (1992)). The scale and location of the section are approximate. For more detailed correlation panels, see Johannesen et al. (1995).

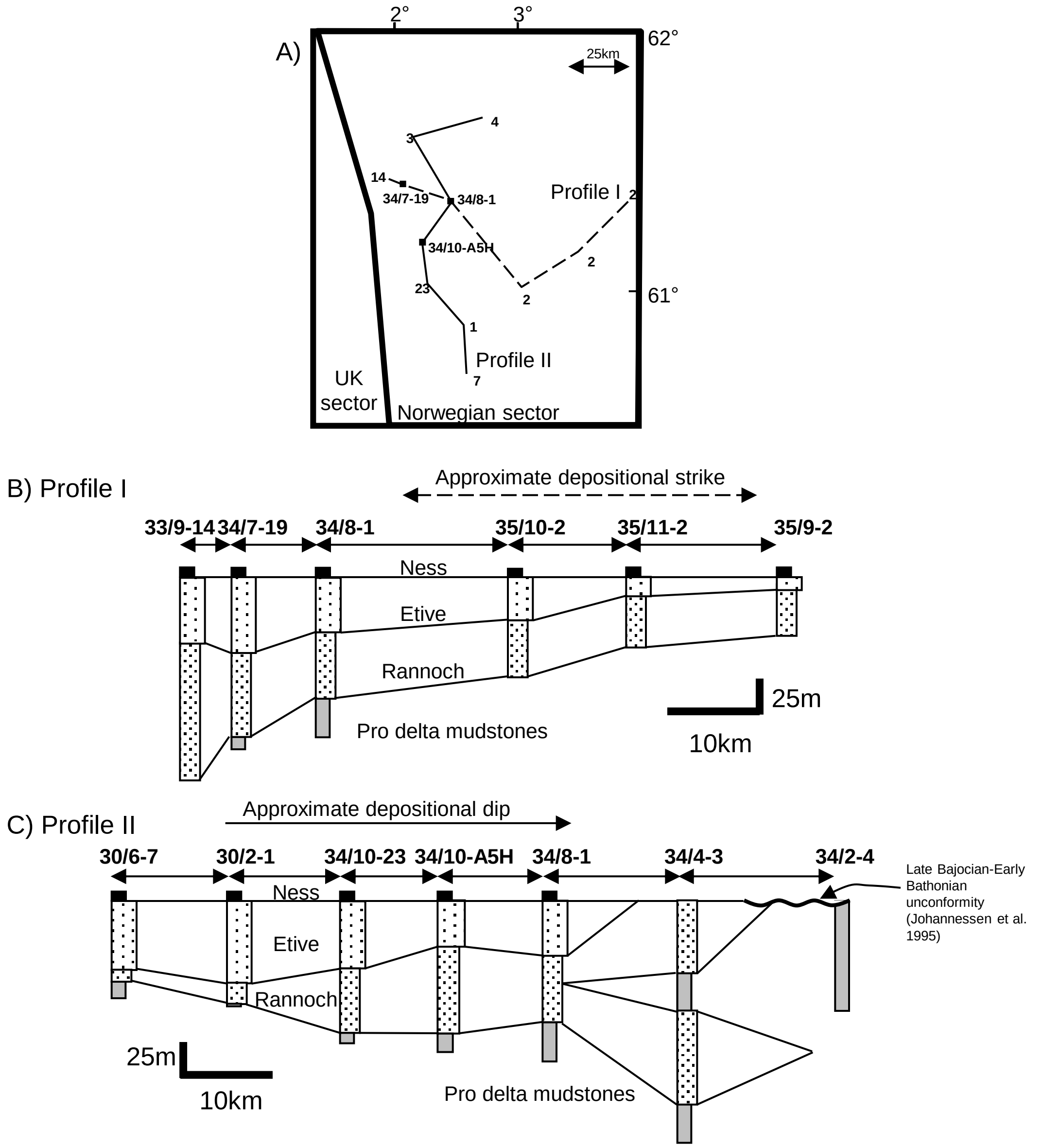

Fig. 5 A) Study area (cf. Fig 4) with location of key wells (black squares) and profiles in b and c indicated. **B)** Strike-directed regional correlation panel for Rannoch-Etive formations. **C)** Dip-directed profile of Rannoch-Etive formations. Correlation panel in b and c are largely based on data provided by Norwegian Petroleum Directorate. Down-dip pinch-out style in profile II is based on Johannessen et al. (1995, their Figs. 26 and 27) and mud logger description of 34/4-3 well.

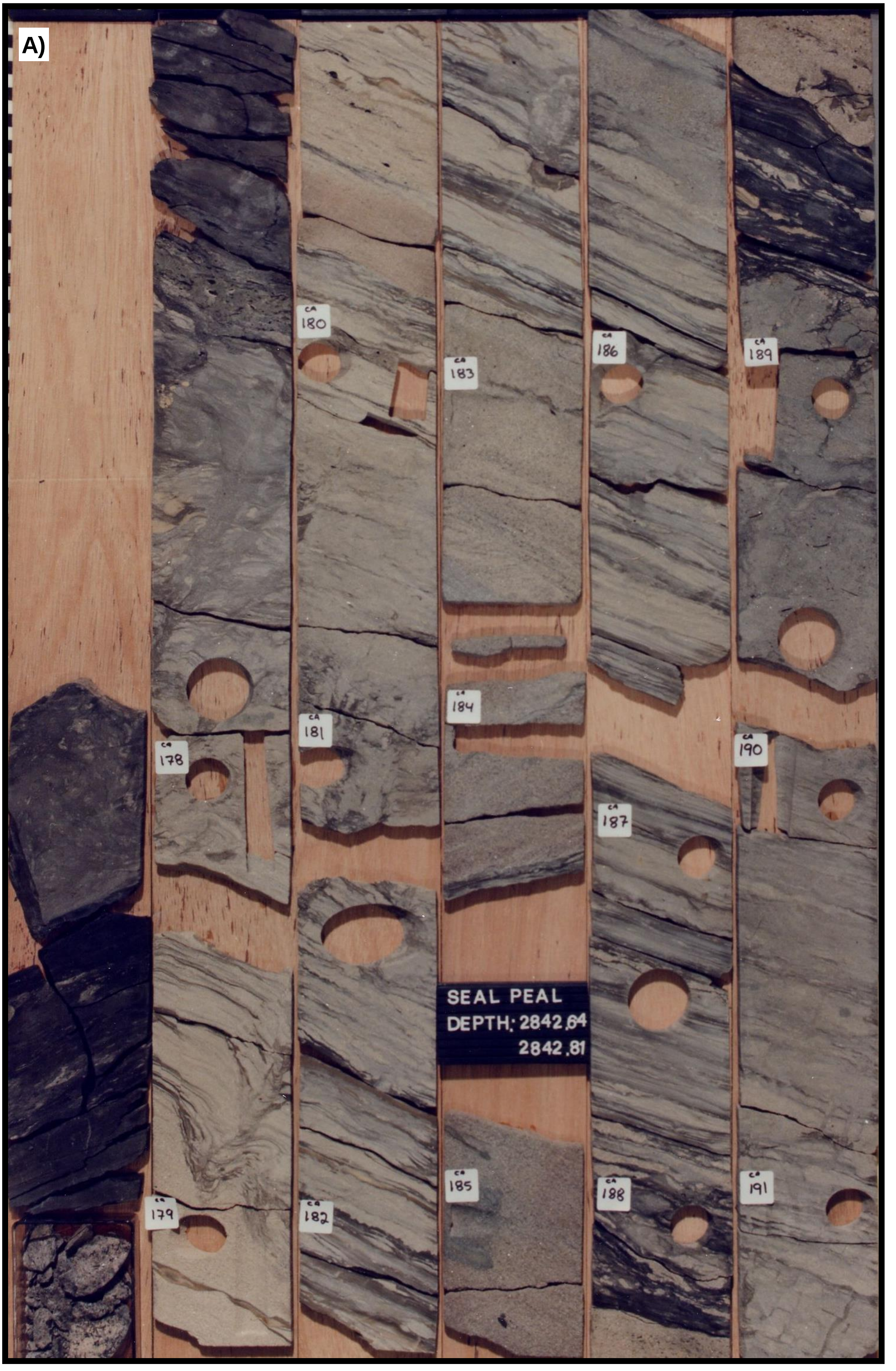

Fig. 6 A) Core photo of the continental plain facies as expressed in well 34/8-1. Each stick 1 m. See Table 2 for description and interpretation. Photos provided by Norwegian Petroleum Directorate.

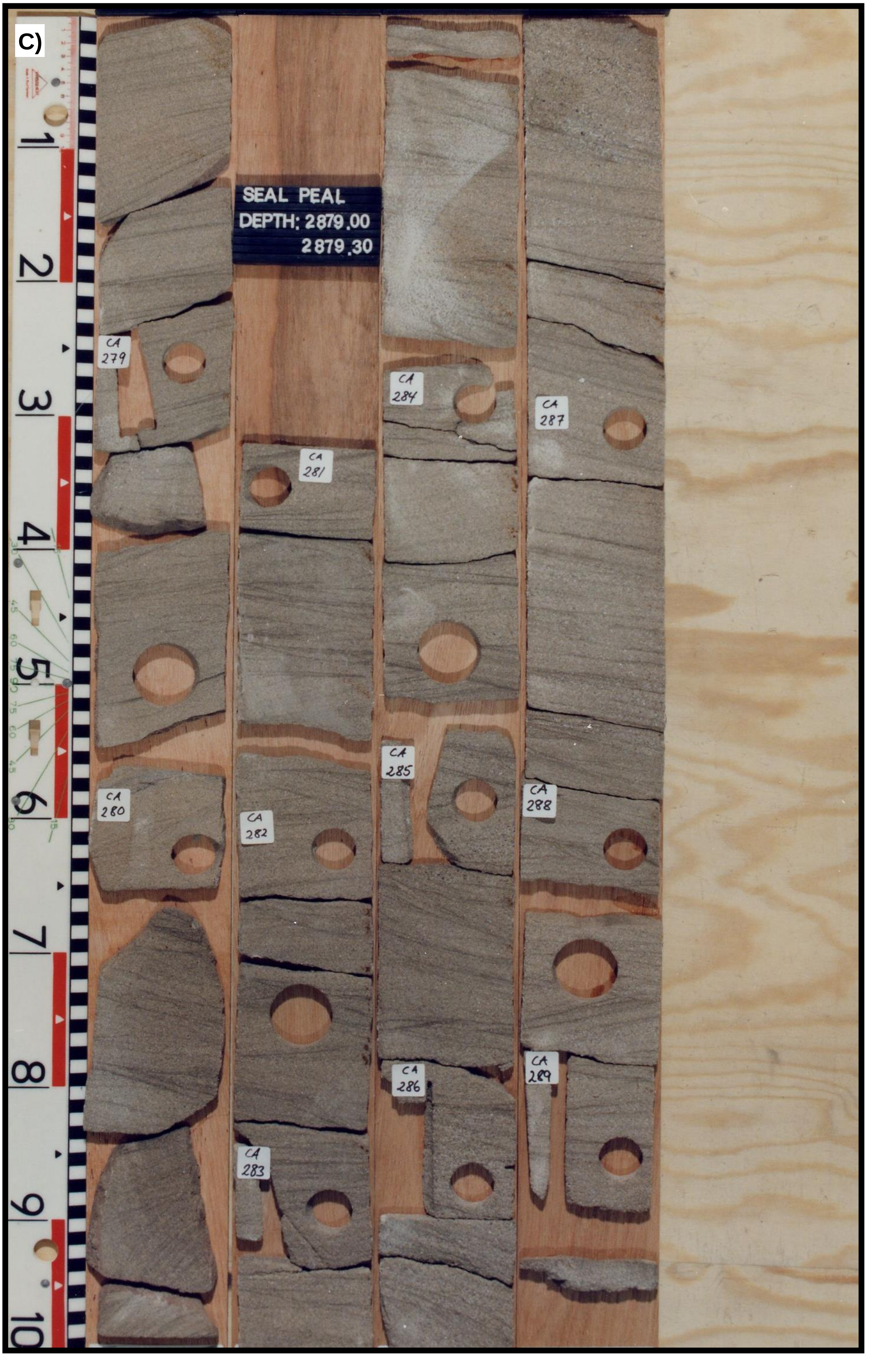

Fig 6 B) Core photo of the upper shoreface facies as expressed in well 34/8-1. Stick totally 1 m. See Table 2 for description and interpretation. Photos provided by Norwegian Petroleum Directorate.

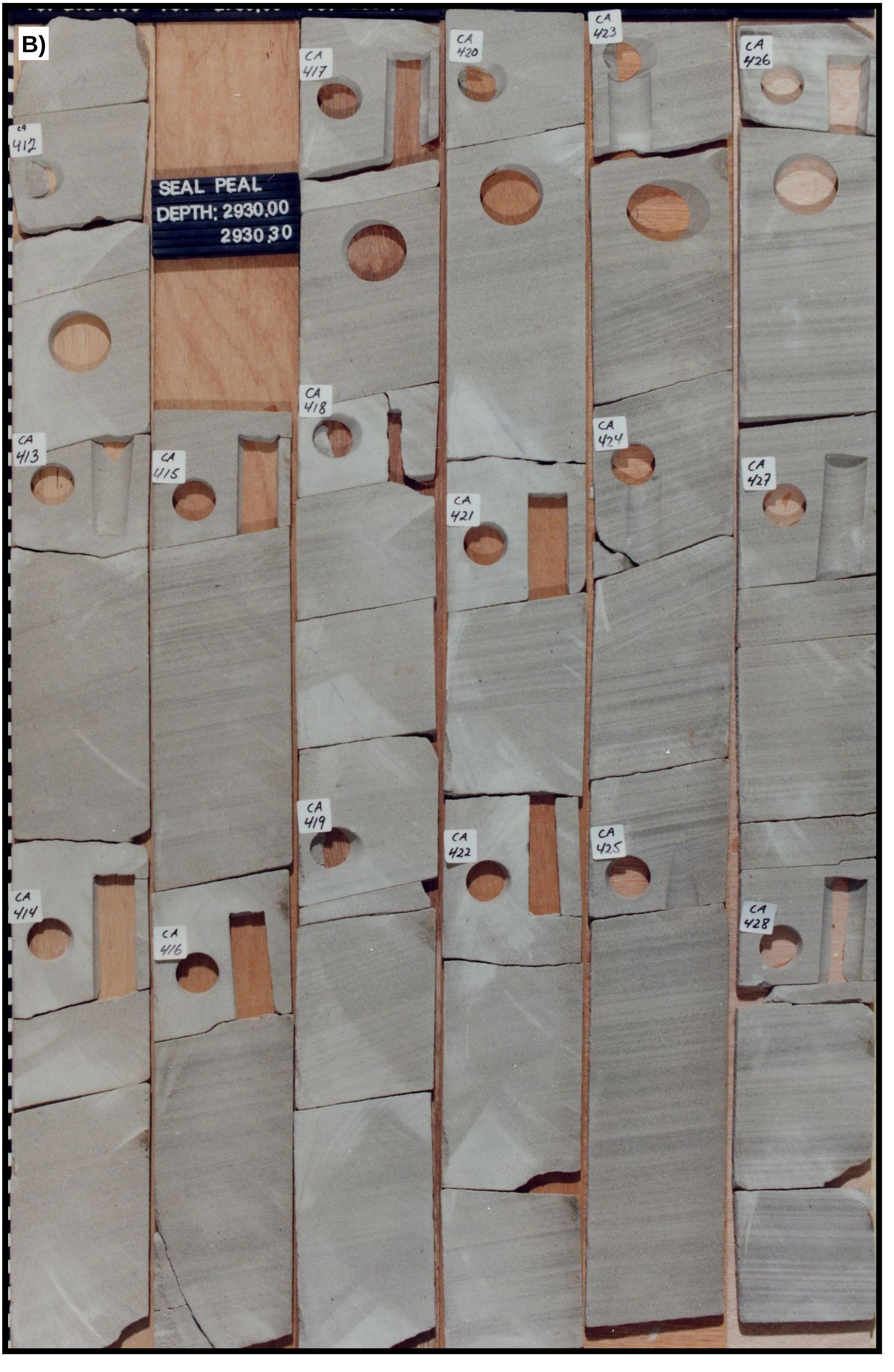

Fig 6 C) Core photo of the lower shoreface facies as expressed in well 34/8-1. Each stick 1 m. See Table 2 for description and interpretation. Photos provided by Norwegian Petroleum Directorate.

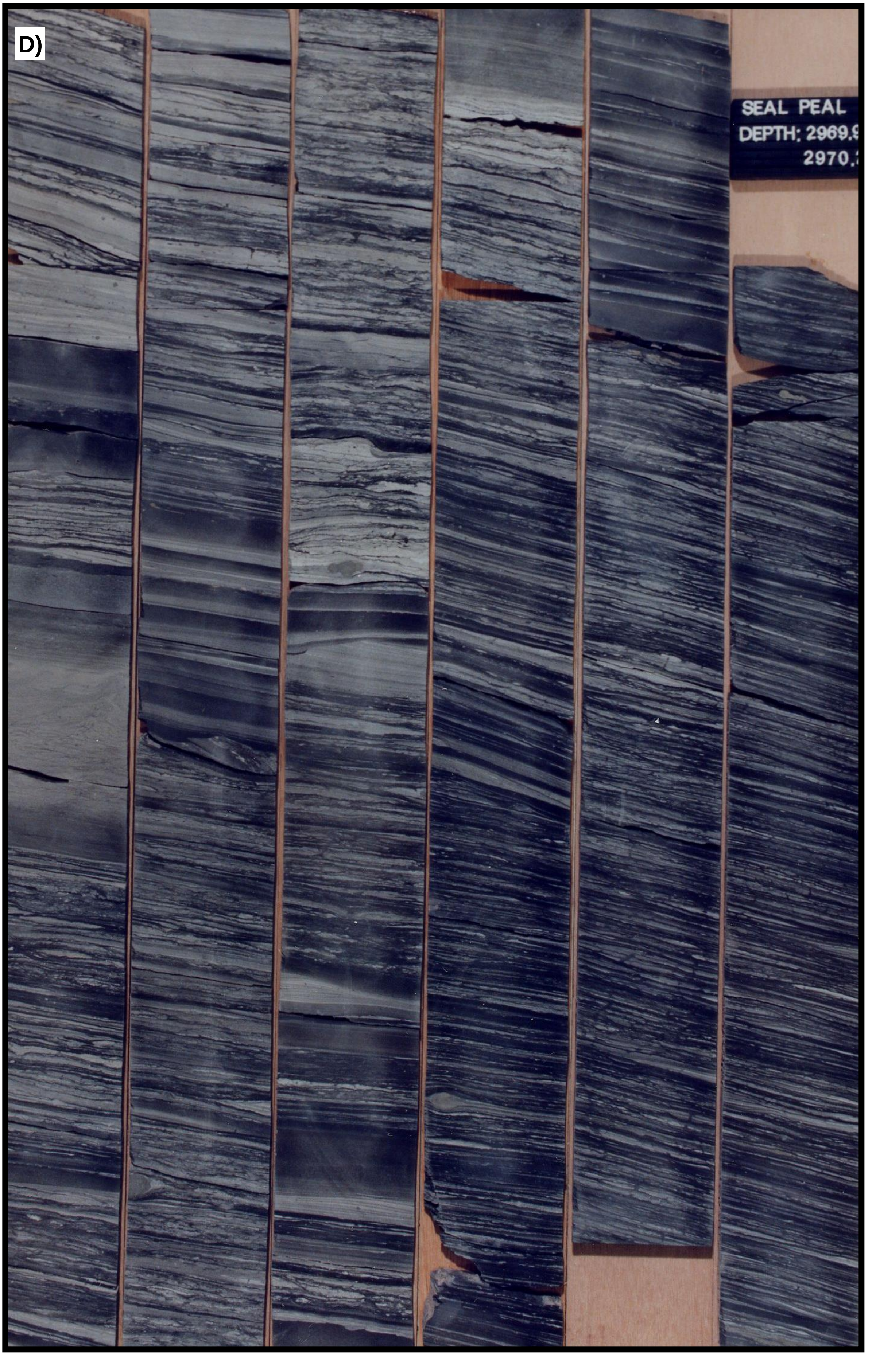

Fig 6 D) Core photo of the gradational lower contact of lower shoreface facies as expressed in well 34/8-1. Each stick 1 m. See Table 2 for description and interpretation. Photos provided by Norwegian Petroleum Directorate.

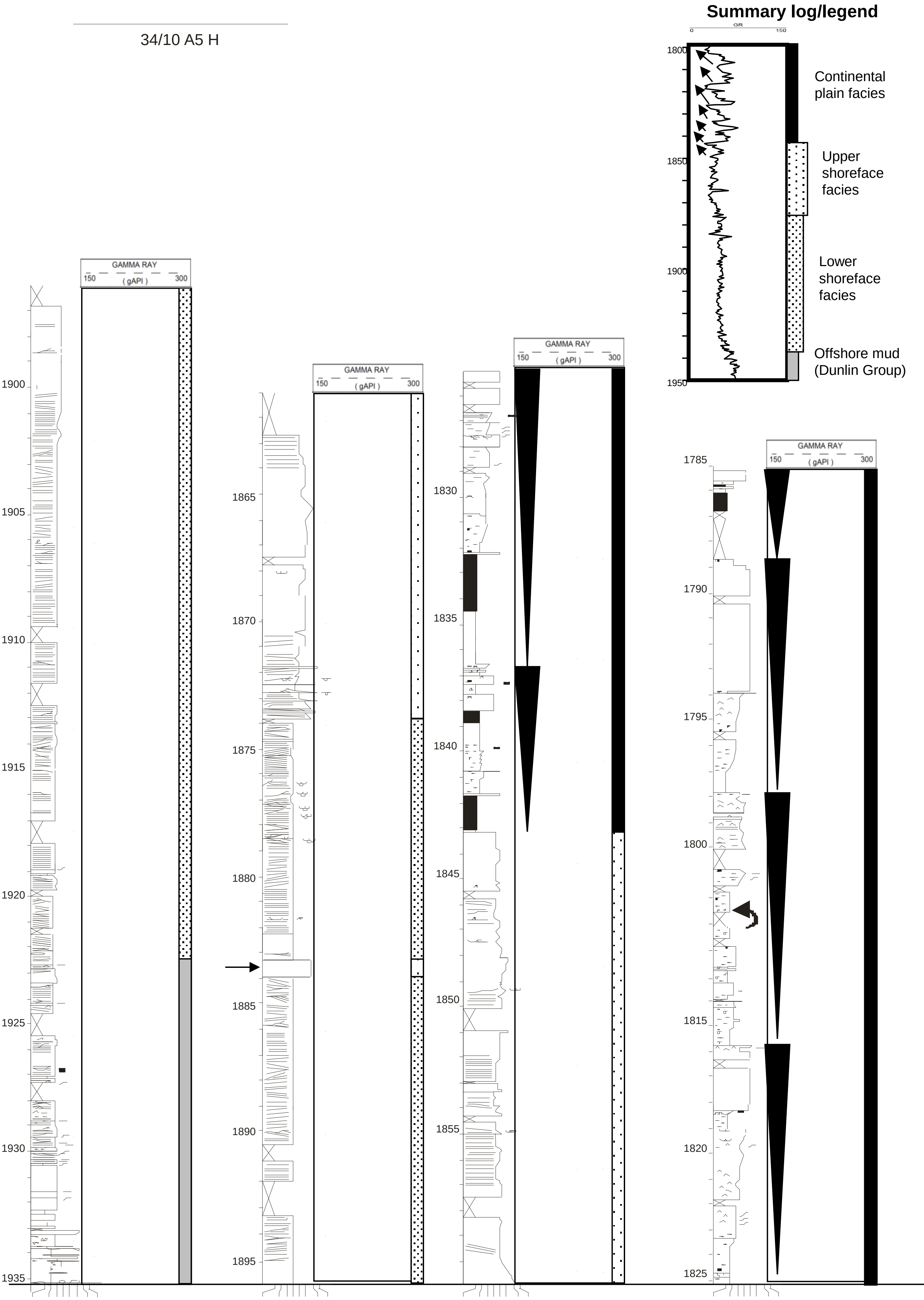
34/10 A5 H
Summary log/legend
GR
0
150
1800
1850
1900
1950
Continental plain facies
Upper shoreface facies
Lower shoreface facies
Offshore mud (Dunlin Group)
GAMMA RAY
150
(gAPI)
300
1900
1905
1910
1915
1920
1925
1930
1935
1865
1870
1875
1880
1885
1890
1895
1830
1835
1840
1845
1850
1855
1785
1790
1795
1800
1815
1820
1825

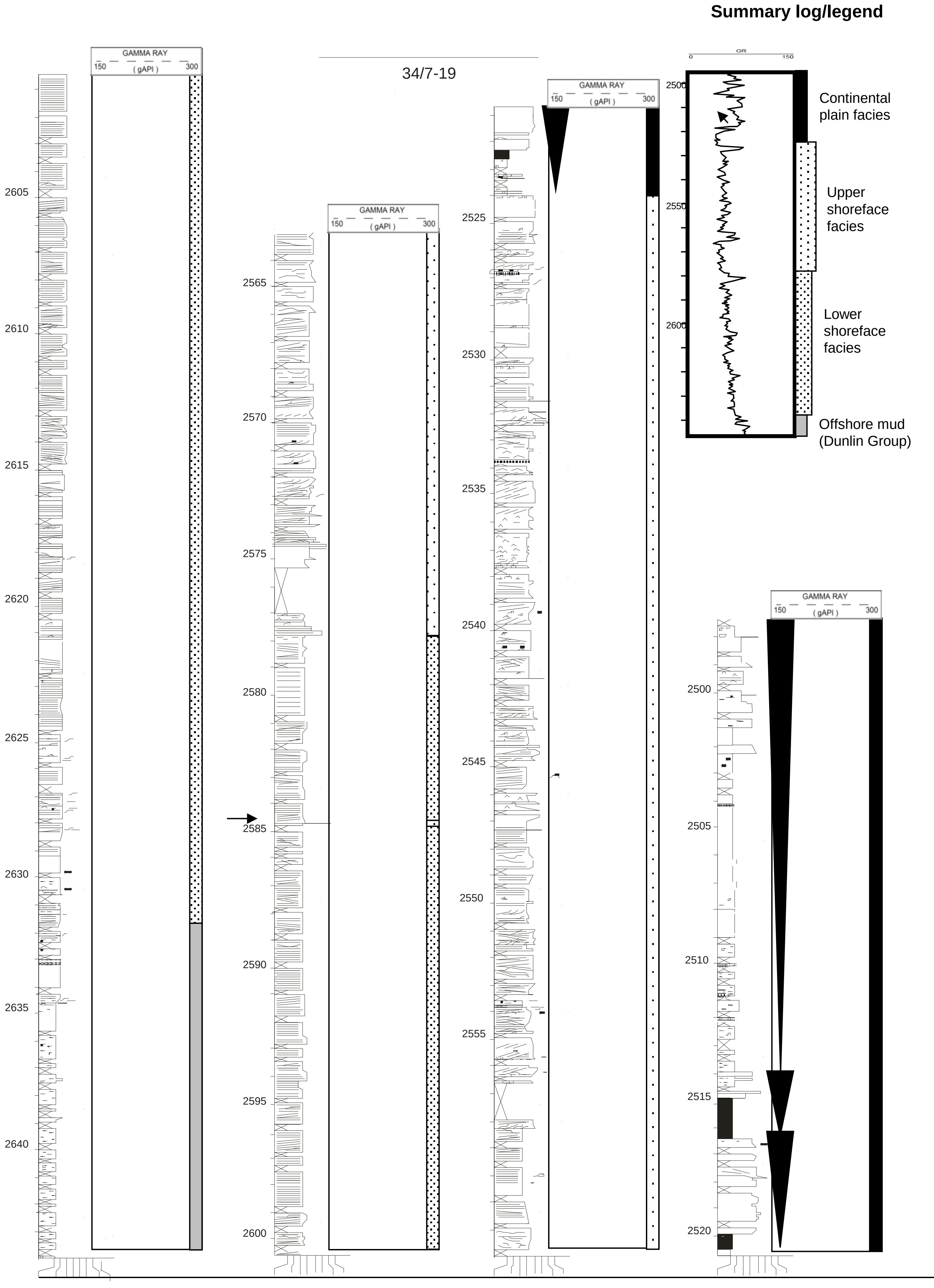

Summary log/legend
34/7-19
GAMMA RAY
150
(gAPI)
300
2605
2610
2615
2620
2625
2630
2635
2640
2565
2570
2575
2580
2585
2590
2595
2600
2525
2530
2535
2540
2545
2550
2555
2500
2505
2510
2515
2520
GR
0
150
2500
2550
2600
Continental plain facies
Upper shoreface facies
Lower shoreface facies
Offshore mud (Dunlin Group)

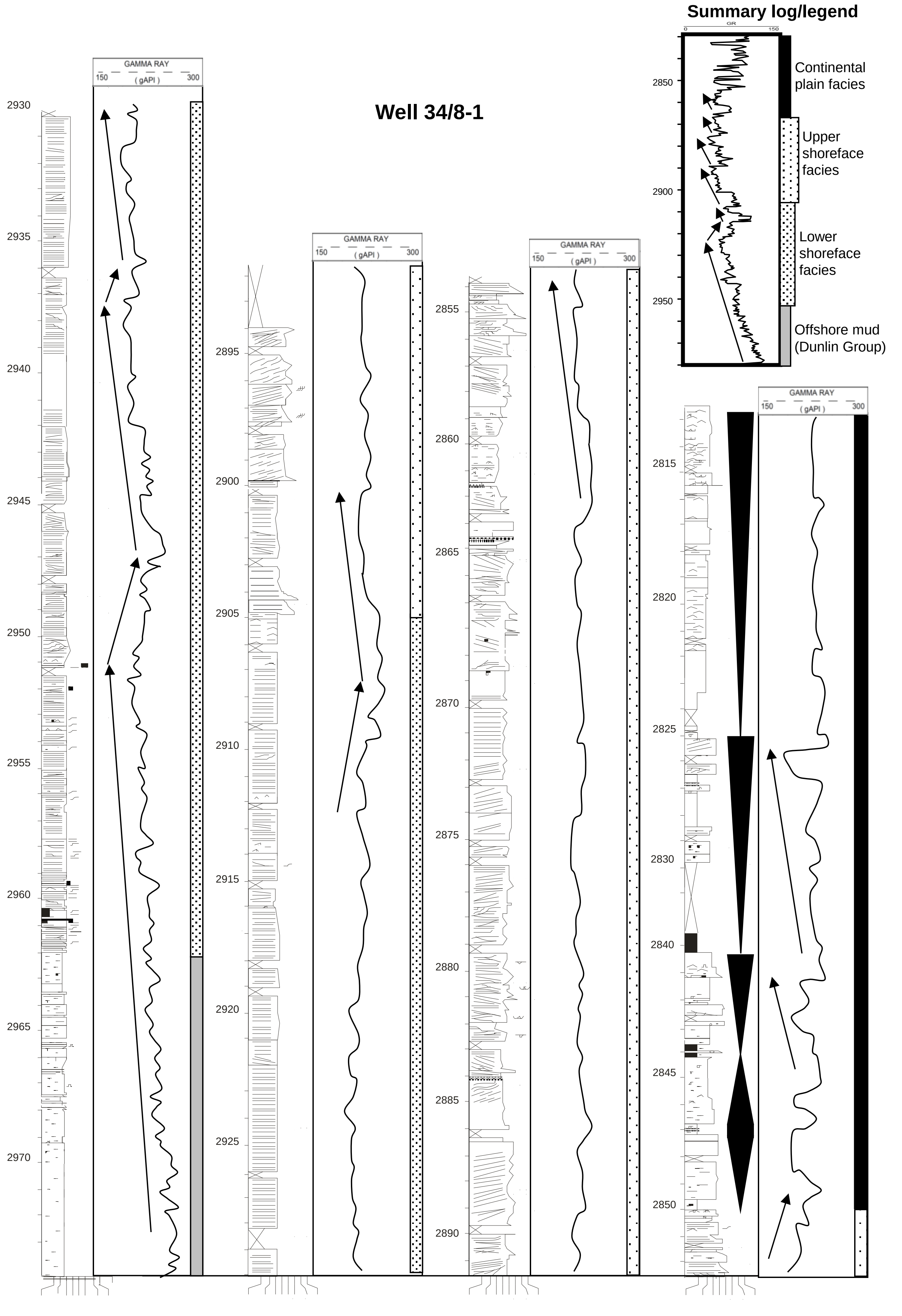
Summary log/legend
GR
0
150
2850
2900
2950
Continental plain facies
Upper shoreface facies
Lower shoreface facies
Offshore mud (Dunlin Group)
Well 34/8-1
GAMMA RAY
150
(gAPI)
300
2930
2935
2940
2945
2950
2955
2960
2965
2970
2895
2900
2905
2910
2915
2920
2925
2855
2860
2865
2870
2875
2880
2885
2890
2815
2820
2825
2830
2840
2845
2850

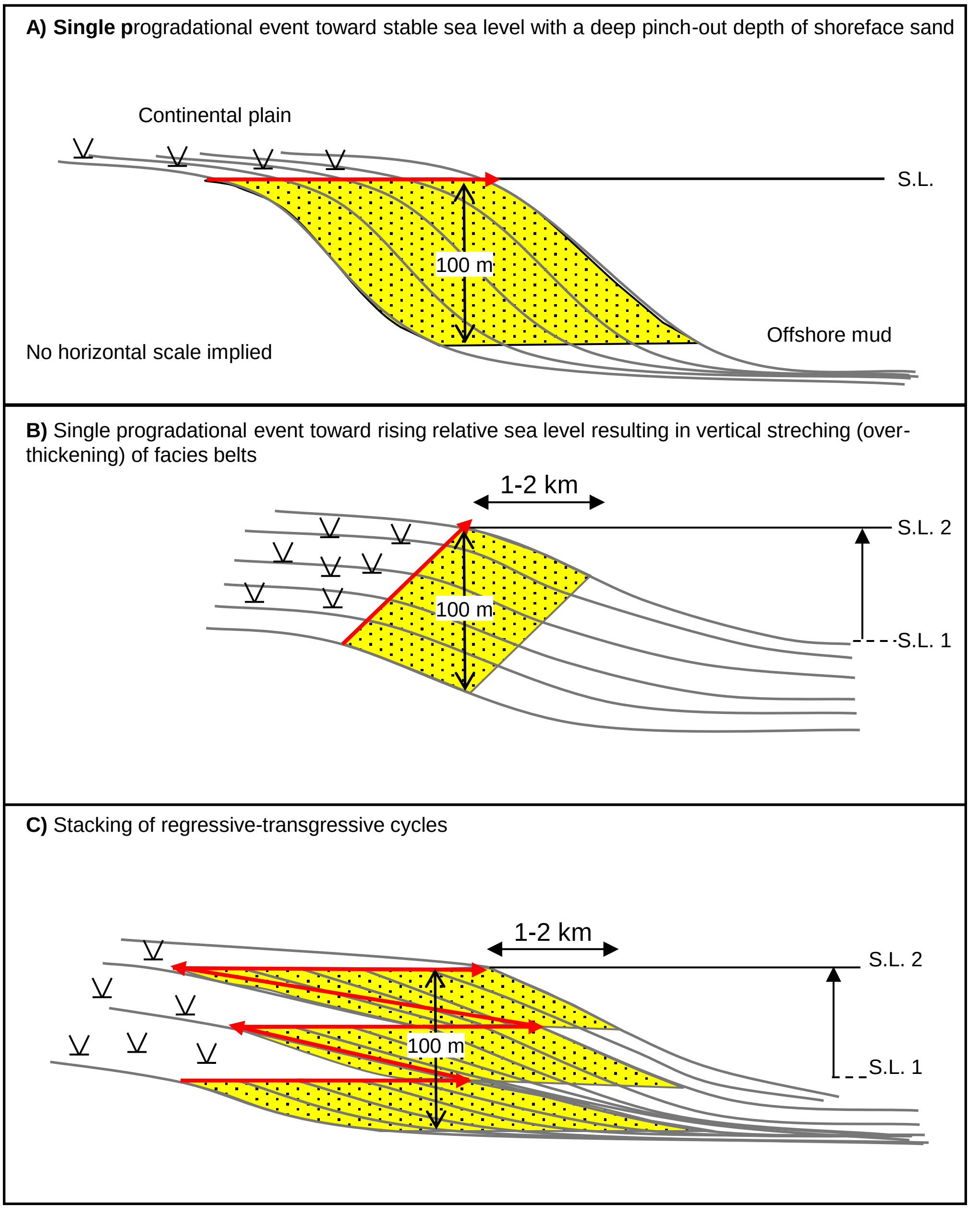

Fig. 8 The possible progradational styles of the Brent coastlines. Either the delta prograded as a single event as indicated in a and b, or the coastline experienced an overall progradation punctuated by multiple transgressions as indicated in c. Also evident: The 3 possible ways to generate a 100 m thick succession of shoreface sandstone (yellow). **A)** Progradation against stable relative sea level with a 100 m deep homogenous shoreface sand pinch out depth would ideally result in a 100 m thick succession of shoreface sandstone. This type of progradation would be associated with facies being stacked in a gradually shallowing up succession and minor accumulation of continental deposits behind the coastline. **B)** Progradation during rising relative sea level will result in vertical stretching of the facies belts during progradation. According to Cant (1991), the vertical shoreface sandstone thickness in such deposits are controlled by: 1) angle of shoreline trajectory; 2) homogenous shoreface sand length; and 3) homogenous shoreface sand pinch-out depth. This type of progradation would also be associated with gradually shallowing-up facies stacking. **C)** Aggradationally stacked regressive-transgressive cycles resulting in local amalgamation of shoreface sandstone and accumulation of continental deposits behind the shoreline. As in b, this model predicts repetitive facies stacking (e.g. repeated intrusions of continental facies into marginal marine facies) and accumulation of continental deposits behind the shoreline. **NOTE:** the stratigraphical climb in option b) and c) is the same, provided the same shoreface sand length and pinch out depth is used.

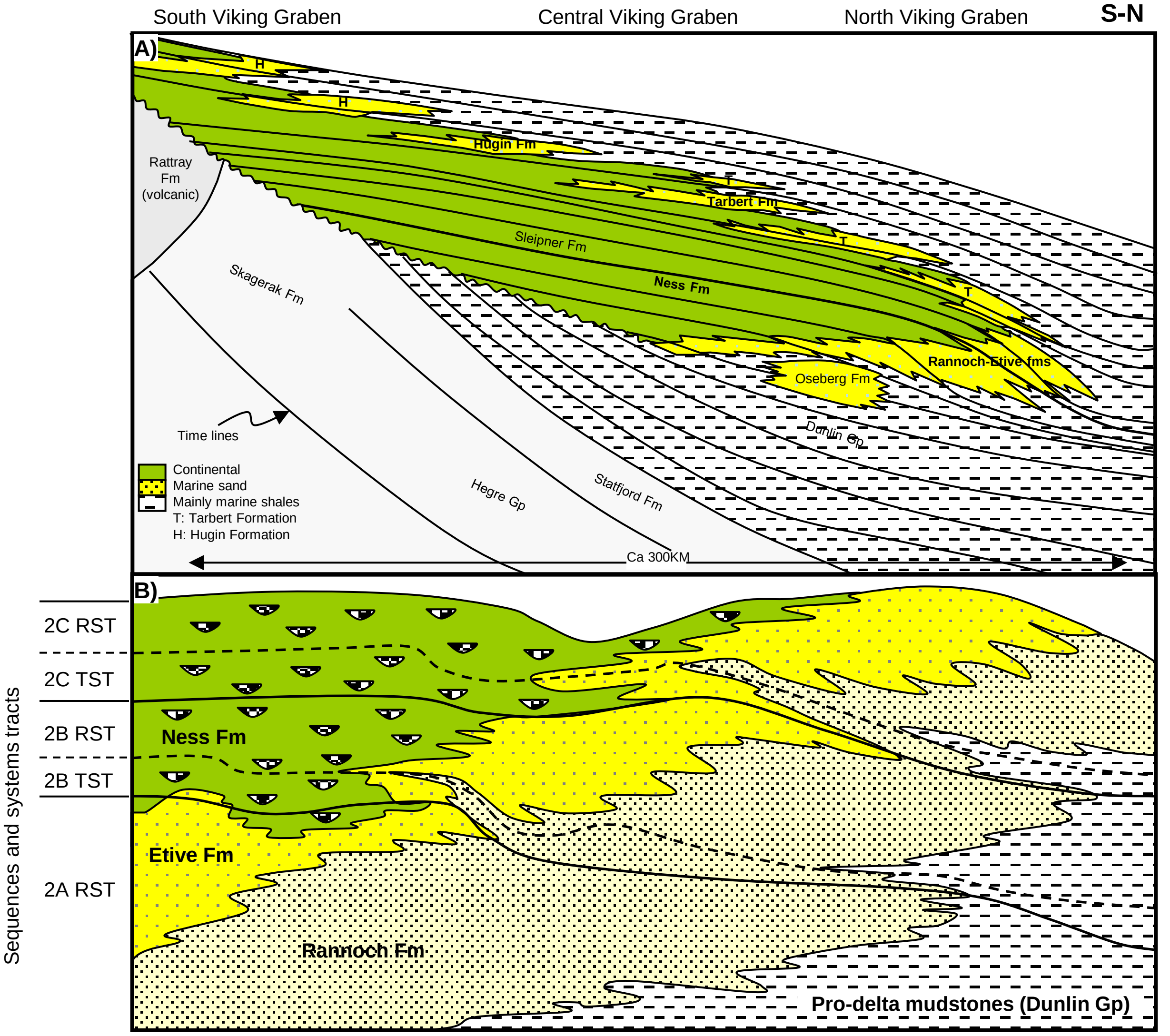

Fig. 9 Previously proposed stratigraphic framework for the progradational part of the Brent delta in Viking Graben. **A)** The Rannoch-Etive formations was originally interpreted to represent a normal regressive succession, not punctuated by transgressions. Modified from Helland-Hansen et al. (1992). **B)** Later, the Rannoch-Etive formations were divided into 3rd order sequences and several higher order cycles (not shown) (e.g. Johannesen et al. 1995; Olsen and Steel 1995). However, the landward migration of the shoreline in the model is highly interpretational and not well documented. Figure modified from Johannesen et al. (1995). RST: Regressive systems tract; TST: Transgressive systems tract.

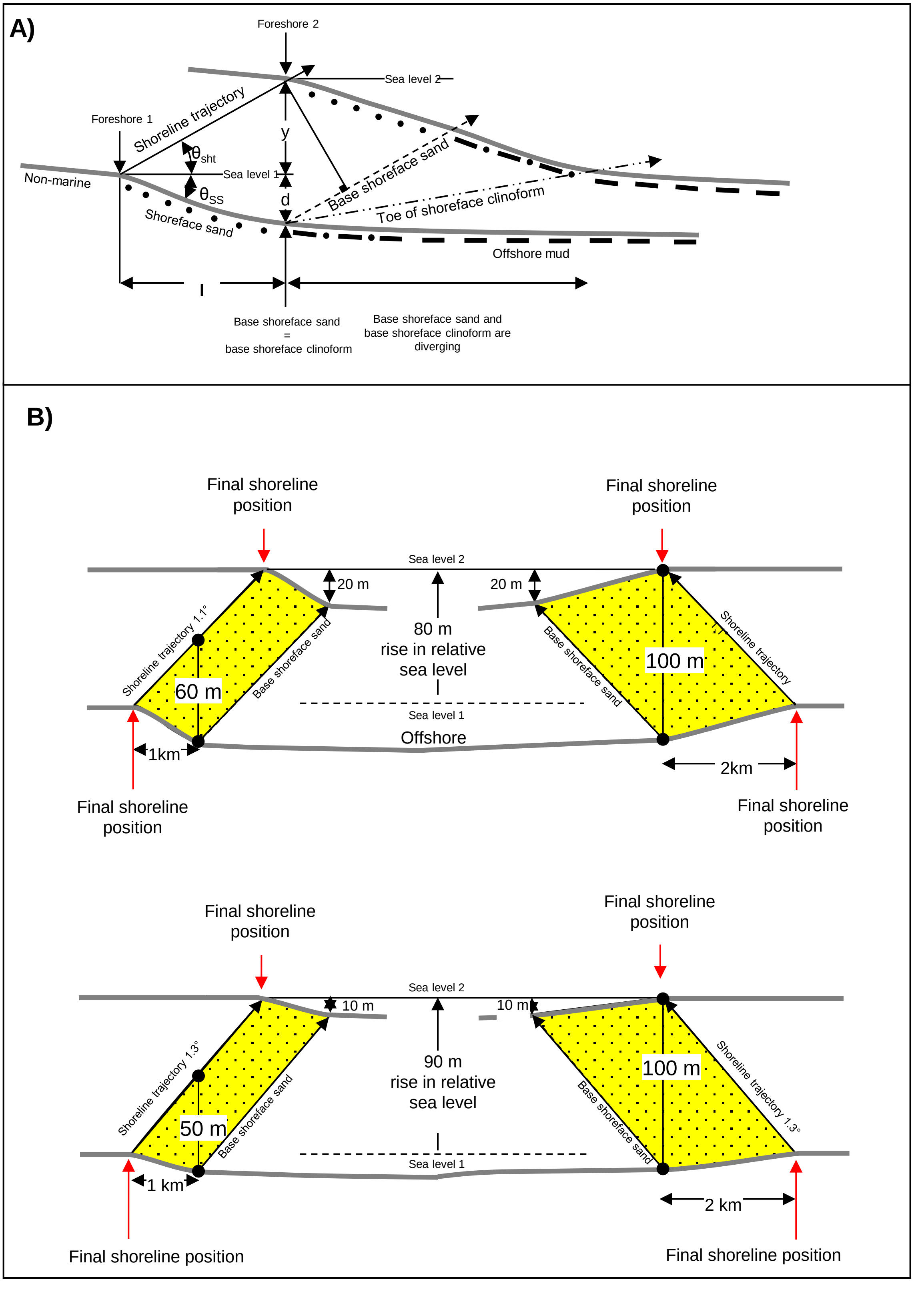

Fig. 10 Geometrical modeling of facies-belt migration in normal regressive, wave-dominated shoreface sandstone tongues. **A)** The vertical thickness of a regressive shoreface sand succession (d+y) is dependent on: 1) angle of shoreline trajectory (θ_{sht}); 2) shoreface sand length (l); and 3) shoreface sand pinch-out depth (d). The latter two can be used to calculate the average angle of the shoreface sand surface (θ_{SS}). Based on Cant (1991). **B)** Progradation with a 20 m deep shoreface sand pinch out depth. The large difference in the resulting shoreface sandstone thickness between prograding with a 1 km shoreface sand length (left) and a 2 km length (right) is evident. **C)** As B) but applying a 10 m shoreface sand pinch-out depth. The above implies that progradation along a coast with large strike variations in shoreface sand length will result in large stratigraphic thickness variations of sandstone along strike. In the the Ebro delta, for example, (Fig. 3), progradation toward stable sea level will result in a 5 m thick shoreface sandstone seawards of the lagoons, whereas a 20 m thick sandstone will be deposited in front of the river outlets. Consequently, the presence of a sandstone body with even strike thickness would therefore suggest a sub-linear coastline. Also see Table 3. Calculations based on formula presented by Cant (1991).

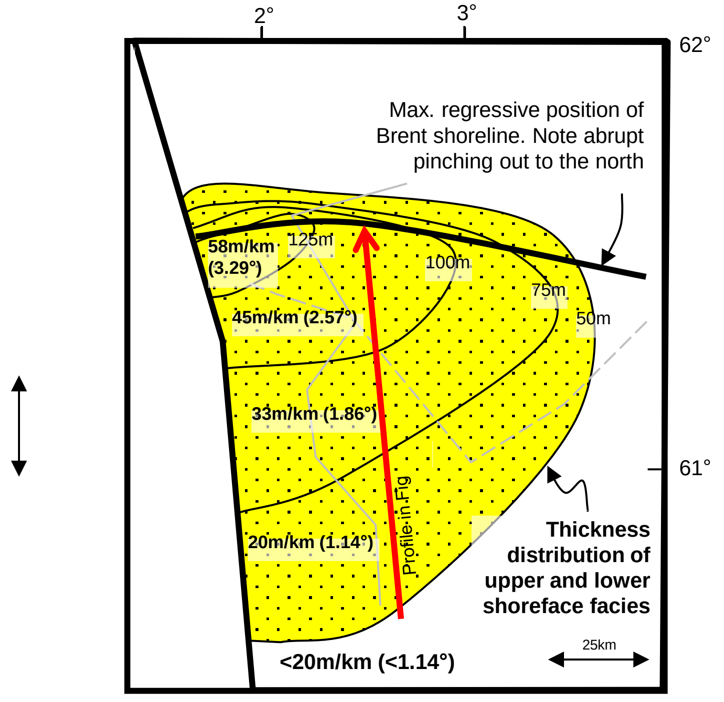

Fig. 11 Facies thickness map of the upper and lower shoreface sandstone facies. Note the gradual thickness increase toward north and the abrupt pinch out. The inferred stratigraphic climb per km and angle of shoreline trajectory is indicated and were calculated based on the facies thickness and assuming a shoreface sand length and pinch-out depth of 2 km and 10 m, respectively (cf. formula in Table 3). Within this framework, the total rise in relative sea level would have been c. 3500 m, further implying that other facies geometries than the ones used here applied to the Brent coast line (also see text). Grey lines indicate position of profiles in Fig. 5.

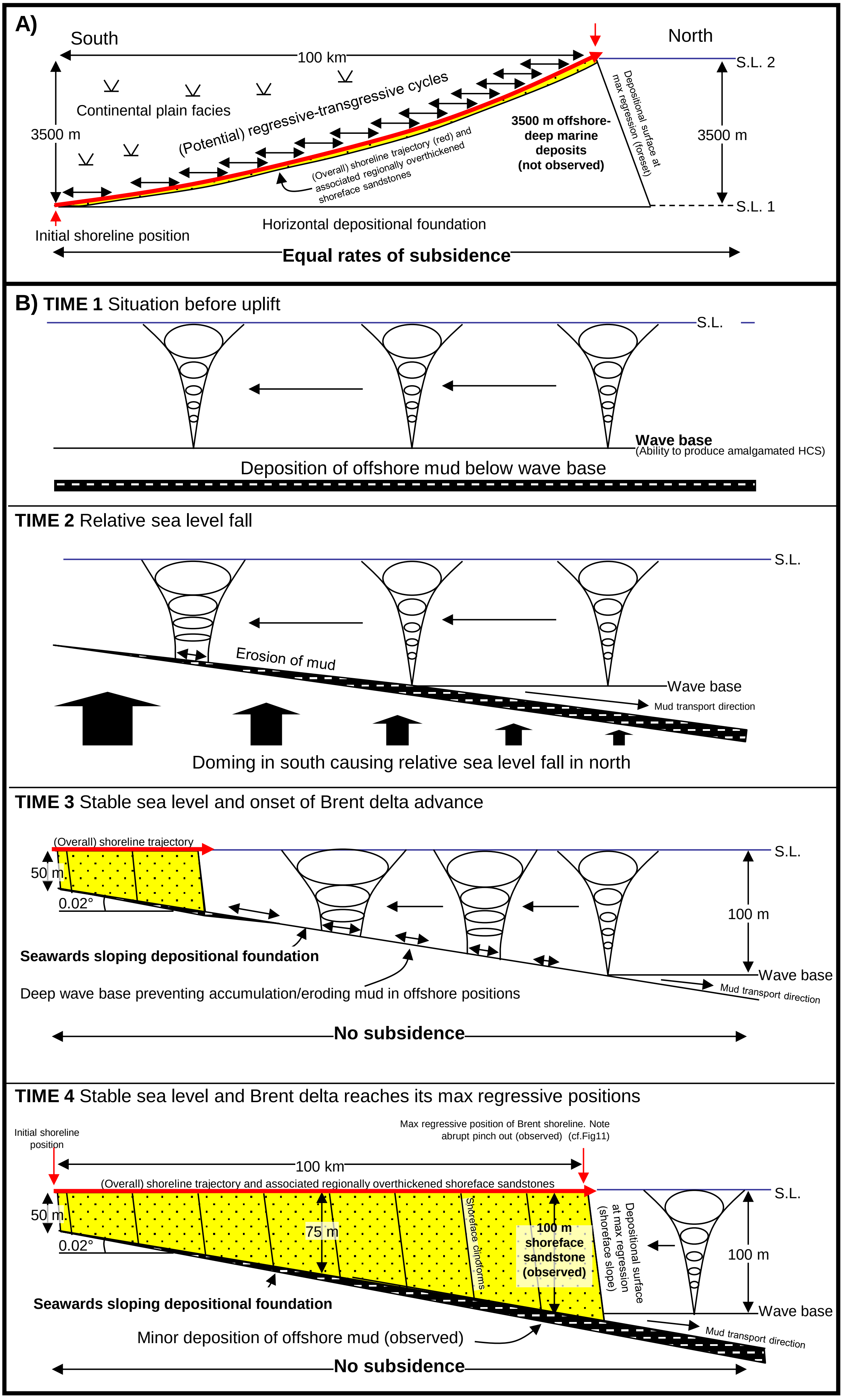
A)
South
North
100 km
3500 m
S.L. 2
S.L. 1
Continental plain facies
(Potential) regressive-transgressive cycles
(Overall) shoreline trajectory (red) and associated regionally overthickened shoreface sandstones
3500 m offshore-deep marine deposits (not observed)
Depositional surface at max regression (foreset)
Initial shoreline position
Horizontal depositional foundation
Equal rates of subsidence
B) TIME 1 Situation before uplift
S.L.
Wave base
(Ability to produce amalgamated HCS)
Deposition of offshore mud below wave base
TIME 2 Relative sea level fall
S.L.
Erosion of mud
Wave base
Mud transport direction
Doming in south causing relative sea level fall in north
TIME 3 Stable sea level and onset of Brent delta advance
(Overall) shoreline trajectory
S.L.
50 m
0.02°
100 m
Wave base
Mud transport direction
Seawards sloping depositional foundation
Deep wave base preventing accumulation/eroding mud in offshore positions
No subsidence
TIME 4 Stable sea level and Brent delta reaches its max regressive positions
Initial shoreline position
Max regressive position of Brent shoreline. Note abrupt pinch out (observed) (cf.Fig11)
100 km
(Overall) shoreline trajectory and associated regionally overthickened shoreface sandstones
S.L.
50 m
0.02°
75 m
Shoreface clinoforms
100 m shoreface sandstone (observed)
Depositional surface at max regression (shoreface slope)
100 m
Wave base
Mud transport direction
Seawards sloping depositional foundation
Minor deposition of offshore mud (observed)
No subsidence

Fig 12 Conceptual sketches showing 2 different ways of generating the regionally anomalously thick shoreface sandstone successions in the study area. NOTE: highly different vertical scale between a and b. A) Sketch of the Brent delta regression with the shoreline trajectory angle inferred from the facies thicknesses of lower and upper shoreface facies and facies geometries in modern wave-dominated coastlines (cf. Fig 11, Table 1, Table 3). This scenario predicts the presence of 3500 m continental plain deposits up dip of the position of maximum shoreline regression, and 3500 m offshore-deep marine deposits stratigraphically below the position maximum shoreline regression. Such thicknesses are not present in the study area, and the model is therefore rejected. **B)** The northward progradation of the Brent delta was initiated by doming in the south (Underhill & Partington, 1993; 1994) which caused relative sea level fall in the study area. The Brent delta shoreface prograded with a 2 km shoreface sand length and 2.9° shoreface slope into a basin with a seaward sloping (0.02°) depositional foundation and stable sea level. The shoreface sandstone thickness increases as water depth increases and the deep wave base is able to generate the lower and upper shoreface facies at successively deeper water depth. Also, the deep wave base prevented mud from being deposited in front of the shoreface sand, efficiently being transported to areas located below wave base.

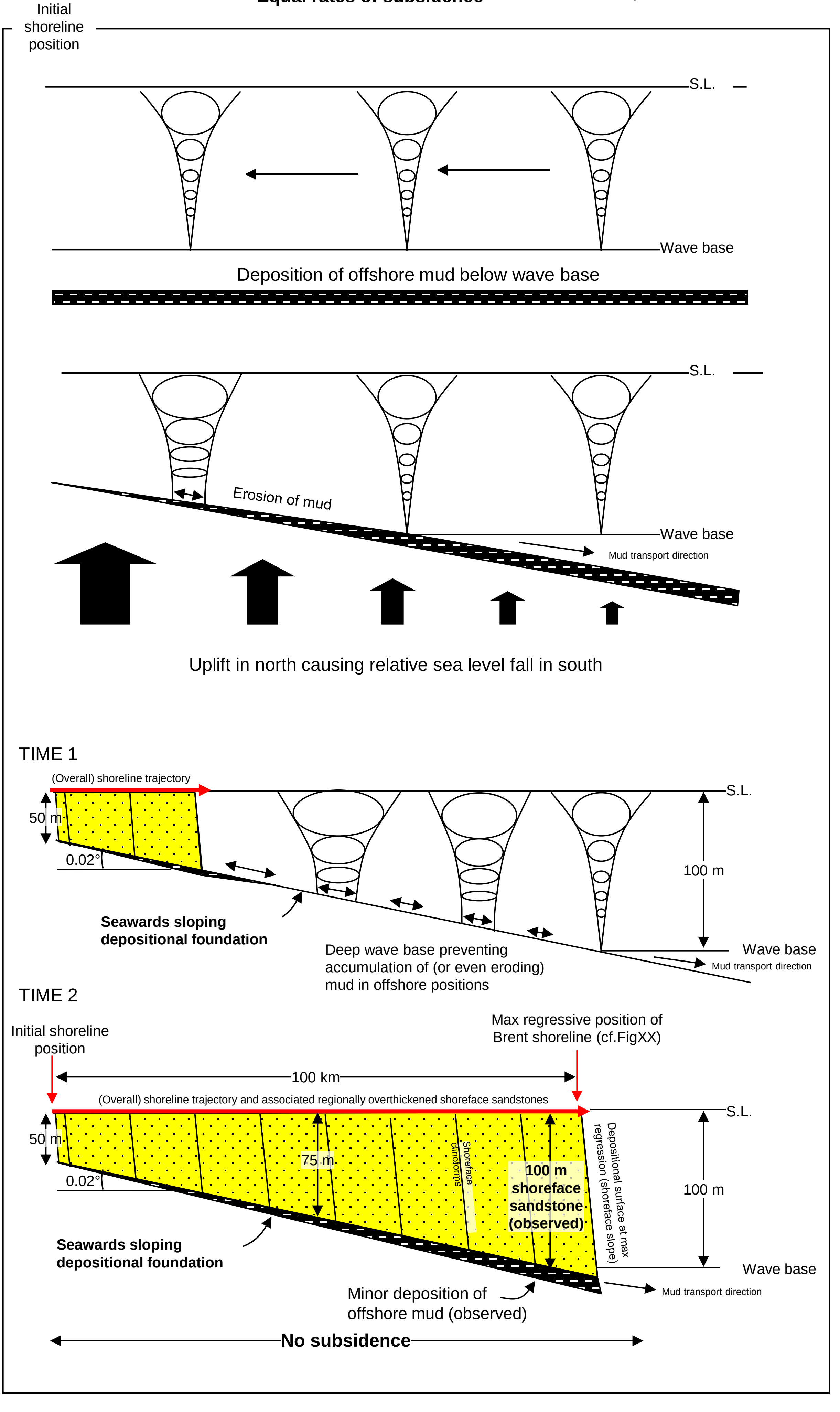

Initial shoreline position
S.L.
Wave base
Deposition of offshore mud below wave base
S.L.
Erosion of mud
Wave base
Mud transport direction
Uplift in north causing relative sea level fall in south
TIME 1
(Overall) shoreline trajectory
S.L.
50 m
0.02°
100 m
Wave base
Mud transport direction
Seawards sloping depositional foundation
Deep wave base preventing accumulation of (or even eroding) mud in offshore positions
TIME 2
Initial shoreline position
Max regressive position of Brent shoreline (cf.FigXX)
100 km
(Overall) shoreline trajectory and associated regionally overthickened shoreface sandstones
S.L.
50 m
75 m
Shoreface clinoforms
100 m shoreface sandstone (observed)
Depositional surface at max regression (shoreface slope)
100 m
0.02°
Wave base
Mud transport direction
Seawards sloping depositional foundation
Minor deposition of offshore mud (observed)
No subsidence

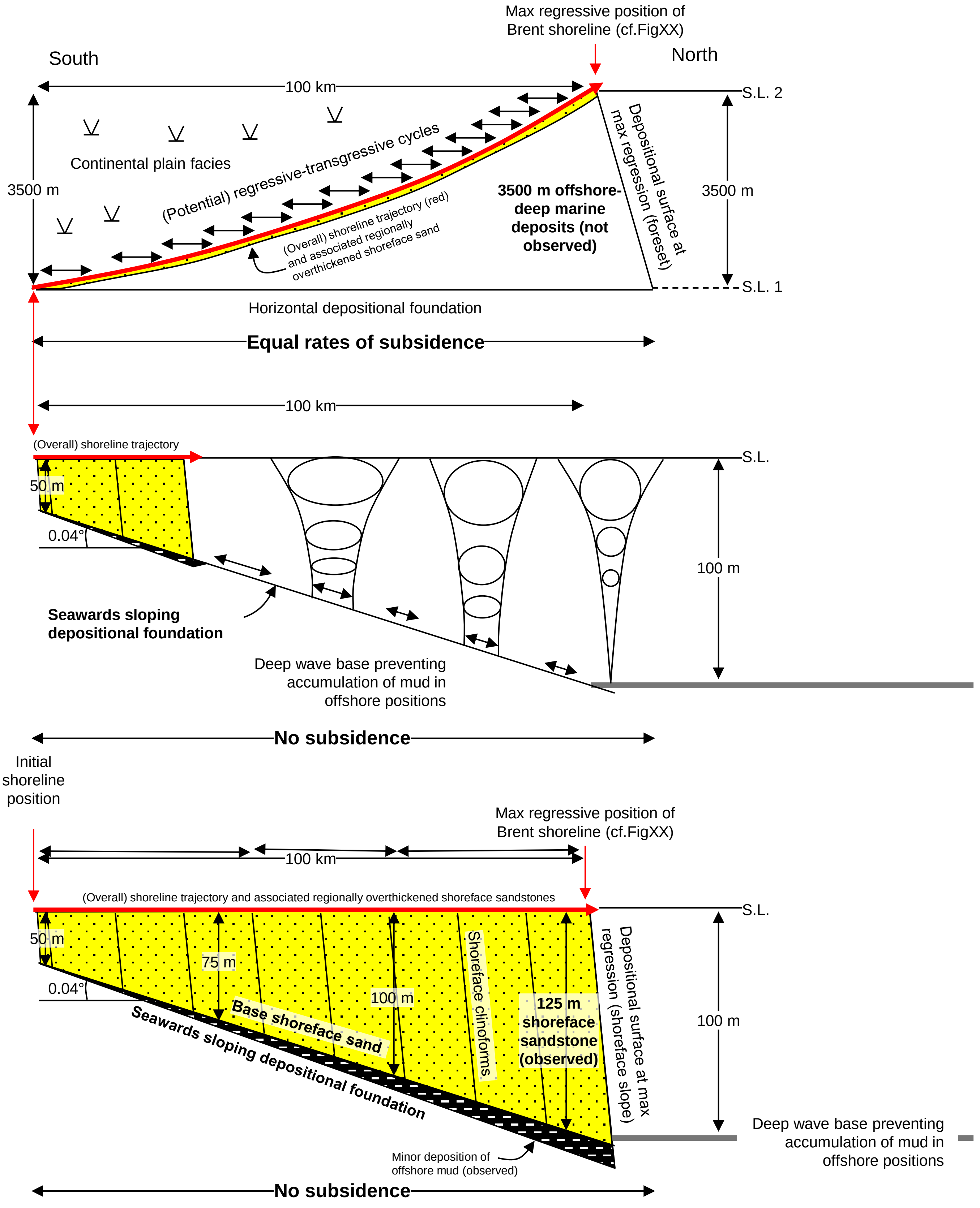

Fig Conceptual sketches showing 2 different ways of generating the anomalously thick shoreface sandstone successions in Rannoch-Etive formations. NOTE: highly different vertical scale. A) Sketch of the Brent delta regression with the shoreline trajectory angle inferred from the thicknesses of the Rannoch-Etive formations and facies geometries in modern wave-dominated coastlines (cf. Table 1, Table 3). Within this scenario, the progradation predicts the presence of 3500 m continental plain deposits up dip of max shoreline regression, and 3500 m offshore-deep marine deposits stratigraphically below max shoreline regression. Such thicknesses are not present in the study area, and the model is therefore rejected. B) Shoreface progradation (2 km shoreface sand length and XX° shoreface slope) toward stable sea level into a basin with a seaward sloping (0.04°) depositional foundation. The shoreface sandstone thickness increases as water depth increases and the deep wave base is able to generate the lower and upper shoreface facies at successively deeper water depth. Also, the deep wave base may have prevented mud from being deposited in offshore position.

A) Model for generating a regionally overthickened succession of shoreface sandstones driven by rise in relative sea level

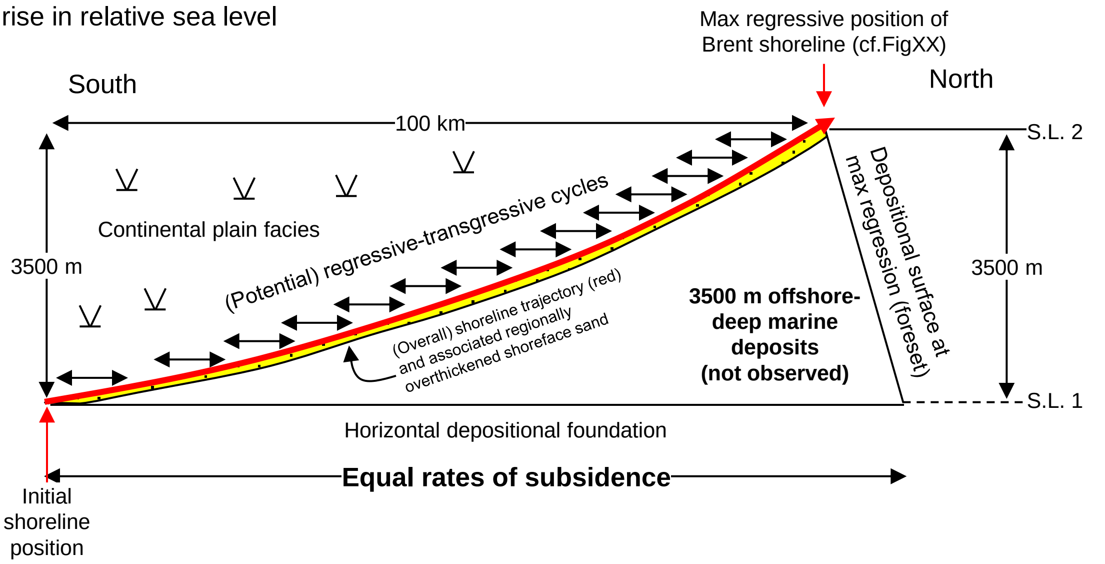

B) Model for generating a regionally overthickened succession of shoreface sandstones driven a deep wave base

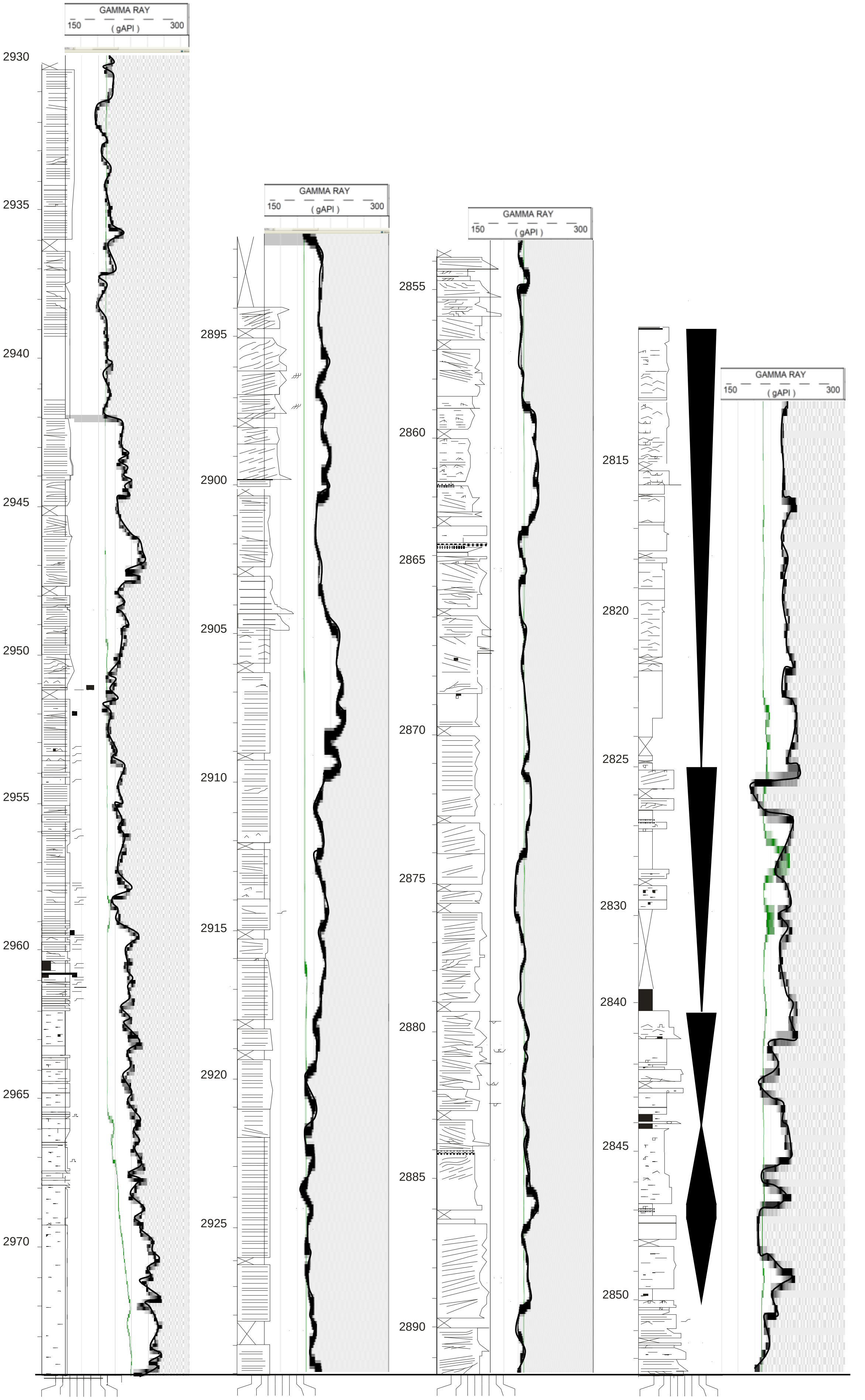
GAMMA RAY
150
(gAPI)
300
2930
2935
2940
2945
2950
2955
2960
2965
2970
GAMMA RAY
150
(gAPI)
300
2895
2900
2905
2910
2915
2920
2925
GAMMA RAY
150
(gAPI)
300
2855
2860
2865
2870
2875
2880
2885
2890
GAMMA RAY
150
(gAPI)
300
2815
2820
2825
2830
2840
2845
2850

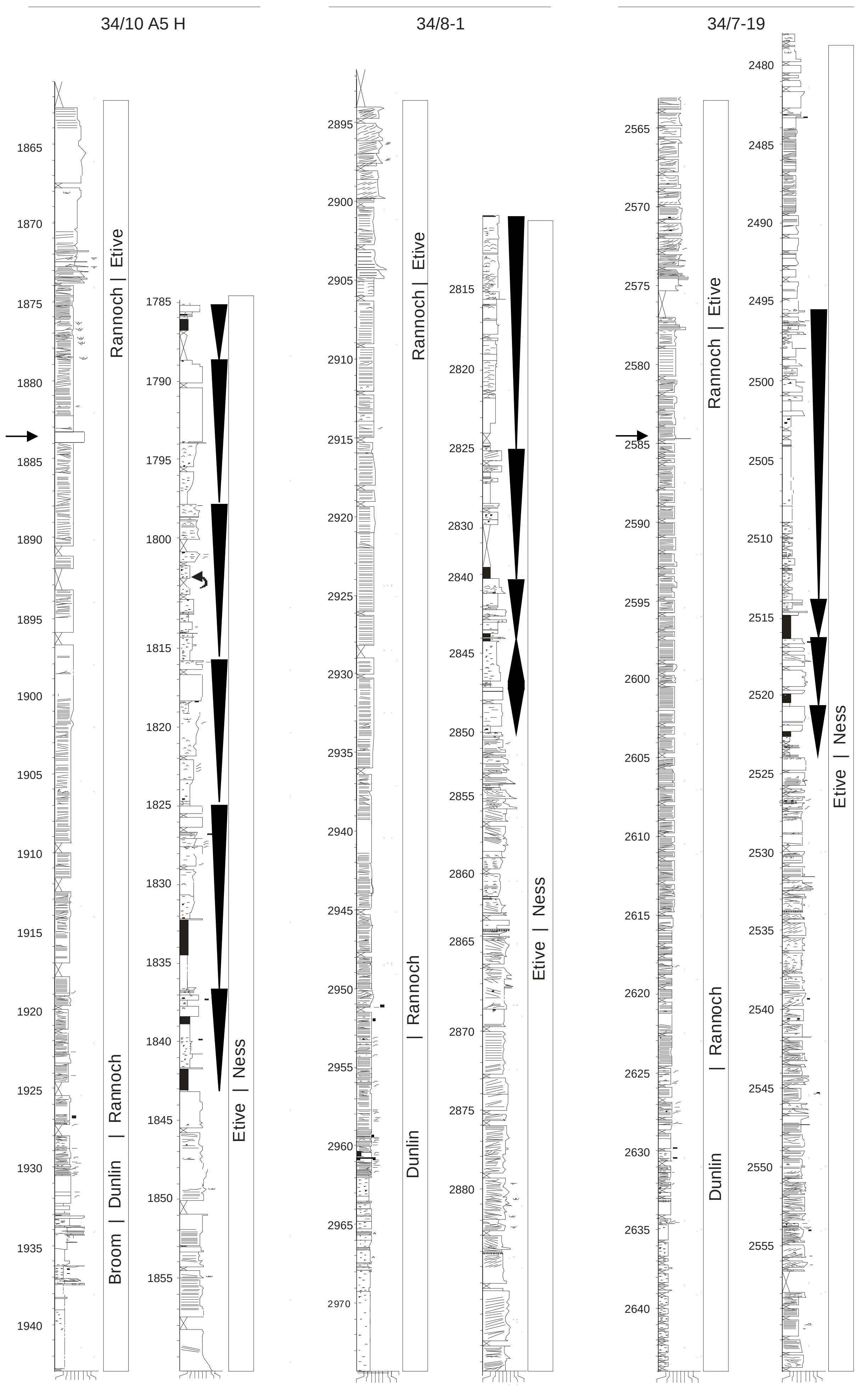
34/10 A5 H
Rannoch | Etive
Broom | Dunlin | Rannoch
Etive | Ness
34/8-1
Rannoch | Etive
Dunlin | Rannoch
Etive | Ness
34/7-19
Rannoch | Etive
Dunlin | Rannoch
Etive | Ness

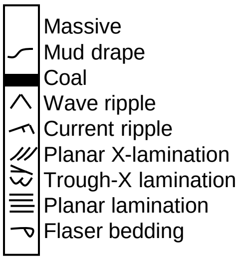

Fig. 7 Core description. The facies are stacked as a gradually upwards shallowing succession and do not display convincing evidence of regressive-transgressive cycles. Horizontal arrows point to Etive facies encased in Rannoch facies. The grain size division is from left toward right: clay, silt, very fine-fine-medium-coarse-very coarse sandstone. See Fig. 5 for location of wells.

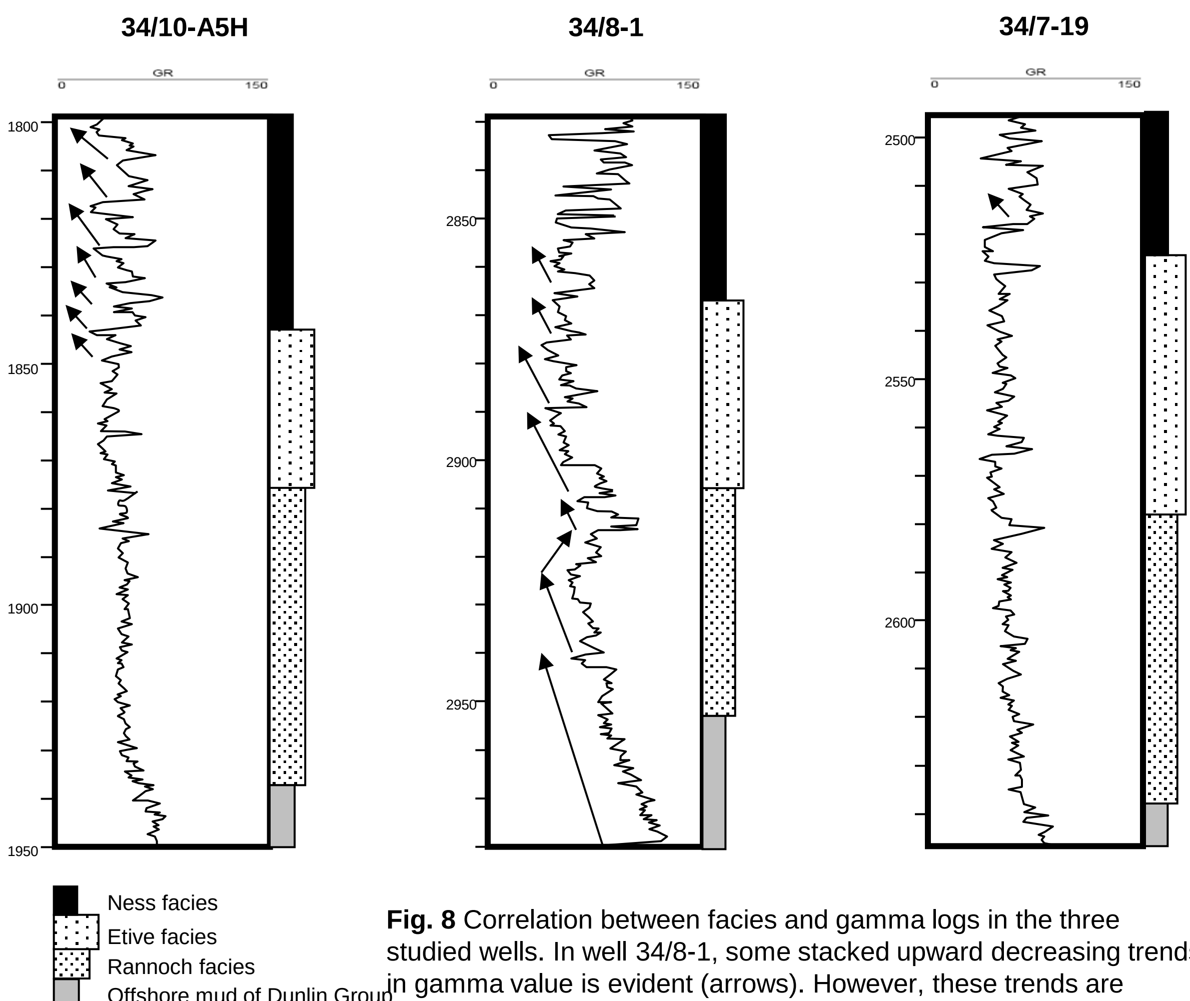

Fig. 8 Correlation between facies and gamma logs in the three studied wells. In well 34/8-1, some stacked upward decreasing trends in gamma value is evident (arrows). However, these trends are correlated to cored intervals where no facies change attributable to regressive-transgressive cycles are evident. See Fig. 7 for detailed sedimentological core description and Fig. 5 for position of wells.

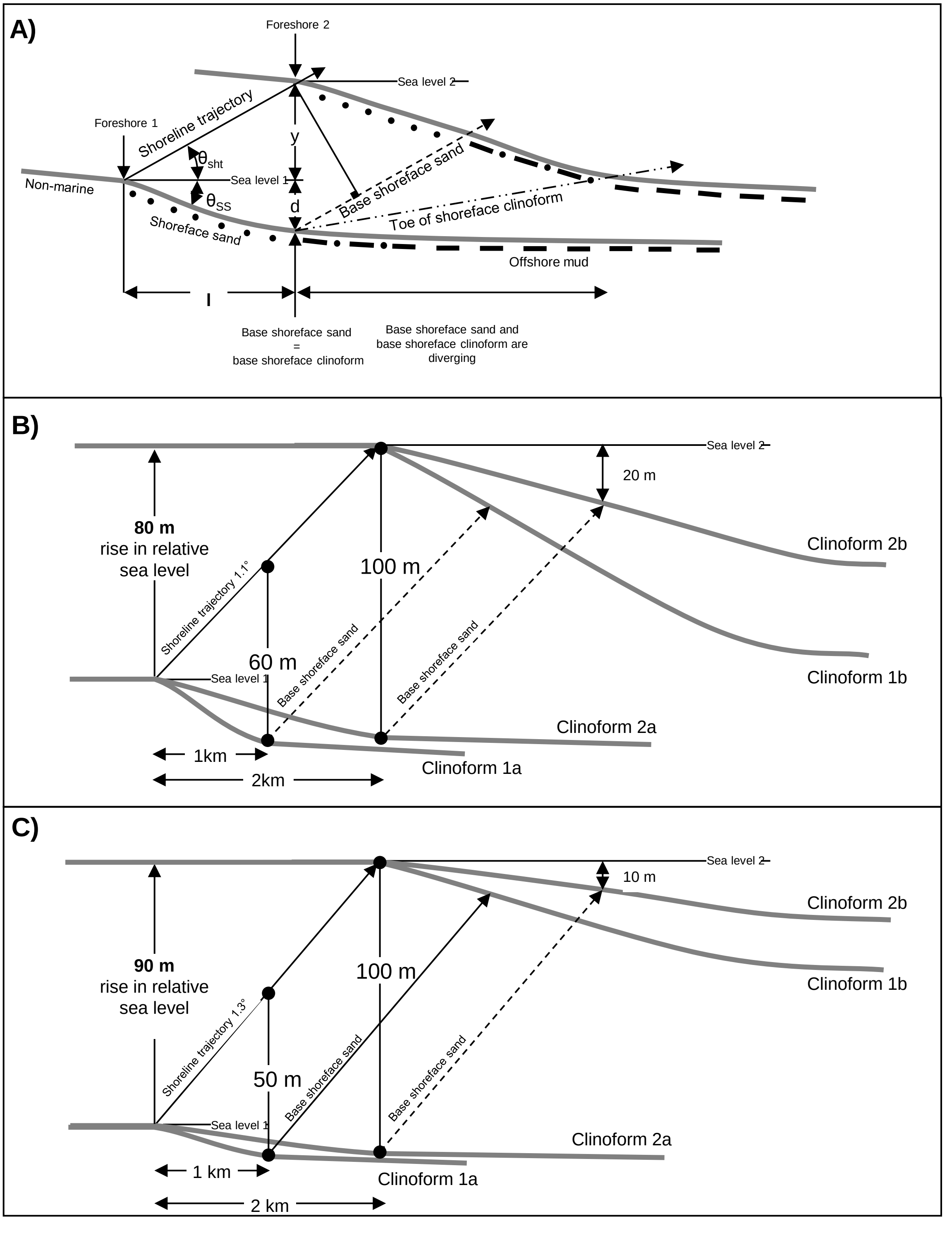

Fig. 10 Geometrical modeling of facies-belt migration in normal regressive, wave-influenced shoreface sandstone tongues. **A)** The vertical thickness of a regressive shoreface sand succession (d+y) is dependent on: 1) angle of shoreline trajectory (θ_{sht}); 2) shoreface sand length (l); and 3) shoreface sand pinch-out depth (d). The latter two can be used to calculate the average angle of the shoreface sand surface (θ_{SS}). Based on Cant (1991). **B)** Progradation with a 20 m deep shoreface sand pinch out depth. The large difference in the resulting shoreface sandstone thickness between prograding with a 2 km shoreface sand length (clinoform 1) and a 2 km length (clinoform 2) is evident. **C)** As B) but progradation with 10 m shoreface sand pinch-out depth. The above implies that progradation along a coast with large strike variations in shoreface sand length will result in large stratigraphic thickness variations of sandstone along strike. The presence of a sandstone body with even strike thickness would therefore suggest a sub-linear coastline. Also see Table 3. Calculations based on formula presented by Cant (1991).

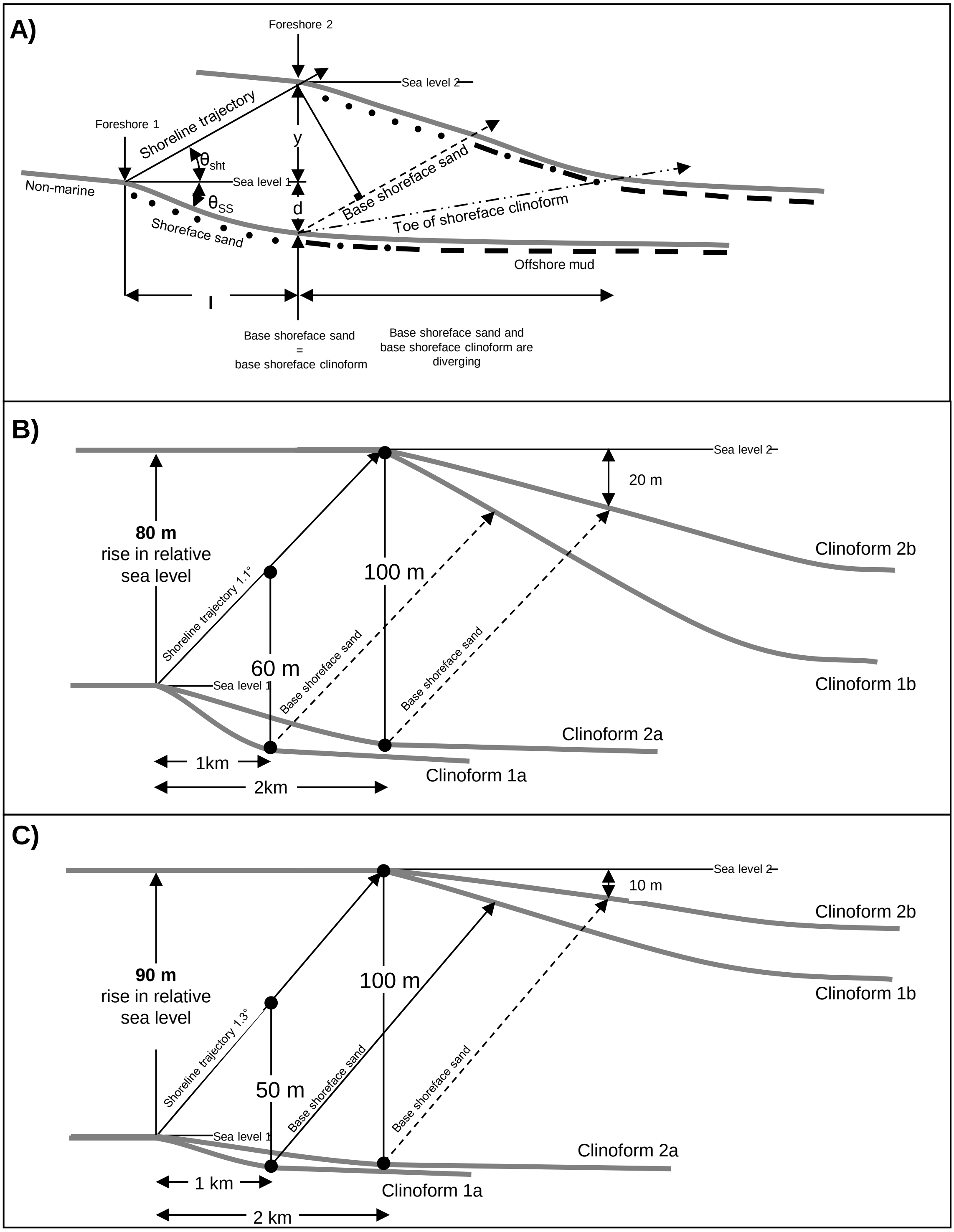

Fig. 11 Geometrical modeling of facies-belt migration in normal regressive, wave-influenced shoreface sandstone tongues. **A)** The vertical thickness of a regressive shoreface sand succession (d+y) is dependent on: 1) angle of shoreline trajectory (θ_{sht}); 2) shoreface sand length (l); and 3) shoreface sand pinch-out depth (d). The latter two can be used to calculate the average angle of the shoreface sand surface (θ_{SS}). Based on Cant (1991). **B)** Progradation with a 20 m deep shoreface sand pinch out depth. The large difference in the resulting shoreface sandstone thickness between prograding with a 2 km shoreface sand length (clinoform 1) and a 2 km length (clinoform 2) is evident. **C)** As B) but progradation with 10 m shoreface sand pinch-out depth. The above implies that progradation along a coast with large strike variations in shoreface sand length will result in large stratigraphic thickness variations of sandstone along strike. The presence of a sandstone body with even strike thickness would therefore suggest a sub-linear coastline. Also see Table 3. Calculations based on formula presented by Cant (1991).

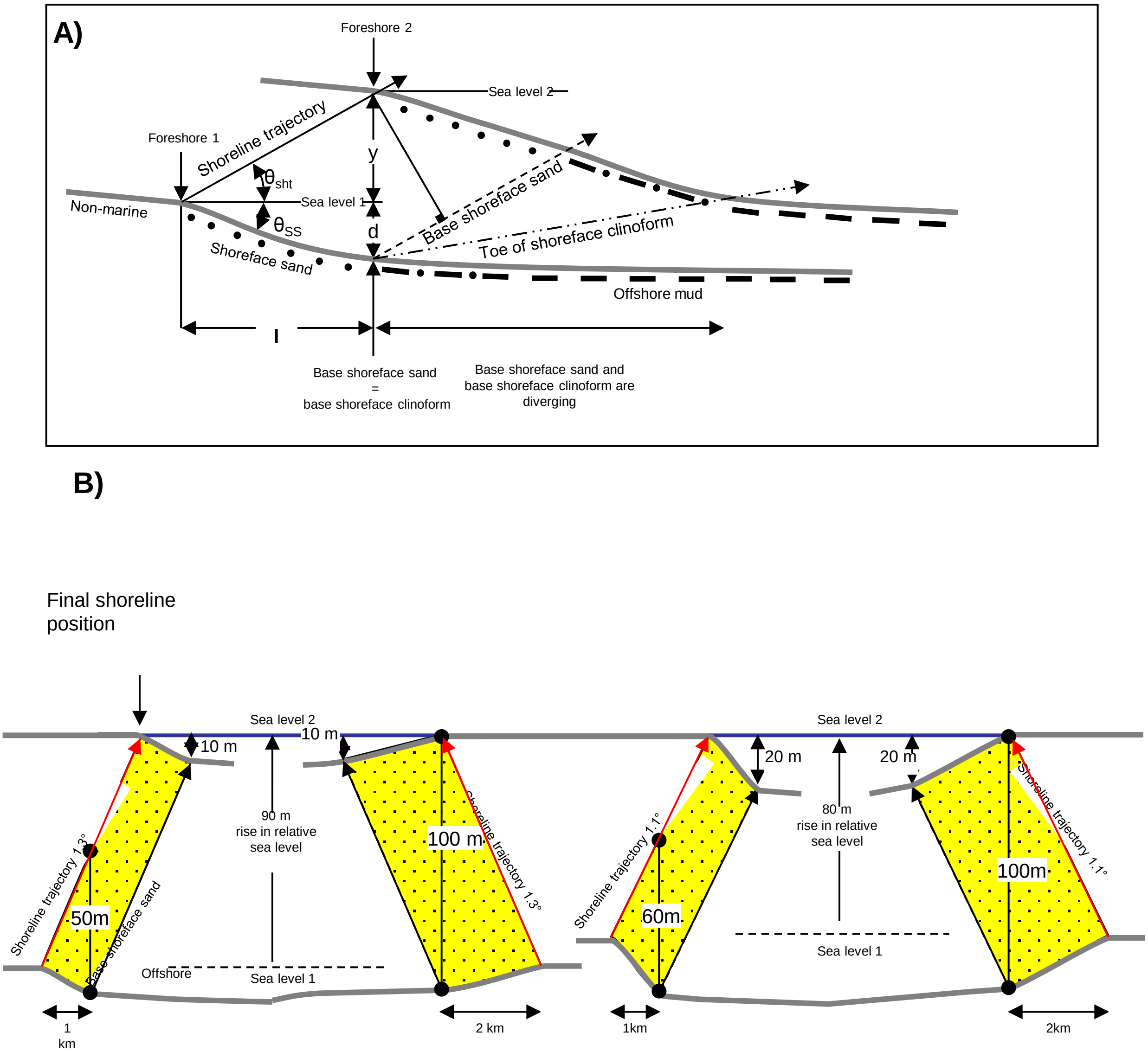

Fig. 10 Geometrical modeling of facies-belt migration in normal regressive, wave-dominated shoreface sandstone tongues. **A)** The vertical thickness of a regressive shoreface sand succession (d+y) is dependent on: 1) angle of shoreline trajectory (θ_{sht}); 2) shoreface sand length (l); and 3) shoreface sand pinch-out depth (d). The latter two can be used to calculate the average angle of the shoreface sand surface (θ_{SS}). Based on Cant (1991). **B)** Progradation with a 20 m deep shoreface sand pinch out depth. The large difference in the resulting shoreface sandstone thickness between prograding with a 1 km shoreface sand length (left) and a 2 km length (right) is evident. **C)** As B) but applying a 10 m shoreface sand pinch-out depth. The above implies that progradation along a coast with large strike variations in shoreface sand length will result in large stratigraphic thickness variations of sandstone along strike. In the the Ebro delta, for example, (Fig. 3), progradation toward stable sea level will result in a 5 m thick shoreface sandstone seawards of the lagoons, whereas a 20 m thick sandstone will be deposited in front of the river outlets. Consequently, the presence of a sandstone body with even strike thickness would therefore suggest a sub-linear coastline. Also see Table 3. Calculations based on formula presented by Cant (1991).

CHAPTER 3

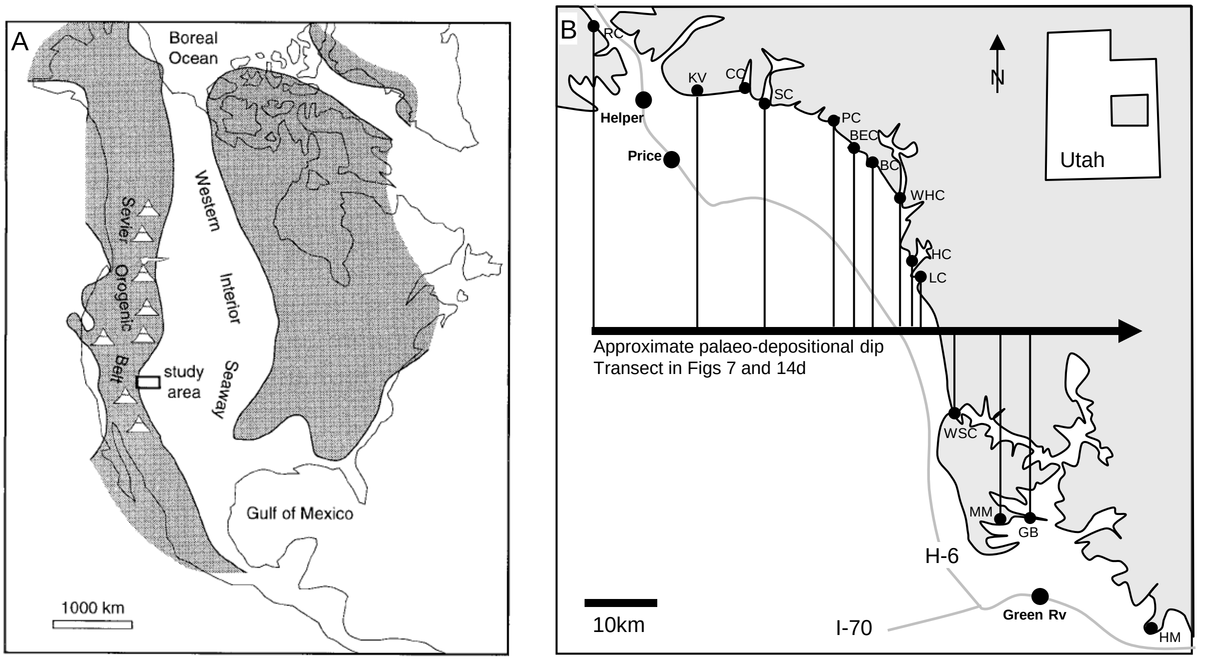

Fig. 1 A) Late Cretaceous palaeogeography of USA and location of study area. Adapted from Hampson et al. (1999), modified from Kauffman and Caldwell (1993). B) Map of the study area in Utah with key localities indicated. RC: Road cut (at Castlegate); KV: Kenilworth village; CC: Coal Canyon; SC: Soldier Canyon; PC: Pace Canyon; BEC: Bear Canyon; BC: B-Canyon; WHC: Whitemoore Canyon; HC: Horse Canyon; LC: Lila Canyon; WSC: Woodside Canyon; MM: Middle Mountain; GB: Gunnison Butte; HM: Hatch Mesa. Modified from Davies et al., (2006).

Fig. 2 The various classes of shoreline trajectories. Heavy line indicates the shoreline trajectory. Adapted from Helland-Hansen and Martinsen (1996).

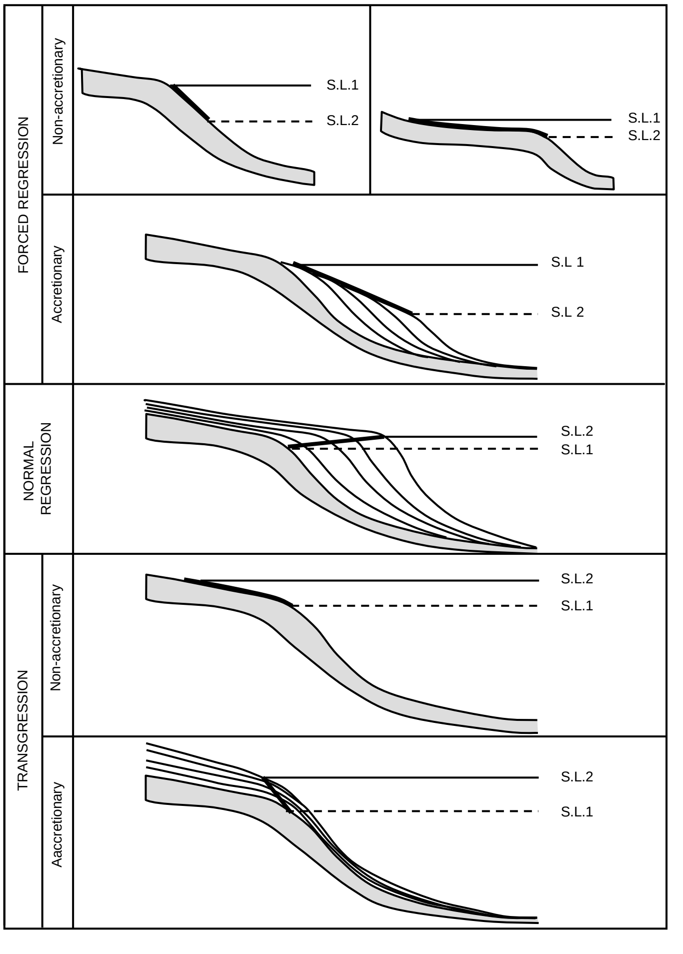

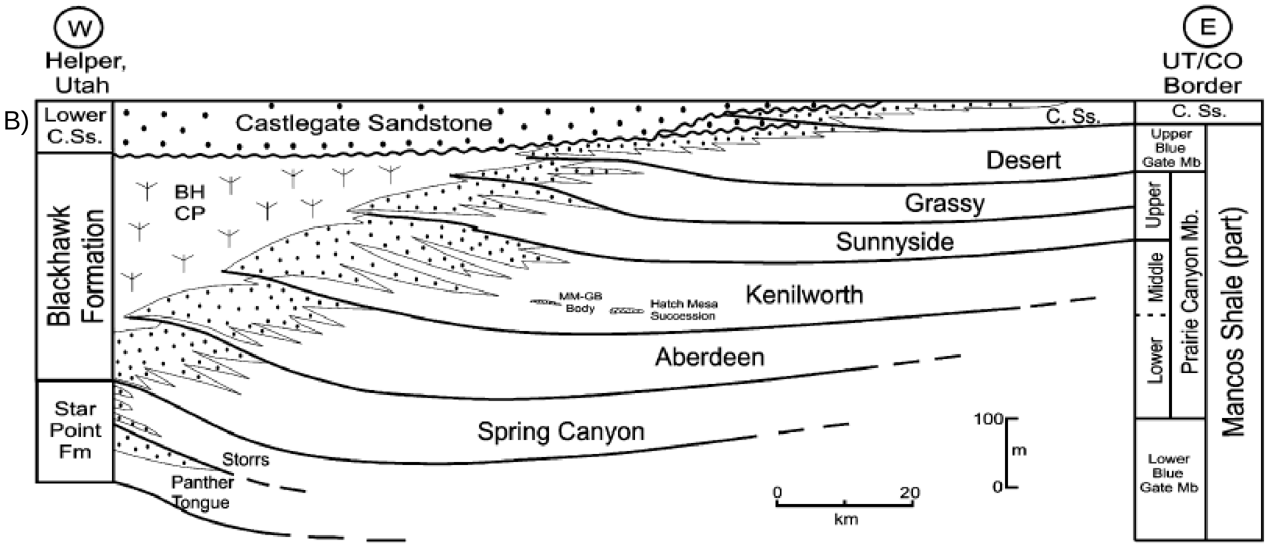

Fig. 3 Lithostratigraphic scheme of Blackhawk Formation. Adapted from Pattison (2005), modified from Young (1955) and Cole (1997).

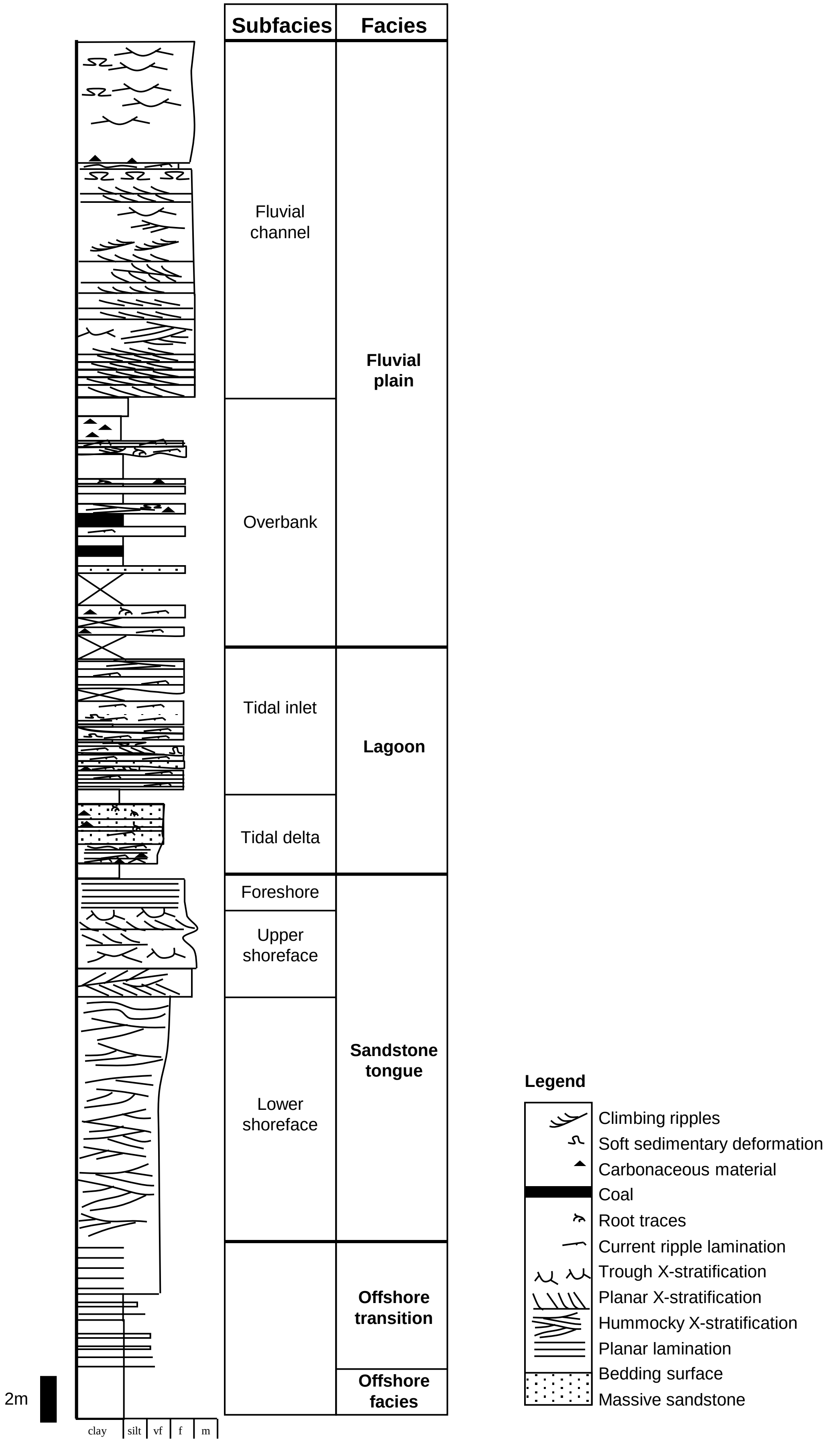

Fig. 4 Composite sedimentary log of the facies and subfacies recognised in this study, collected from Woodside Canyon, Soldier Canyon and at road cut locality (cf. Fig. 1). See Table 1 for description and interpretation of facies and Fig. 5 for photos.

Fig. 5 Facies and subfacies recognised in this study. Division on stick 10 cm. **A)** Fluvial channel subfacies, note internal channel geometry. **B)** Overbank subfacies, sheet sands, small scale channelisation and heterolithic character evident. Person for scale. **C)** Tidal inlet subfacies; note low angel channelisation. **D)** Tidal delta subfacies; planar sheet sandstones. Cliff c. 2.5 m tall. **E)** Foreshore subfacies; planar lamination origin from swash zone. Pen for scale. **F)** Upper shoreface subfacies; trough cross lamination with palaeoflows parallel to coastline. **G)** Lower shoreface subfacies; HCS dominated. **H)** Offshore transition facies; bioturbated heterolithics. **I)** Offshore facies grading up into offshore transition facies. Cf. Table 1.

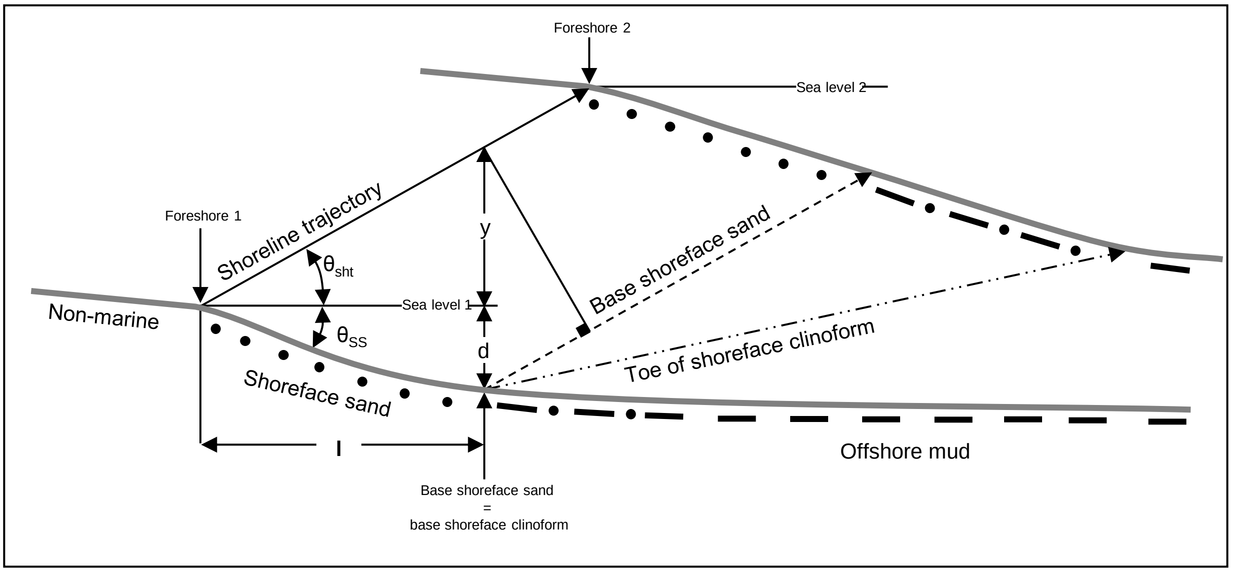

Fig. 6 Geometrical modeling of facies belt migration. Progradation during rising relative sea level is associated with vertical stretching of facies belts. d: Pinch-out depth of homogenous sand; y: amount of vertical stretching of homogenous shoreface sand during progradation with rising sea level; l: length of homogenous shoreface sand; θ_{sht}: angle of shoreline trajectory; θ_{SS}: angle of sediment surface. Modified from Cant (1991).

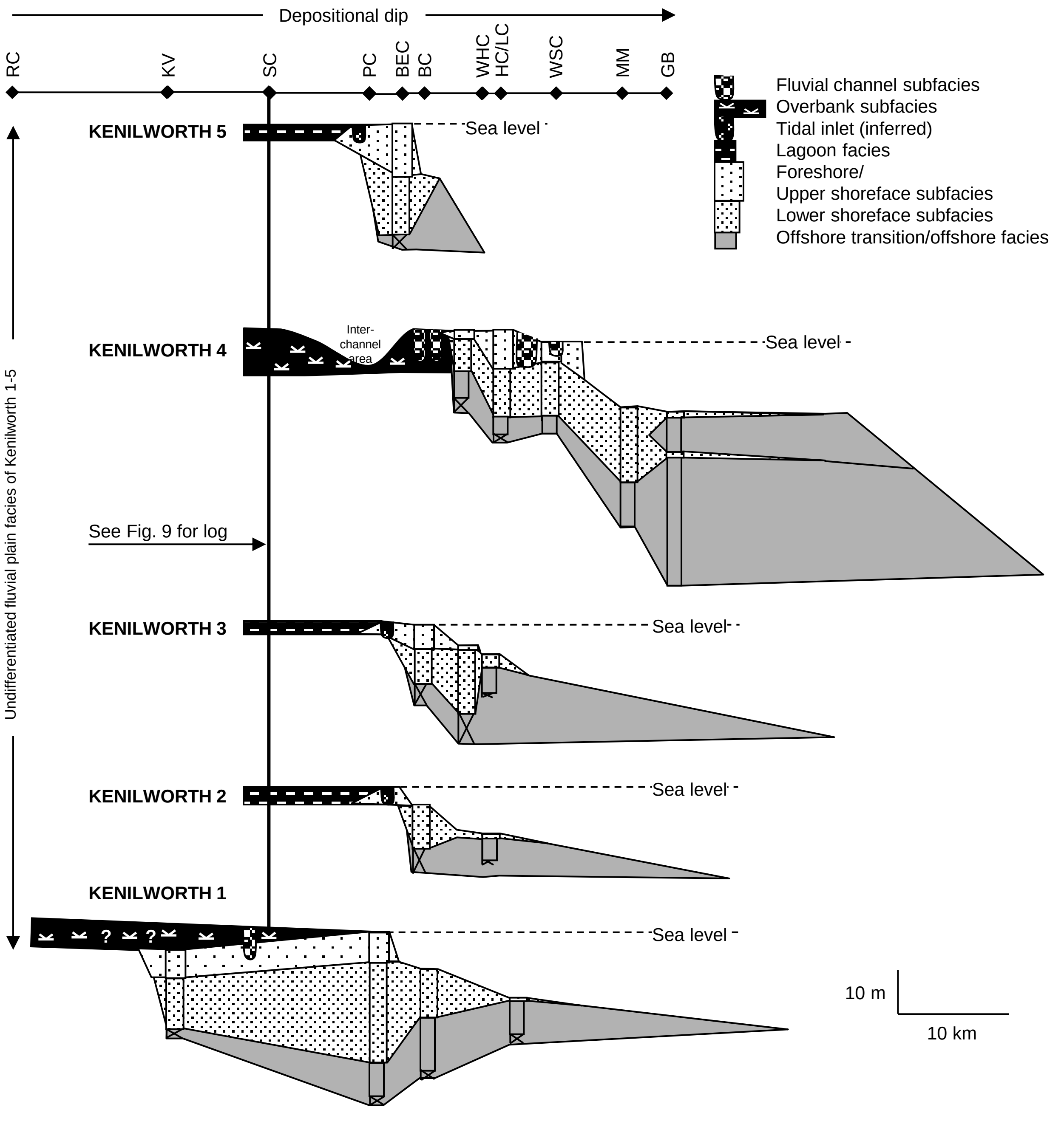

Fig. 7 Correlation scheme for the parasequences in the Kenilworth Member. Outcrops have been projected to an east-west directed depositional dip profile as indicated in Fig. 1b. The parasequences with short regressive distances (Kenilworth 2, 3 and 5) are associated with lagoon-barrier coasts whereas parasequences with long regressive distances are associated with deltaic coasts (Kenilworth 1 and 4). The pinch-out water depth of lower shoreface sand is assumed to be approximately 15 m along deltaic coasts and 10 m along lagoon-barrier coasts (see text). Note that the top surface in the continental part of Kenilworth 4 have topographical relief, suggesting the presence of a slope extending away from the main channel belts. See Fig. 1 for abbreviations. Parasequence numbering correspond to Taylor and Lovell (1995). For more detailed correlation diagrams for the marine part of Kenilworth Member along the Book Cliffs section, see figs. 3-7 in Pattison (1995) and figs. 10 and 11 in Taylor and Lovell (1995).

Fig. 8 Sharp base of Kenilworth 1 sandstone tongue as expressed in Pace Canyon. Amalgamated sandstones belonging to lower shoreface subfacies directly overlies offshore facies without being separated by offshore transition facies.

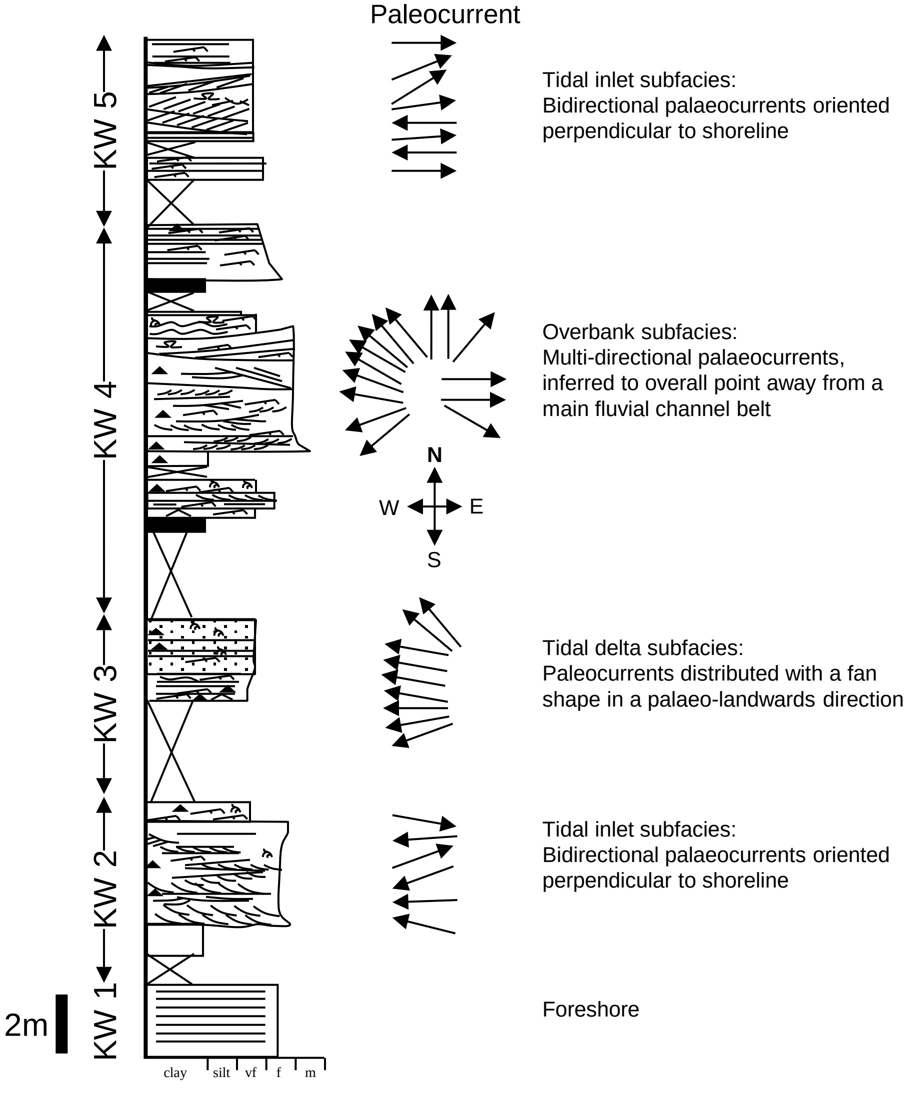

Fig. 9 The stratigraphic succession between top Kenilworth (KW) 1 and top Kenilworth 5 (32 m) as exposed in Soldier Canyon. Note slightly more coarse grained and thicker development of Kenilworth 4 compared to the other parasequences. See Fig. 4 for legend, Table 1 and Fig. 5 for facies description.

Fig. 10 Model for the development of *regressive* lagoons (continuous arrow indicate shoreline trajectory). If interpreting the short distance regressive lagoon-barrier coasts to be strike equivalent to the longer distance regressive deltaic coasts, this gives two possible palaeogeographic models: **A)** An asymmetric delta system with lagoons present down drift from channel outlets as a result of the fresh water plume from the river preventing longshore drifted sediments to be deposited in this area. The model predicts that the main channel belts are located down-drift of long regressive strand plains and up-drift of lagoon-barrier complexes. Based on Bhattacharya and Giosan (2003)'s model for asymmetric deltas. **B)** Preferred model for the Kenilworth Member: a symmetric delta with lagoons located on both sides of the channel belt. Fluvial channel belts are observed to cut the Kenilworth 4 sandstone tongue numerous places along strike (cf. Fig. 7), suggesting main sediment transport to the coastlines occurred on top of the sandstone tongue, and not down drift of these as predicted in an asymmetric model. See text for further discussion.

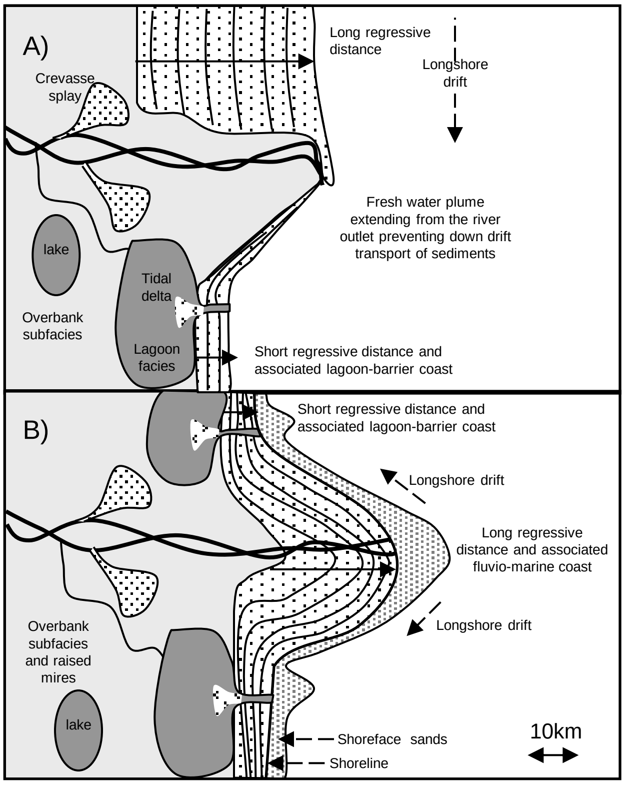

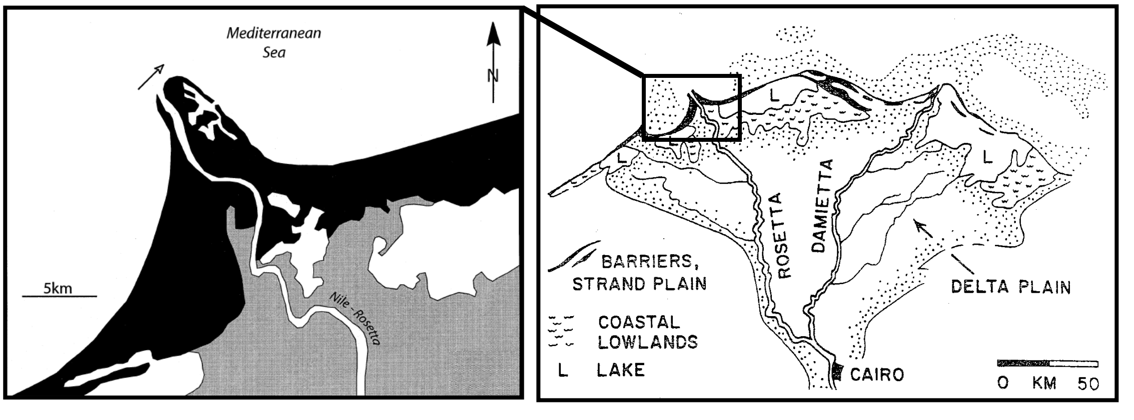

Fig. 11 The Rosetta lobe (inset) of the Nile delta is the preferred modern analogue for the Kenilworth Member palaeogeography. Lagoon-barrier coasts are associated with short regressive distances, whereas deltaic coasts are associated with long regressive distances. Black areas indicate sands, whereas deltaic plain lithologies other than sand is colored grey. Arrow indicate predominant direction of longshore drift. Inset figure modified from Sestini (1989) and Fanos et al. (1995), adapted from Bhattacharya and Giosan (2003). Overview figure (right) after Fischer and McGowen (1969) and Sestini (1989), adapted from Bhattacharya and Walker (1992).

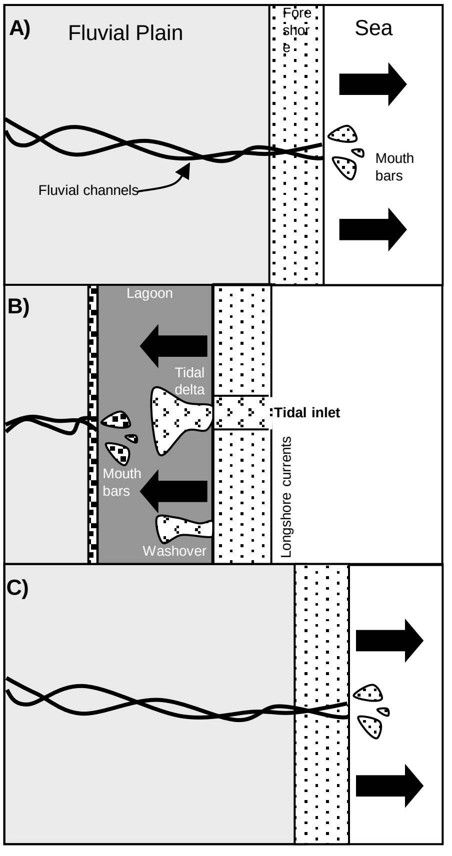

Fig. 12 Model for development of *transgressive* lagoons. **A)** The shoreline initially prograded seawards during stable sea level. During the regression, the continental-marine transition is direct from fluvial plain to marine facies. **B)** When the regression is terminated by a rise in relative sea level, the shoreline migrates landward and the fluvial plain and sandstone tongue facies is separated by lagoon facies. **C)** When rate of rise in relative sea level slows down, the lagoons start to fill up by fluvial mouth bars, flood tidal deltas and washovers fans. Finally, the fluvial channels break through to the coastline and the shoreline start to prograde until the next rise in relative sea level. Arrows indicate the migration direction of facies belts. Modified from Howell and Flint (2003).

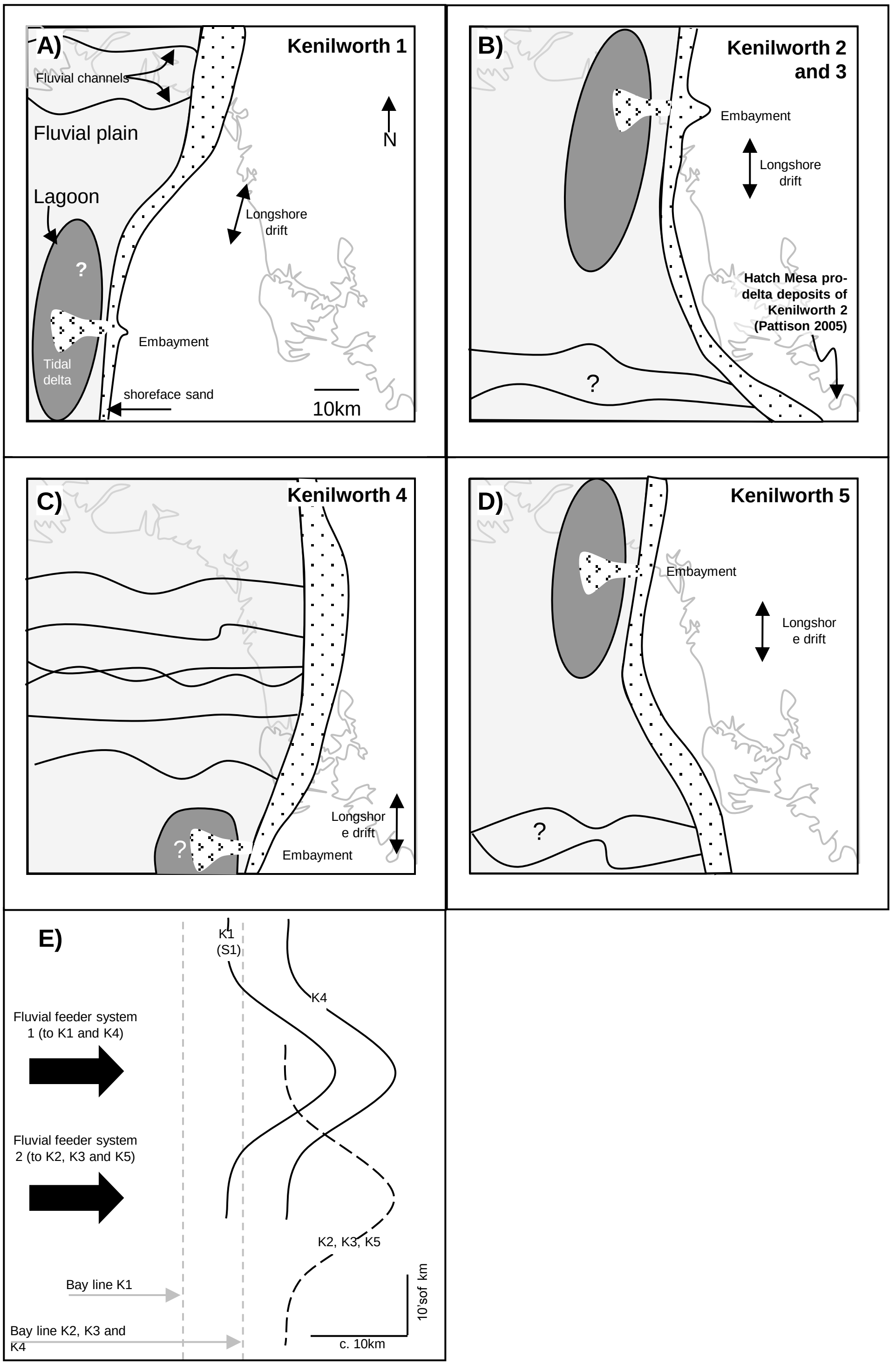

Fig. 13 Tentative palaeogeographic sketches (cf. Fig. 1) of the maximum regressive position of the Kenilworth parasequences (K1-K5), based on the palaeogeographic model proposed in this study (Fig. 10b). The parasequences are interpreted to be the result of compensation style stacking caused by over-extension of the fluvial system (see text). **A)** K1: An embayment with a lagoon-barrier complex is inferred to have been located to the south in the study area. **B)** K2 and K3: The main channel outlets and associated deltaic lobe is interpreted to fill in the inferred embayment of the underlying K1, whereas an contemporaneous embayment and lagoon-barrier coast is inferred to have been located in the north of the study area. The Hatch Mesa delta front deposits are time equivalent to the K2 parasequence (Pattison, 2005d), supporting the interpretation of a major seaward protuberance of the coastline in the Hatch Mesa area. **C)** K4: The focus of deposition shifted back into the Book Cliffs transect and is interpreted to fill in the inferred embayment of the underlying K2 and K3 parasequences. **D)** K5: The delta lobe is inferred to have shifted away from the study area resulting in an embayment located approximately at the same position as K2 and K3. **E)** Regional palaeogeographic sketch of the interpreted stacking of Kenilworth Member delta lobes. Onset of deposition of the Kenilworth Member was initiated by the strike-stepping of K1 into the Book Cliffs. K2 and K3 are strike and basinward-stepping compared to the underlying K1 lobe, whereas K4 and K5 are only strike-stepping. The above Sunnyside parasequence (S1) is back-stepping and is located in approximately the same area as K1.

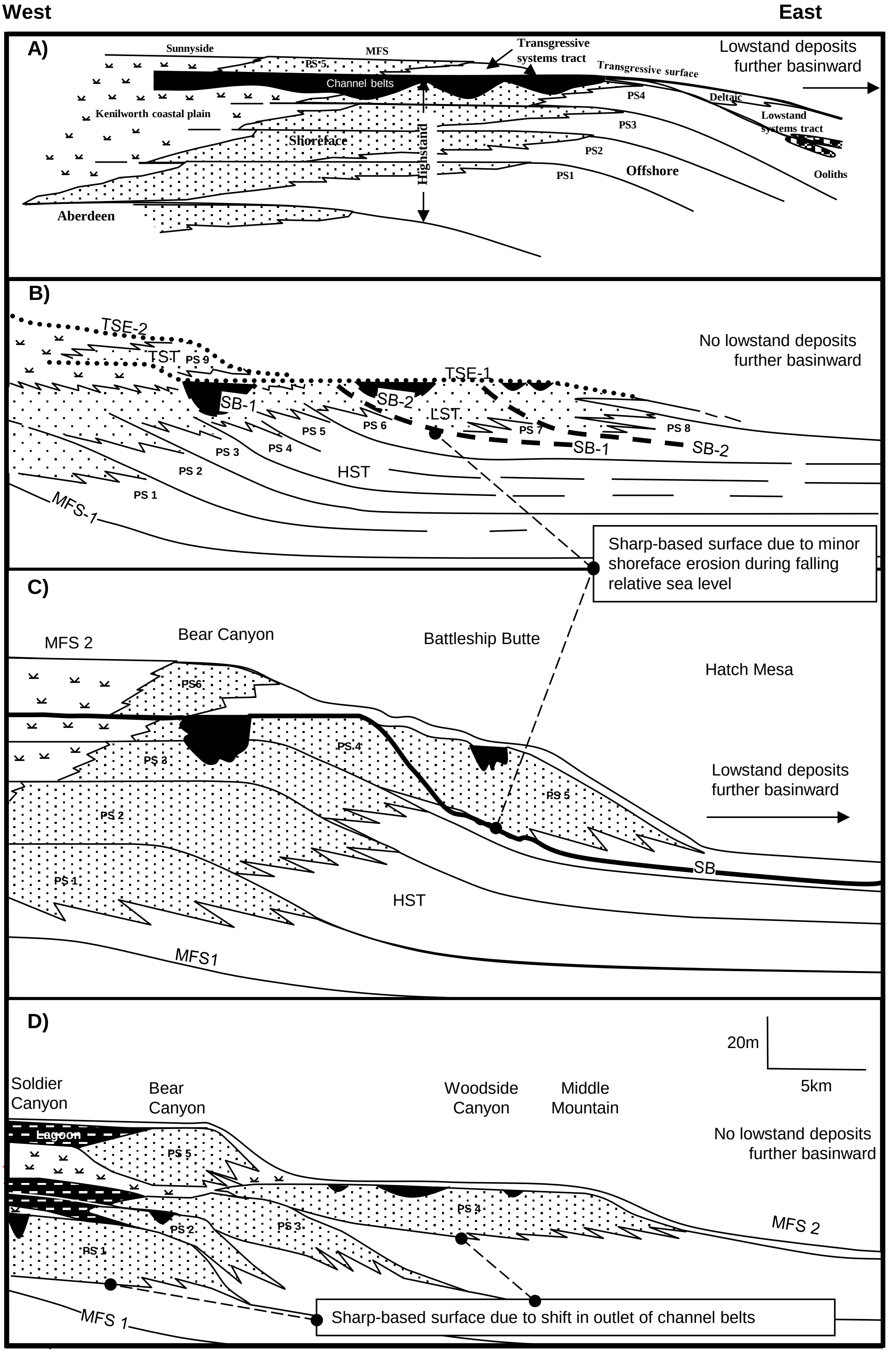
West
East
A)
Sunnyside
MFS
PS 5
Transgressive systems tract
Transgressive surface
Lowstand deposits further basinward
Channel belts
PS4
Deltaic
Kenilworth coastal plain
PS3
Lowstand systems tract
Shoreface
Highstand
PS2
Ooliths
PS1
Offshore
Aberdeen
B)
TSE-2
TST
PS 9
No lowstand deposits further basinward
TSE-1
SB-1
SB-2
LST
PS 5
PS 6
PS 7
PS 8
PS 3
PS 4
SB-1
SB-2
PS 2
HST
PS 1
MFS-1
Sharp-based surface due to minor shoreface erosion during falling relative sea level
C)
MFS 2
Bear Canyon
Battleship Butte
Hatch Mesa
PS6
PS 4
PS 3
Lowstand deposits further basinward
PS 5
PS 2
SB
PS 1
HST
MFS1
D)
20m
5km
Soldier Canyon
Bear Canyon
Woodside Canyon
Middle Mountain
No lowstand deposits further basinward
Lagoon
PS 5
PS 4
MFS 2
PS 2
PS 3
PS 1
MFS 1
Sharp-based surface due to shift in outlet of channel belts

Fig. 14 Different interpretations of the high resolution sequence stratigraphy of Kenilworth Member. The predicted detached lowstand deposits in models A and C remain undocumented. **A)** Taylor and Lovell (1995) placed a sequence boundary on top of Kenilworth 4 parasequence and predicted detached lowstand shorelines down-dip of the study area. **B)** Pattison (1995) subdivided the Taylor and Lovell's (1995) parasequence 4 into three (Pattison's PS 6, 7, 8) and argued that 2 sequence boundaries run through the sandstone tongue. The sandstone bodies were interpreted as attached lowstand deposits. **C)** Howell and Flint (2003) divided the same shoreface tongue into two (their parasequence 4 and 5) separated by a sequence boundary. As the model in A, this model also predicts the presence of detached lowstand shorelines down-dip of the study area. **D)** Approximately scaled high resolution sequence stratigraphic model proposed in this study. The entire Kenilworth Member is interpreted as a part of highstand systems tract (cf. Fig. 13e) and there is no sequence boundary implied. Consequently, the model exclude the presence of detached lowstand shorelines and predicts the presence of deltaic lobes along strike from parasequences 2, 3 and 5, as well as lagoon-barrier complexes being located along strike from Kenilworth 1 and 4. Note that parasequence 5 is interpreted to be located within inter-channel belt depressions in parasequence 4. SB: Sequence boundary; TSE: Transgressive surface of erosion; LST: Lowstand systems tract; TST: Transgressive systems tract; HST: Highstand systems tract; MFS: Maximum flooding surface; PS: parasequence.

CHAPTER 4

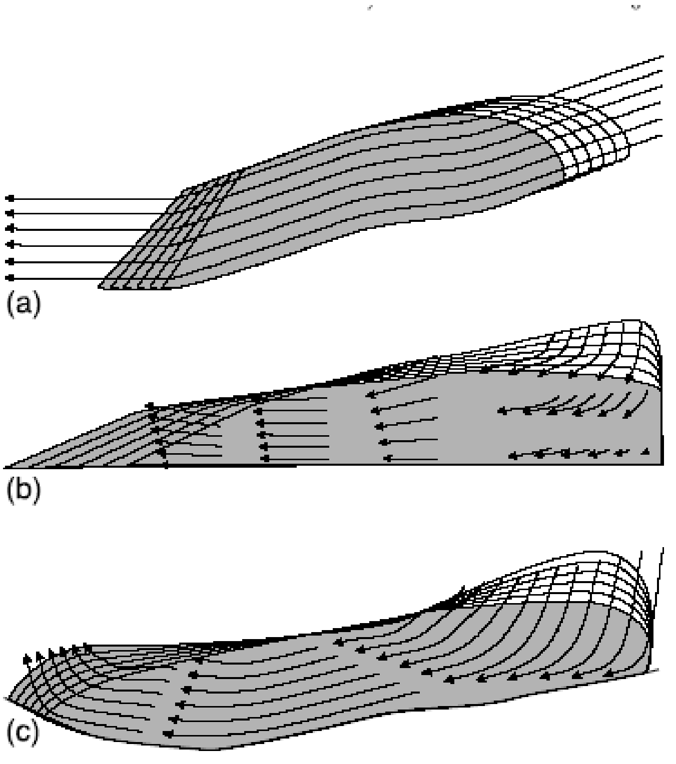

Fig. 1 Gravity-driven deformation. **A)** Gravity gliding, in which a rigid block slides down a detachment. **B)** Gravity spreading, in which a rock mass distorts under its own weight by vertical collapse and lateral spreading. **C)** Mixed-mode deformation. Shaded areas are the final stages and arrows show material movement vectors. Adapted from Rowan et al. (2004).

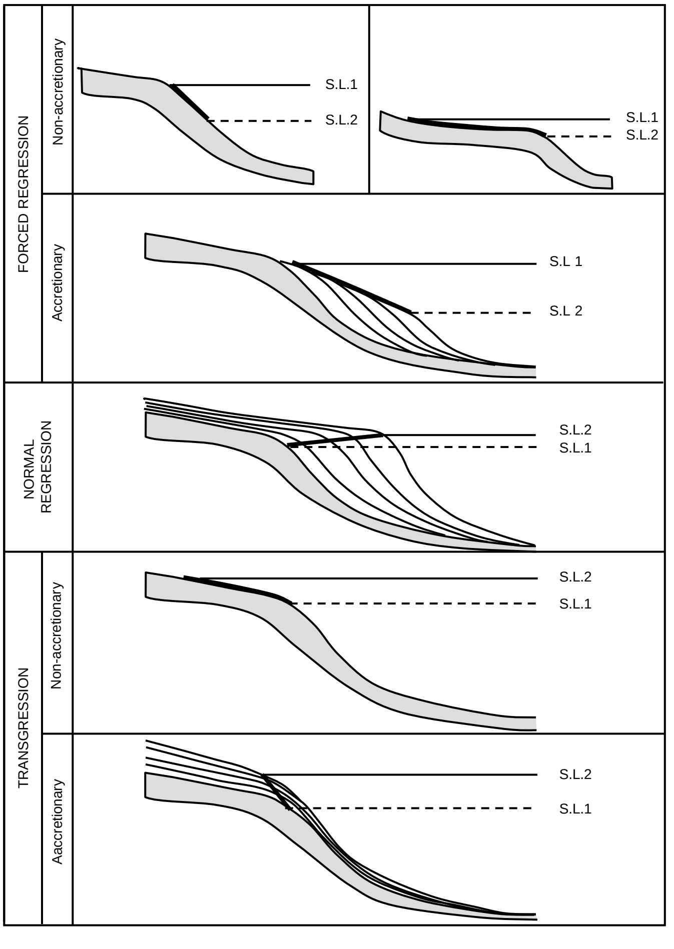

Fig. 2 The various classes of shoreline trajectories. Heavy line indicates the shoreline trajectory. Adapted from Helland-Hansen and Martinsen (1996).

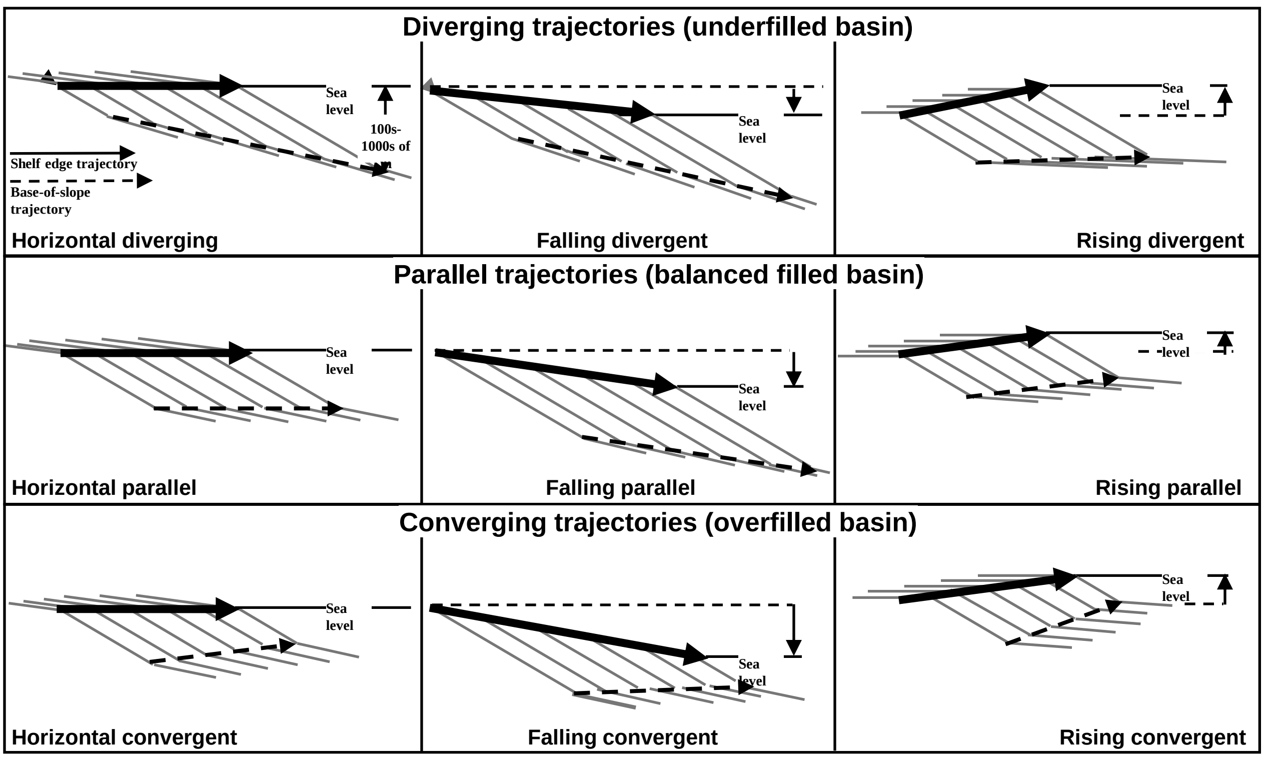

Fig. 3 Concepts of shelf edge trajectory and base-of-slope trajectory. The shelf edge trajectory can either be rising, horizontal or falling as it responds to long term rising, stable or falling relative sea level, respectively. The base-of-slope trajectory is dependent upon sediment supply to the basin floor, basin physiography and subsidence. Coupling of the shelf edge and base-of-slope trajectories result in 3 main types of trajectory patterns: 1) converging trajectories resulting in successively decreasing clinoform size with time (decreasing foreset length and relief); 2) parallel trajectories resulting in constant clinoform size; and 3) diverging trajectories resulting in increasing clinoform size with time (increasing foreset length and relief). The patterns can further be divided into rising convergent, rising parallel, rising divergent; horizontal convergent, horizontal parallel etc., where rising, horizontal and falling refers to the shelf edge trajectory orientation. The coupling of base-of-slope and shelf edge trajectories can be used to decide if the accommodation seaward of the shelf edge was increasing (indicative of a underfilled basin) or decreasing (indicative of a overfilled basin) during progradation. Parallel trajectory pattern suggest that the sediment supply balanced accommodation. Diverging trajectories are indicative of build-up of gravitational potential along the clinoform, whereas converging trajectories are indicative of the oposite.

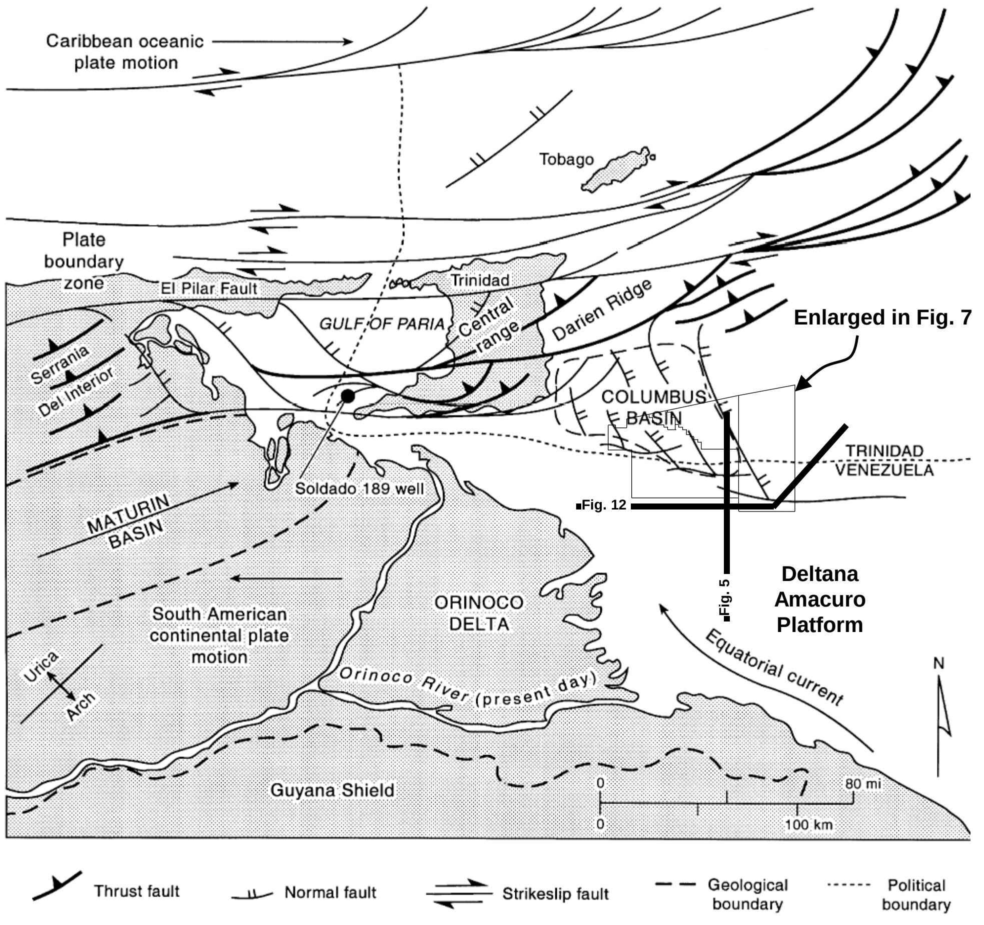

Fig. 4 Structural framework of the eastern part of Eastern Venezuelan Basin. Convergence between Caribbean and South American plates resulted in uplift in the north and the generation of a foreland basin in the south. The uplift changed the drainage pattern of northern part of South America, and the proto-Orinoco delta system started to prograde parallel to the axis of the foreland basin. Frames indicate position of license blocks. After Pocnall 1999, adapted from Wood 2000.

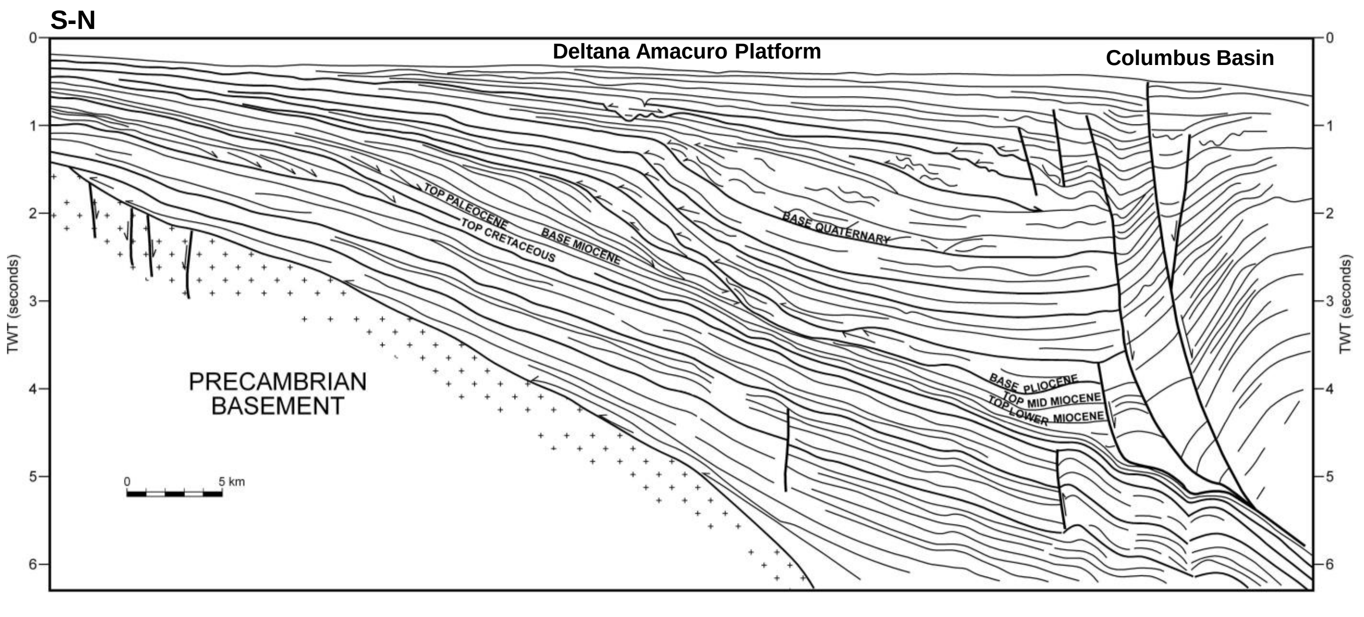

Fig. 5 Cross-section extending from the tectonic stable Delta Amacuro Platform in the south to the growth faulted Columbus Basin in the north. The stratigraphic thickness increases considerably toward the thrust front. Key horizons and time lines indicated. See Fig. 4 for position of transect. Modified from Di Croce et al. (1999).

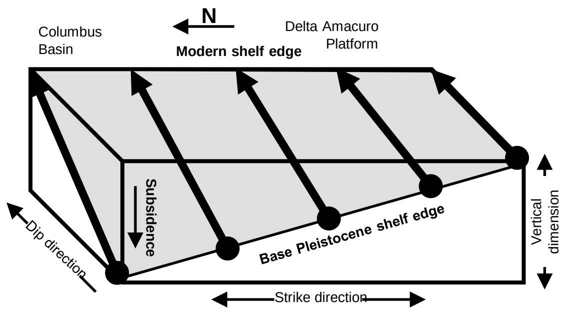

Fig. 6 3D sketch showing the inferred spatial relation of the shelf edge trajectory orientation in the study area. The trajectory is horizontal in areas with no subsidence (south) whereas it gradually steepen toward the area with maximum subsidence (north). Grey area represent plane of shelf edge trajectory progradation. See Fig. 4 for geographic position of basins.

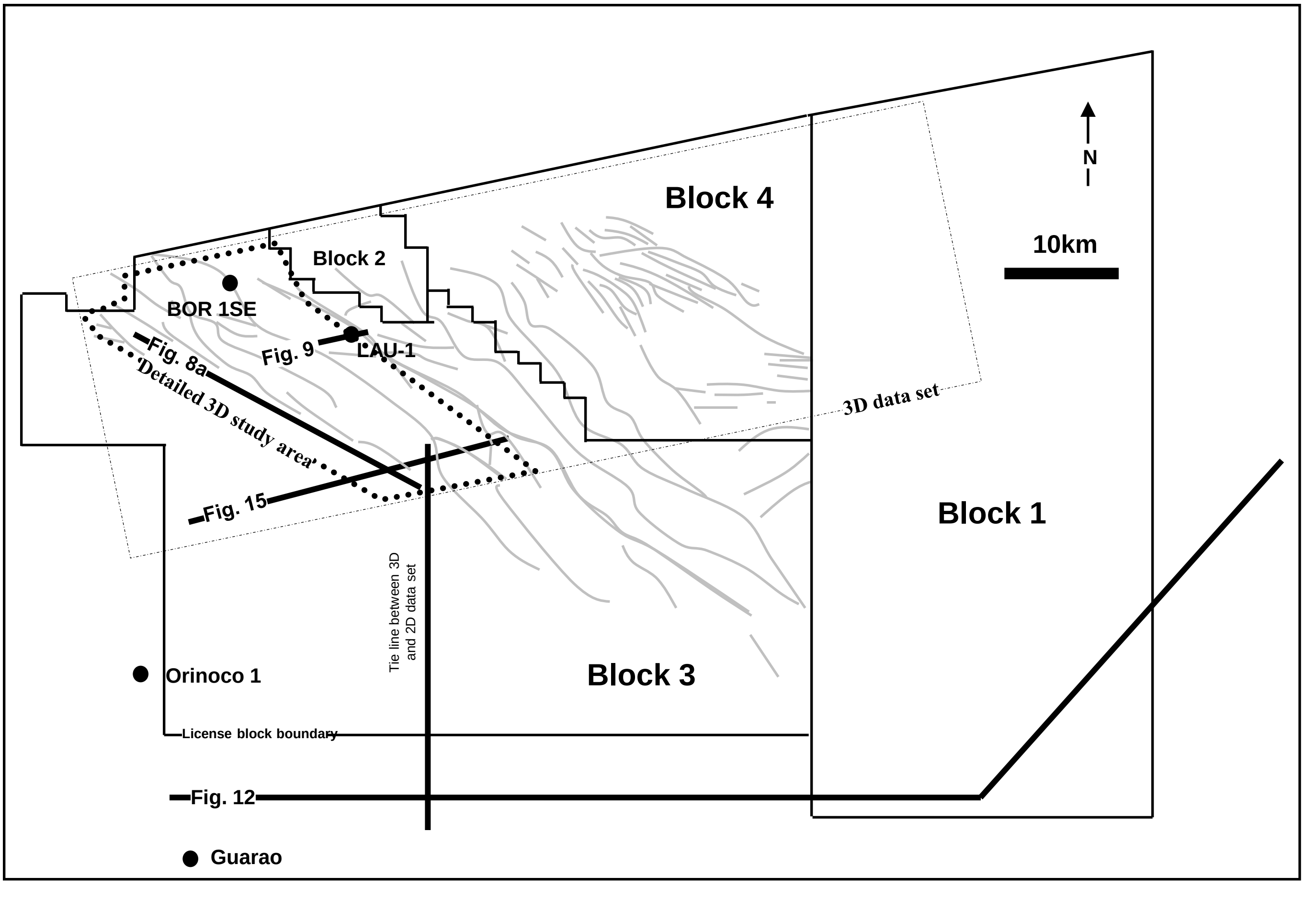

Fig. 7 License block boundaries and position of detailed 3D seismic study area. Grey lines indicate faults (down thrown to the northeast). Columbus Basin (cf. Fig. 4) is represented within the faulted areas, whereas Deltana Amacuro Platform (cf. Fig. 4) is located in the relatively tectonically undisturbed area to the south. Position of key wells indicated by black circles.

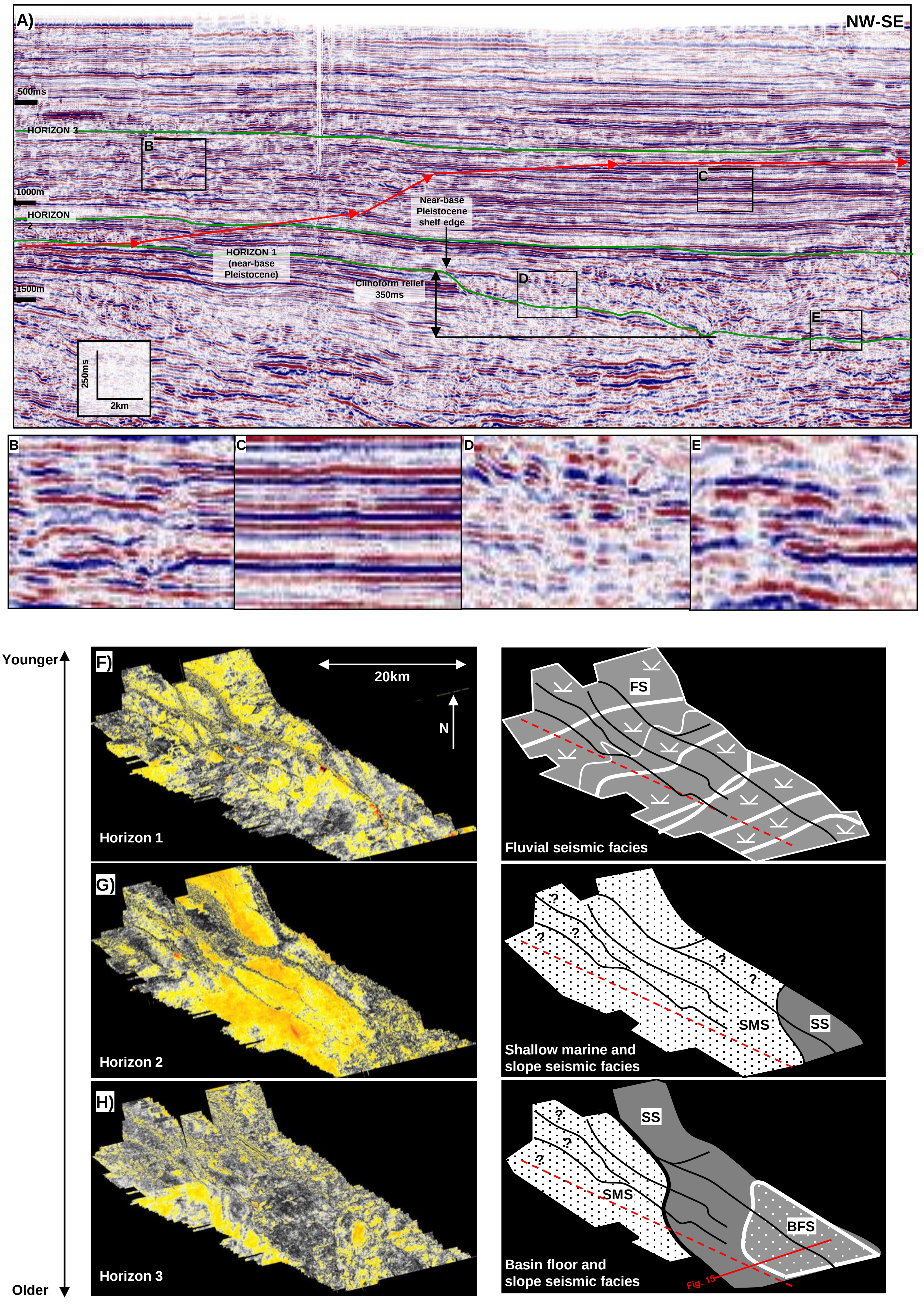
A)
NW-SE
500ms
HORIZON 3
1000m
HORIZON 2
Near-base Pleistocene shelf edge
HORIZON 1 (near-base Pleistocene)
Clinoform relief 350ms
1500m
250ms
2km
B
C
D
E
Younger
Older
F)
20km
N
Horizon 1
FS
Fluvial seismic facies
G)
Horizon 2
SMS
SS
Shallow marine and slope seismic facies
H)
Horizon 3
SS
SMS
BFS
Fig. 15
Basin floor and slope seismic facies

Fig. 8 The seismic facies recognised in this study. A) Oblique depositional dip cross-section comprising an overview of the facies signatures. Position of profile indicated in Fig. 7 and as red stippled line in f,g,h. B) Fluvial seismic facies (FS). C) Shallow marine seismic facies (SMS). Note Horizon 1 cut SMS at the shelf edge. D) Slope seismic facies (SS). E) Basin floor seismic facies (BFS). Down-dip transition from fluvial seismic facies to shallow marine seismic facies is interpreted to represent a change from fluvial to basinal processes and to represent the approximate position of the shoreline. When interpolated, this lateral facies change display the approximate orientation of shoreline trajectory. F) RMS-map expression of fluvial seismic facies (horizon 1); G) RMS-map expression of shallow marine seismic facies (horizon 2); H) RMS-map expression of slope and basin floor seismic facies (horizon 3). Black lines indicate faults. See A for stratigraphic position of horizons and Fig. 7 for position of detailed 3D study area.

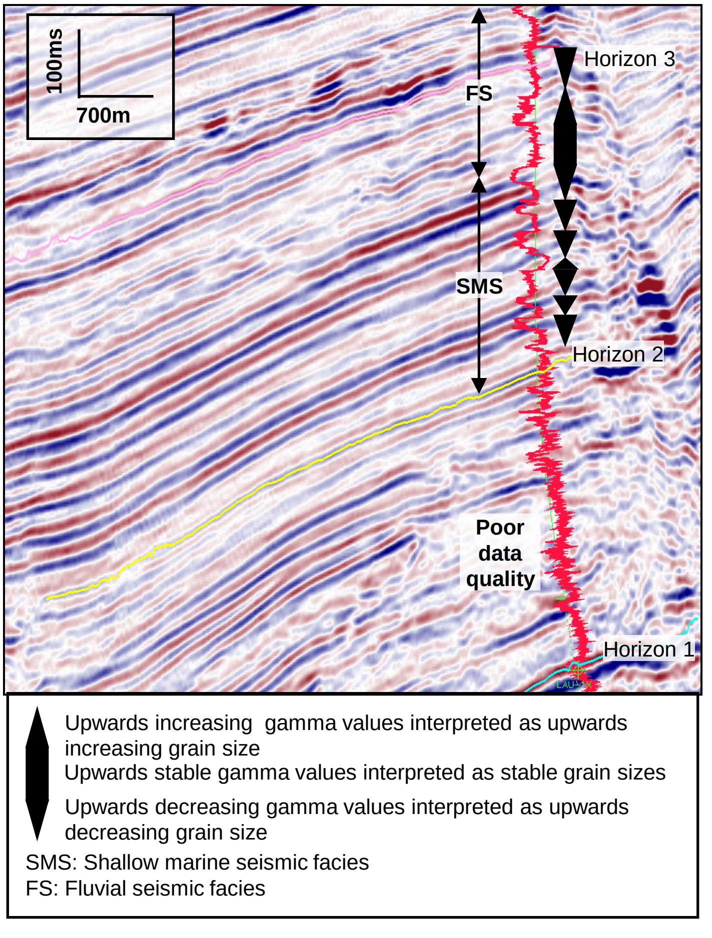

Fig. 9 Correlation of fluvial seismic facies (FS) and shallow marine seismic facies (SMS) to LAU-1 well. The former display repeated 35-55 ms (35-55 m) thick, blocky to upwards decreasing gamma values separated by abrupt increases in gamma value. This is interpreted as stacked shoreline-shelf parasequences. Fluvial seismic facies display a different gamma ray pattern; it is characterized by thicker (ca 100 ms/100 m) upwards decreasing and increasing gamma values interpreted to reflect progradation and retrogradation of the delta system. See Fig. 7 for position of profile and LAU-1 well. Horizons 1-3 refer to horizons in Fig. 8.

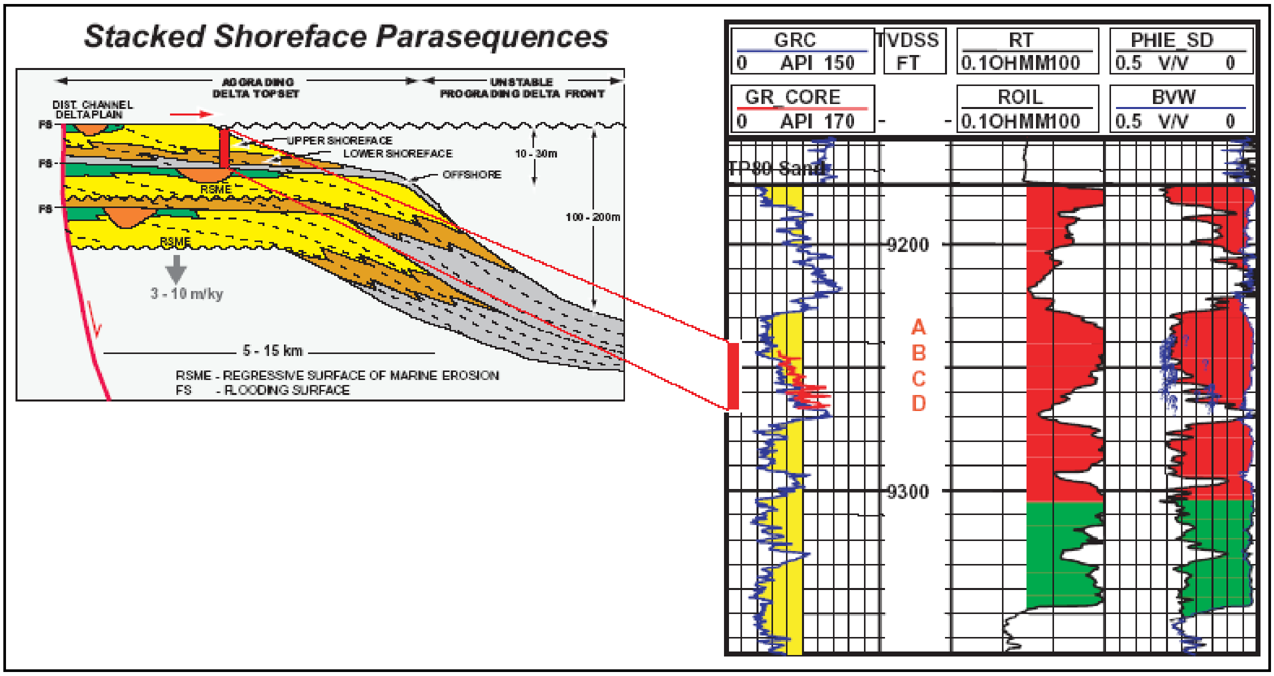

Fig. 10 Interpreted depositional setting (from cores and well logs) comprising upwards coarsening, stacked shoreface parasequences (ps). Cored interval marked with red column (for core description see Sydow et al. (2003)). A: upper shoreface (top of parasequence); B: mid shoreface; C) lower shoreface; D) offshore silts. Adapted from Sydow et al., (2003).

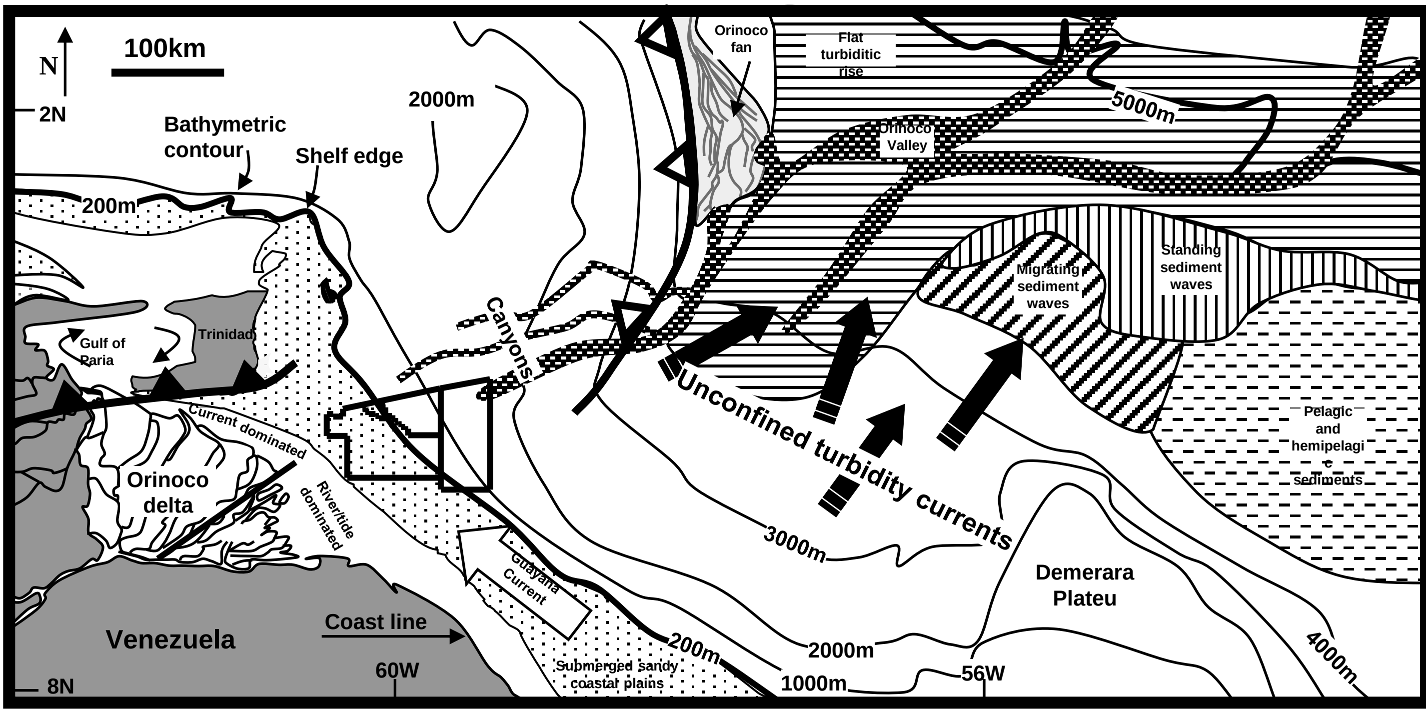

Fig. 11 Regional geography of the modern Venezuelan margin and the Orinoco delta system. Sediments are transported 100s-1000 km down dip of the study area. Wind and wave predominantly travel from east toward west. Frames indicate position of license blocks. Data sources include: Di Croce et al. (1999) (regional framework); Belderson (1984) (Orinoco fan); Embley and Langseth (1977), Faugeres et al. (1993), Ercilla et al. (2002), Gonthier et al. (2002) (canyons/sediment waves); Warne et al. (2002) and references therein (Orinoco delta and shelf).

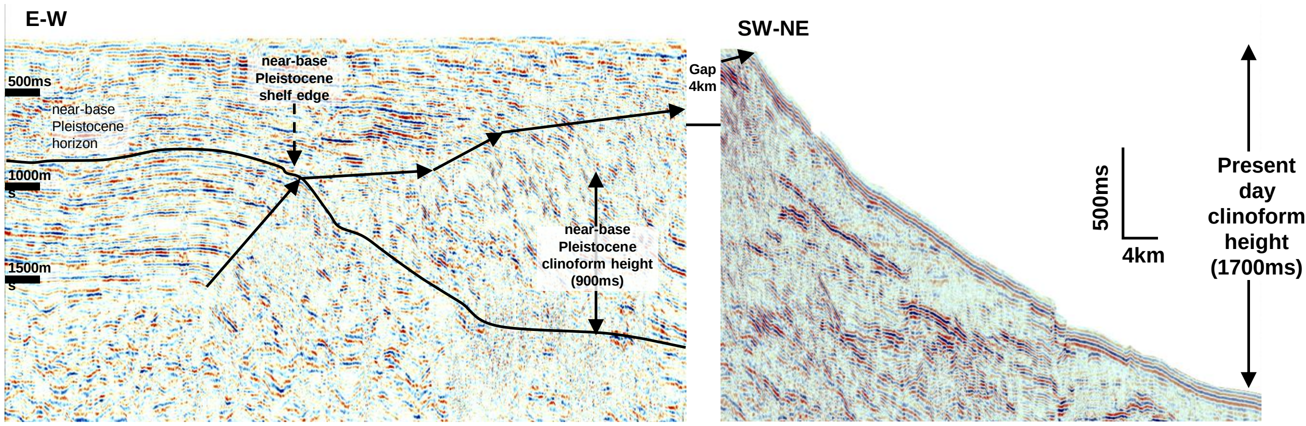

Fig. 12 Seismic cross-section from the relatively structurally undeformed Deltana Amacuro Platform. Shelf edge trajectory (continuous arrow) indicated; a change in accommodation/sediment supply ratio resulting in a decrease in angle of shelf edge trajectory is evident at the lowermost interpreted horizon (near-base Pleistocene). See Fig. 7 for position of cross-section.

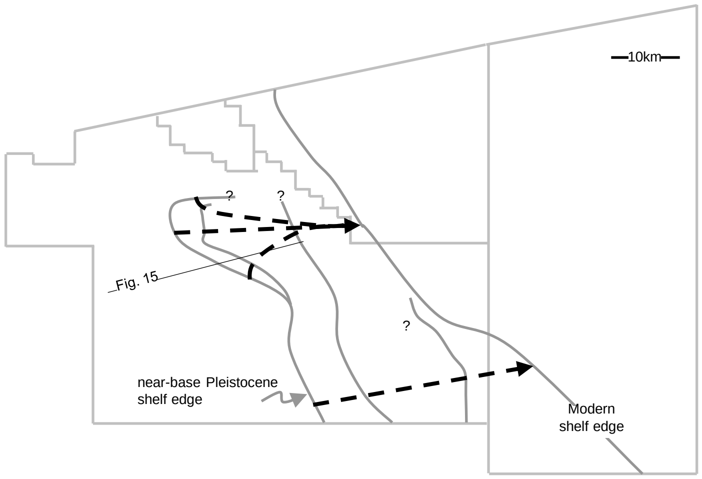

Fig. 13 Map view of the successive positions of the shelf edges in the study area from near-base Pleistocene to Recent. Note concave profile of the near-base Pleistocene shelf edge. This type of concavity is created by shelf edge failures and down slope transport of sediments. Stippled arrows indicate direction of shelf edge migration; note that the trajectory deviates horizontally to heal the erosional concavity resulting from slumping. Position of blocks shown in Fig. 4.

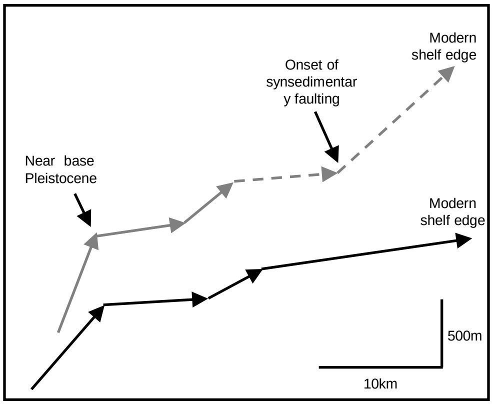

Fig. 14 Sketch showing the difference between the shelf edge trajectories of Columbus Basin (grey line) and Delta Amacuro Platform (black line). Continuous line represent observed shelf edge trajectory whereas stippled line indicates inferred trajectory. Scale approximate.

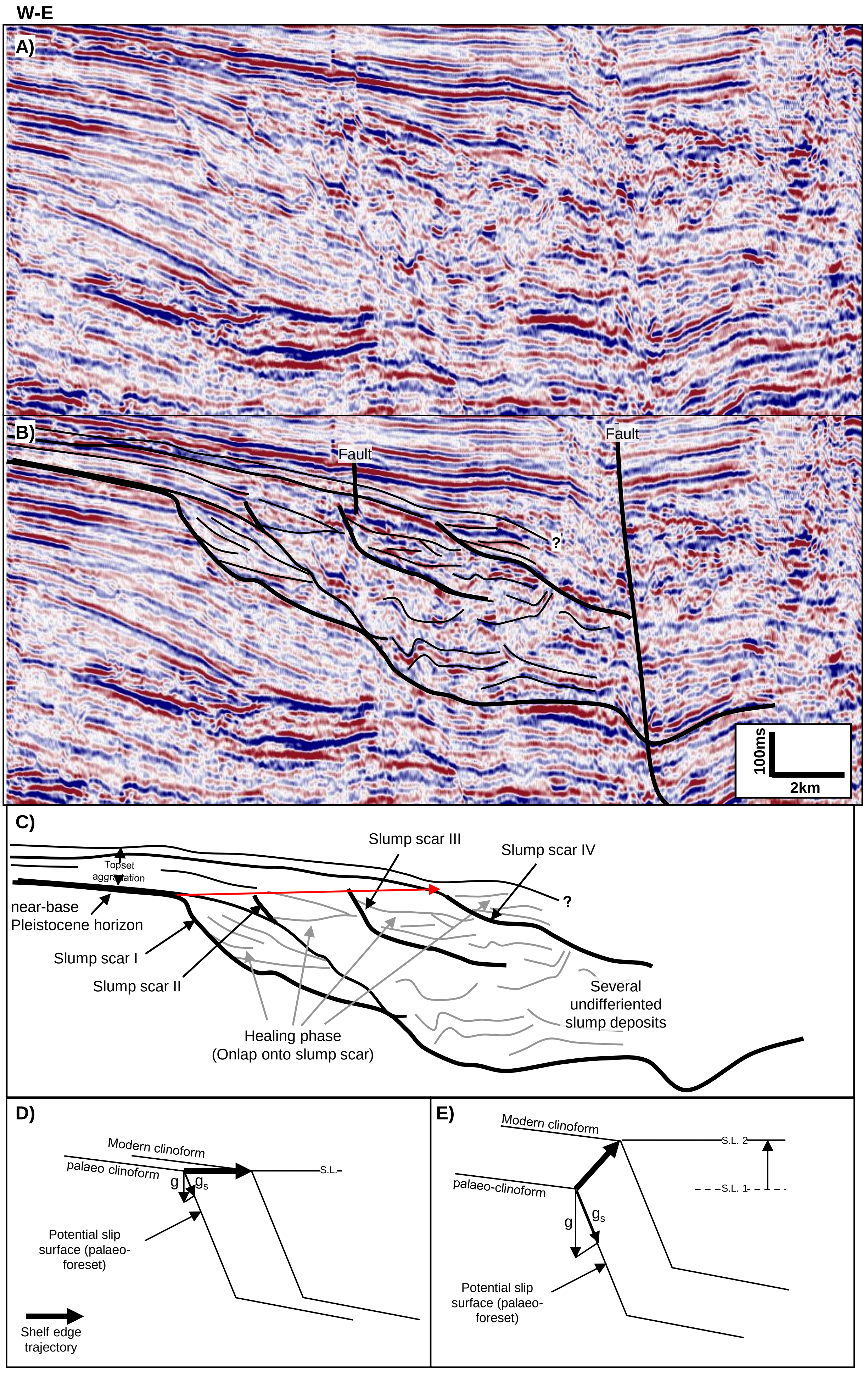

W-E
A)
B)
Fault
Fault
?
100ms
2km
C)
Slump scar III
Slump scar IV
Topset
aggradation
?
near-base
Pleistocene horizon
Slump scar I
Slump scar II
Several
undifferiented
slump deposits
Healing phase
(Onlap onto slump scar)
D)
Modern clinoform
palaeo clinoform
S.L.
g
g_s
Potential slip
surface (palaeo-
foreset)
Shelf edge
trajectory
E)
Modern clinoform
S.L. 2
palaeo-clinoform
S.L. 1
g
g_s
Potential slip
surface (palaeo-
foreset)

Fig. 15 Repeated shelf edge progradations and collapses. **A)** Uninterpreted cross-section. **B)** Interpreted cross-section showing slump scars and healing phases followed by renewed progradation. Note topset aggradation during progradation, suggesting a rising shelf edge trajectory. **C)** Interpretative sketch rotated so topset reflectors appear in sub-horizontal position. Red line indicates the overall shelf edge trajectory. **D)** Sketch showing the inferred relation between steep shelf edge trajectory and high amount of shelf edge failures: *(D1)* Progradation with horizontal shelf edge trajectory is associated with little accumulation of sediment along the shelf edge. *(D2)* Increasing steepness of the shelf edge trajectory is associated with increased accumulation of sediment at the shelf edge. The increased loading is associated with increased shear stress component of gravity along potential seawards dipping slip surfaces (palaeo-continental slopes). In addition, progradation during rising relative sea level is associated with steepening of the upper slope (e.g. Ross et al. 1994). Gravity gliding is initiated when the shear stress component of gravity parallel the slip surface exceed the shear strength of the surface (Ramberg, 1981). g= vertical gravity resulting from overburden, gs= shear component of gravity. Position of profile indicated in Fig. 7. RMS map of near-base Pleistocene horizon is shown in Fig. 8h.

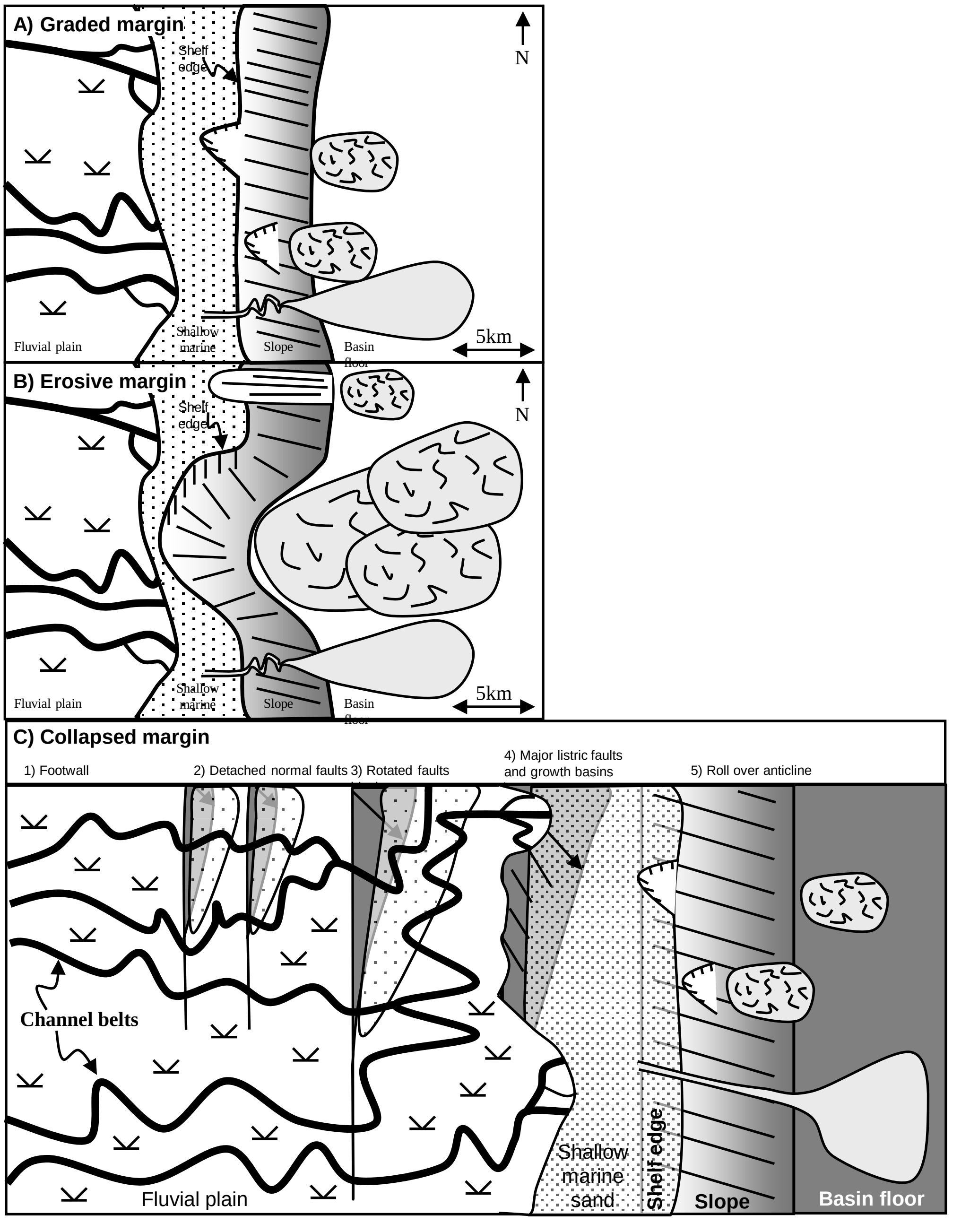

Fig. 16 Palaeogeographic sketches of the study area. **A)** Graded margin progradation (Deltana Amacuro Platform). Only small scale syn-sedimentary deformation evident. **B)** Palaeogeographic sketch of the near-base Pleistocene Orinoco Delta system in its most regressive positions, based on the dip-stacking of seismic facies. An aggrading fluvial plain supplied sediments to a wave/storm dominated coastline. Down continental slope sediment transport to the basin floor was dominated by mass-wasted sediments resulting from shelf edge failures. The shelf edge prograded as repeated shelf edge failure-healing cycles and followed the model of slope readjustment typical for an erosive margin (sensu Hedberg 1972, Ross et al. 1994).
C) Paleogeographic sketch of the study area after onset of growth faulting. The gravity failure was associated with basinward transport of fault domains and caused lowering of the depositional profile across the margin. This further led to a reduction in large scale shelf edge failures compared to pre-collapse palaeogeography in B. In detached normal faults domain, sediments were deposited at a high rate, but palaeoflows were only affected to a limited extent. In contrast, in the rotated fault blocks domain, palaeoflows of the fluvial system were directly affected and fluvial channels are observed to trend parallel to strike of faults in some stratigraphic intervals. The majority of the sediments were captured in major listric faults and growth basins domain, and the accommodation created here prevented the margin from further basinward progradation.

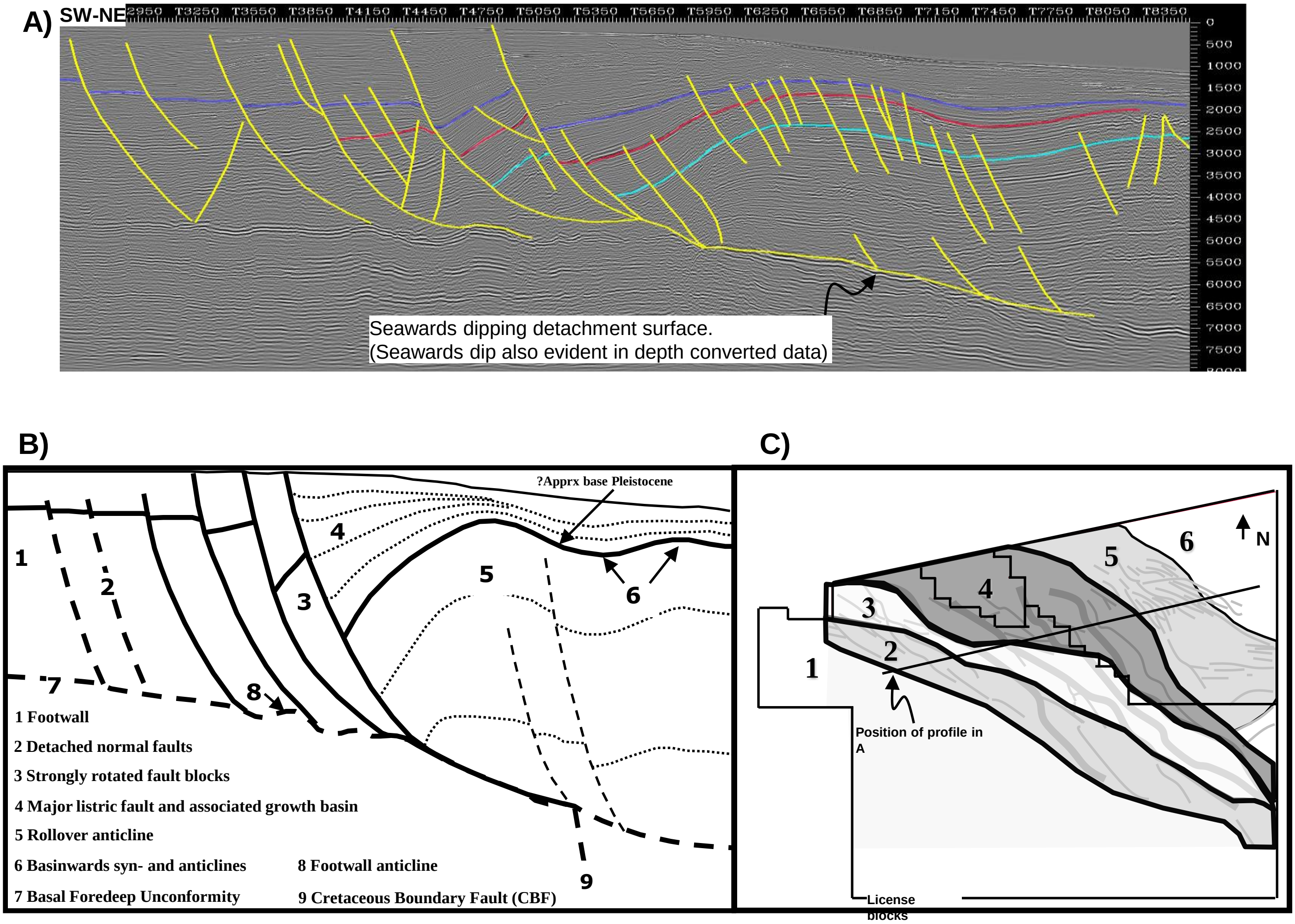

Fig. 17 Fault domains recognised in this study. **A)** Seismic cross-section showing interpreted faults and detachment surface. Position of line indicated in C. **B)** Conceptual cross-sectional sketch of the fault domains in the Columbus Basin, based on A. **C)** Map view of fault domains. Numbers refer to domains indicated in B). See Fig. 4 for position of blocks.

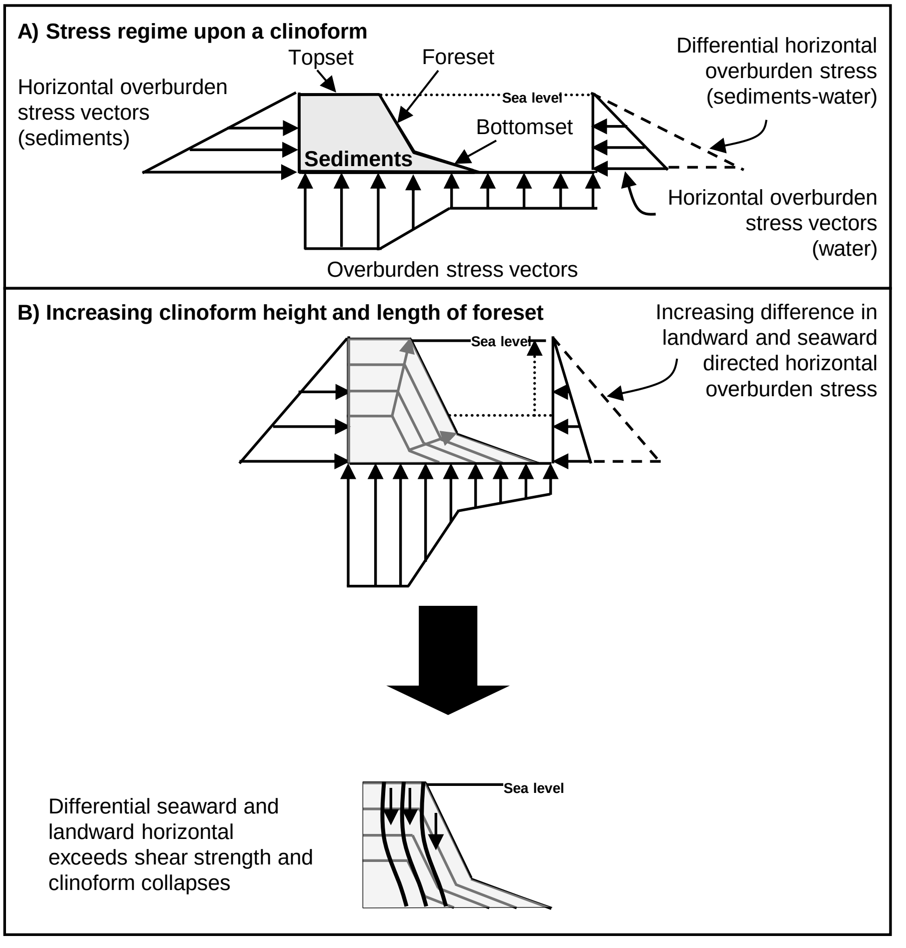

Fig. 18 Horizontal overburden stress versus clinoform size (relief and length of foreset). The slope of the foreset is equal in A and B. **A)** Stress regime upon a clinoform. Overburden decreases basinwards as rocks are more dense than water. The associated landward directed horizontal overburden stress is therefore lower than seaward directed horizontal overburden stress. However, in this example, the difference in horizontal overburden stress is less than the shear strength of sedimentary package and onset of gravitational failure (growth faulting) is prevented. **B)** Increasing clinoform size (increasing relief and length of foreset). As the clinoform increases in size due to diverging shelf edge and base-of-slope trajectories, the difference in overburden and associated horizontal overburden stress increases. Eventually, this difference will reach critical shear stress in the sedimentary package and growth faulted gravitational failure will commence.

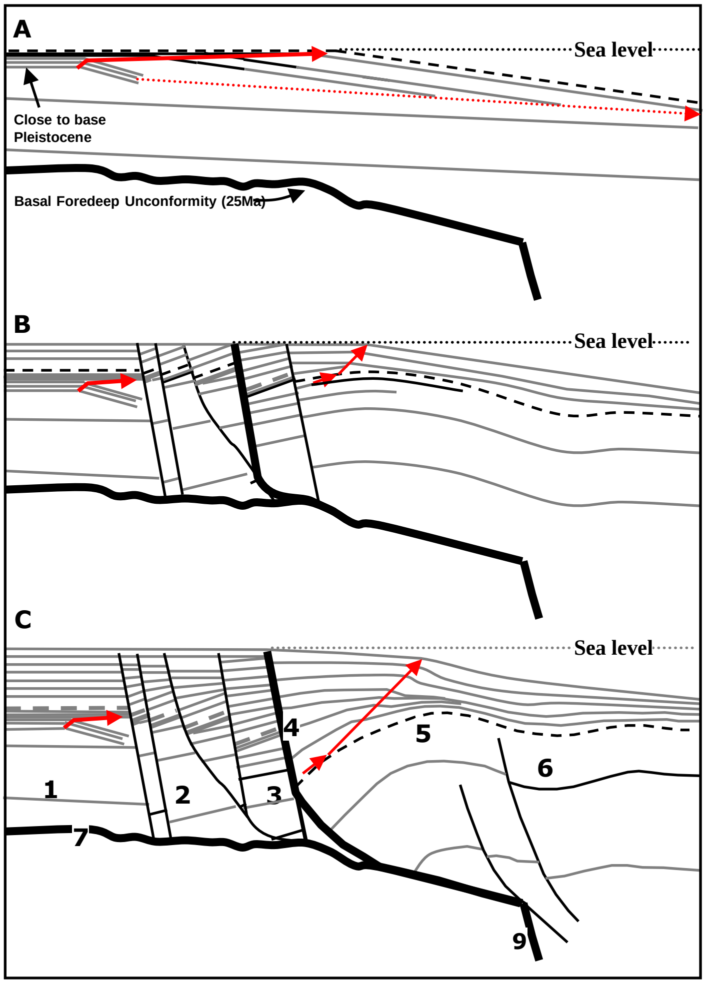

Fig. 19 Conceptual sketch showing the evolution of growth faulting in the Columbus Basin. **A)** At near-base Pleistocene, the depositional system stepped basinward with diverging shelf edge (red arrows) and base-of-slope trajectories (stippled red arrows). This resulted in an increase in clinoform size and associated increasing difference in seaward and landward directed horizontal overburden stress. Stippled black line represent reference horizon. **B)** The difference in seaward and landward directed horizontal overburden stress exceeded shear strength along incompatible horizons, and planar faulting commenced. Thick line indicates fault plane with main movement. **C)** The present day situation. The main fault shifted basinwards and a large growth faulted basin has developed. This basin trapped so much sediments that it halted the progradation of the entire margin. The loading of these sediments further contributed to maintaining movements along the fault planes. Numbers in the figure refer to fault domains in Figs 17b.

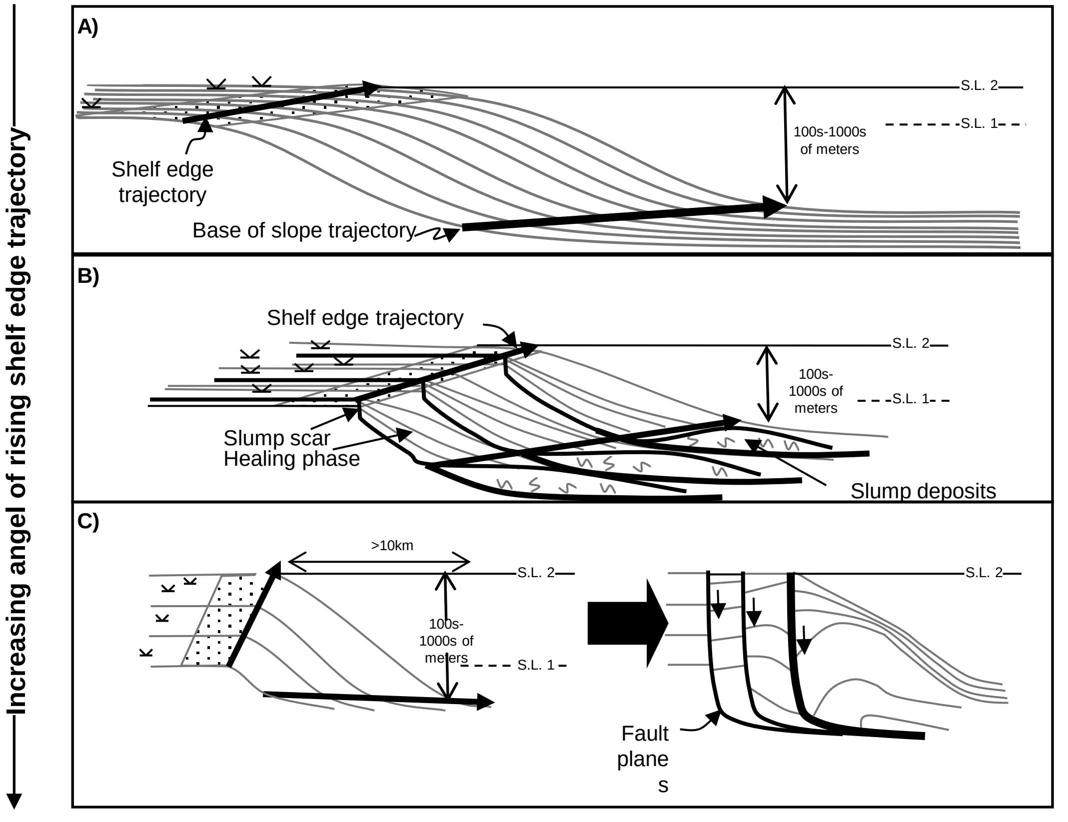

Fig. 20 Model for the development of a margin prograding with successively increasing steepness of a rising shelf edge trajectory. **A)** Progradation as a graded margin (sensu Hedberg 1972; Ross et al. 1994). The margin is prograding steadily without major shelf edge collapses and down slope mass wasting processes. Sediment transport to the basin floor is predominantly by minor mass transport movement and unconfined turbidity currents. **B)** As the shelf edge trajectory steepens, the margin transforms into a erosive margin (sensu Hedberg 1972; Ross et al. 1994) where progradation occurs as repetitive shelf edge failure-healing cycles. **C)** If progradation of the margin prevails with diverging shelf edge and base-of-slope trajectories, the margin will eventually experience major gravitational failure with the development of growth faulting.